RECOMBINANT ESCHERICHIA COLI DERIVED OUTER MEMBRANE VESICLES FOR SAFE AND EFFECTIVE SUBUNIT ANTIGEN DELIVERY

A Dissertation

Presented to the Faculty of the Graduate School

of Cornell University

In Partial Fulfillment of the Requirements for the Degree of

Doctor of Philosophy

by

Hannah Christine Watkins

January 2017

RECOMBINANT ESCHERICHIA COLI OUTER MEMBRANE VESICLES FOR SAFE AND EFFECTIVE SUBUNIT ANTIGEN DELIVERY

Hannah Christine Watkins, Ph. D.

Cornell University 2017

Subunit vaccines rely on adjuvants to drive an immune response against antigens of interest. Improved adjuvant platforms, capable of interaction with specific pathogen recognition receptors in the innate immune system, can lead to more effective and longer lasting vaccines. Recombinant outer membrane vesicles (rOMVs) are a recently developed adjuvant system that harnesses the natural pathogen associated molecular patterns present in the outer membrane of *E. coli* to direct an immune response against recombinant antigens displayed on the rOMV surface. Though rOMV vaccines have demonstrated promise against viral antigens in murine models, their high lipopolysaccharide (LPS) content hinders translation to humans. This dissertation will present ways in which the LPS in rOMVs can be modified, through use of 'detoxified' commercial *E. coli* strains, as well as through genetic manipulation of probiotic *E. coli* strains, to generate rOMVs with greatly improved safety profiles. Additionally, it will profile the development of a potential pandemic influenza vaccine using detoxified rOMVs, demonstrating their feasibility in achieving protective immune responses.

BIOGRAPHICAL SKETCH

Hannah was born on April 17th, 1989 in Dumas, Texas. After nine too many years in Texas, she moved to Kenai, Alaska in 1998. She graduated from the University of Rochester in May 2011, with a B.S. in Biomedical Engineering and minors in Chemical Engineering and Biology. While at Rochester, Hannah conducted research under Danielle Benoit in polymer systems for targeted drug delivery. Hannah then spent 14 months at Imperial College London on Whitaker and Fulbright Fellowships, working under Professor Molly Stevens on assay development using gold nanostars. Hannah received an M.Phil in Materials Engineering from Imperial College London in Aug. 2013. Hannah started her PhD in Biomedical Engineering at Cornell in fall 2012, with the support of a National Science Foundation Graduate Research Fellowship. At Cornell, she worked under the guidance of David Putnam to develop outer membrane vesicles as a safe and effective adjuvant platform.

‘OMG! OMV!’ –anonymous

ACKNOWLEDGMENTS

First, thank you to my advisor, David Putnam. Thank you, Dave, for the support and enthusiasm you have provided over the past four and a half years. Thanks for always asking 'What can I do to help?', connecting me to others in the field, giving me freedom to design my own project, and providing me with many cookies. I am lucky to have had an advisor who supports work-life balance as much as you do. Thank you also to my minor committee members: Gary Whittaker and Matthew DeLisa. Thank you, Gary, for welcoming me into your lab (and lab meetings and lab outings) and for providing valuable insight about influenza. Thank you, Matt, for suggesting the Clearcoli project and for giving me freedom to take it in my own direction. Though not an official committee member, this work would not have been possible without the assistance and guidance of Cynthia Leifer. Thank you, Cindy, for sharing your wealth of immunology knowledge, helping to troubleshoot experiments, and providing me with resources for studying the interactions of rOMVs with the innate immune system.

The Putnam Lab is a pretty special place and I have had the privilege of working with many interesting people throughout the years. Thank you to the following PhD students for helping to make the Putnam Lab a warm and welcoming environment: Jen, who introduced me to the Ithaca Concert Band; Joseph, who patiently trained me in rOMV techniques, gave me project guidance, and knew all the answers to all the questions; Mingchee, for being a bouldering buddy; Lindsey, who brightened my mornings with dancing and singing; Jose, the best post-doc undergrad ever; Nicole, my go-to person for all professional advice and an amazingly skilled e-mail crafter; Bailey, who even when overloaded with work still helped others and left emergency chocolate under desks; Zhexun, for answering chemistry questions and translating labels; Sarah, for her tree knowledge and informative signs, and finally, Dave, for taking over the rOMV

project—I can't wait to see in which directions the project goes. Lab life also would not have been the same without the post-docs Janis, Cassie, and Can, as well as all of the assorted m'enges and undergrads. Herein, I would be remiss to not specifically thank Garrett, whose successful development of the M2e4xHet antigen significantly affected my PhD, giving me a great test antigen as I studied the effects of LPS acyl chain manipulation. Thanks Garrett, for training me on influenza work, always sharing your tips with me, and providing a soundtrack for ELISA-ing by. I also must thank Cassie for doing such a wonderful job training the team rOMV members I got to work with: Garrett, Catalina, and Annie. Additionally, I have many other students to thank for helping to complete this work: thank you Aditya, for your endless enthusiasm and curiosity; Joey, for your early hours and tireless pipetting; Sara, for your positive attitude and attention to detail; Hannah, for your organization and cranking out of 100+ ELISAs, and Jaclyn for your classiness and resilience to devastation in the face of mold (plus professional behavior, organization, troubleshooting ability, etc.).

Many non-Putnam Lab people contributed to this dissertation as well. Thank you to phlebotomist extraordinaire, Jeff, and all of my anonymous blood donors- you rock! – and so does your blood! (well…mostly). Thank you to Sylvie and Frank, as well as the other mouse core facility members for taking such good care of my mice, training me in mouse techniques, and always alerting me to any issues. Thank you to John in the CCMR for training me in TEM and helping when things went awry. Thank you to Dorian for getting the flow core back in shape, patiently assisting me through many flow-associated crises, and setting up the high throughput sampler. Thank you to Jody and Erika in the Leifer Lab for taking care of cell lines and training me in various *in vitro* experiments. Thank you to Taylor in the DeLisa lab for teaching me phage knock out and for providing me with *E. coli* strains. Finally, thank you to

Marco in the Whittaker Lab for help with the plaque assay and to Michele in the Whitaker Lab for assistance in growing up virus from egg stocks.

In addition to all of the lab-related and experimental assistance I received, thanks to my friends for helping to make getting a PhD an enjoyable experience. Thanks to the Man Cave for making my final semester at Cornell a great one (ugh, and for making me not want to leave). Also, thanks to long-term housemate and friend since PhD day one, Julie, for always being available to listen to my rants, go for walks, watch movies, and discuss the merits of various cookies. Thank you especially to friends Marie, for providing me with support and scones even when far away; Liz, for being my swim swim and exercise buddy and regularly feeding me; Jacob, for not killing me despite enjoying sprinting up hills and climbing routes sans locatable rap stations; Dan, for constantly showering me in compliments; Lauren, for culinary and rock climbing adventures; Suruh, for yurt advice and artistically arranged treats, and Amanda, for tasty meals and long walks. Thank you also to the Spotify playlists of Lesley Chow, without which, the writing up process would have been much more miserable.

Finally, thank you to my family—especially master proofreader Molly. Thank you for your constant support and for being my primary source of entertainment as I traipse between home and campus. Thank you for not finding me too crazy as I rush to wrap up my PhD, just so that I can jump into doing more research and more writing (aka a post-doc). We might be scattered across the country and world, but it's nice to know that family is only a phone call away.

TABLE OF CONTENTS

CHAPTER 1

INTRODUCTION

Adjuvants: a critical component to many vaccines

Vaccines represent one of the most successful public health interventions in prevention of disease. Through vaccination, smallpox has been completely eradicated, and great progress has been made towards the elimination polio and tetanus[1,2]. More recently, vaccines against human papilloma virus (HPV) have already led to significantly fewer high grade cervical lesions[3]. While vaccines against certain pathogens have resulted in great success and high levels of protection, vaccines for other diseases remain elusive; highly effective vaccines against human immunodeficiency virus (HIV), malaria, influenza, and many others remain to be developed[4].

Currently, most vaccines can be roughly divided into the categories of live attenuated, inactivated, or subunit. Live-attenuated vaccines are often generated via passage of the pathogen through a non-human cell type, causing the pathogen to become less adept at infecting human cells. For example, to create the chickenpox vaccine, varicella zoster virus was passaged numerous times through guinea-pig embryo cultures[5]. Inactivated vaccines are created by killing/inactivating the pathogen, preventing it from being infectious. VAQTA, a hepatitis A vaccine produced by Merck, is comprised of formalin inactivated hepatitis A virus. Subunit vaccines are made by using only select components of the pathogen, typically proteins[6,7]. For example, the hepatitis B vaccine contains only the protein hepatitis B surface antigen (HBsAg), which is produced using yeast. Historically, vaccines were made primarily via attenuation or inactivation; however, both of these strategies require working with large amounts of pathogen[8]. Additionally, attenuated vaccines, while often the longest lasting, can have drawbacks of being unable to be administered to immune-compromised individuals, reliance on refrigeration, and—

in extremely rare cases—reversion to a more pathogenic form. Inactivated vaccines are generally safer than attenuated vaccines, and can be given to immune compromised individuals. However, they typically require multiple doses to elicit long-term effects. Additionally, producing inactivated pathogens for vaccines can be costly; the attenuated oral polio vaccine costs ~20x less per dose than the inactivated polio vaccine[9]. Subunit vaccines offer the advantage of only requiring antigens from pathogens, which can be expressed using recombinant DNA techniques in non-pathogenic organisms, such as lab strains of *Escherichia coli* (*E. coli*)[10]. These pathogen-derived antigens are often poorly or non-immunogenic, and thus require addition of an adjuvant to elicit a sufficient immune response[11].

Adjuvants, immune response 'helpers,' are common additions in inactivated vaccines and are almost always found in subunit vaccines[12]. Vaccines work by tricking the body into responding as if it were exposed to the actual pathogen. Thus, the immune system responds by making neutralizing antibodies against the vaccine antigen, just as it would a true pathogen. When the actual pathogen invades, vaccination-induced antibodies neutralize the pathogen, preventing infection. Pathogens contain conserved pathogen associated molecular patterns (PAMPs) that send danger signals to the immune system upon infection[13]. Because of this, attenuated vaccines rarely require addition of adjuvant, as the live pathogen in the vaccine is able to produce sufficient danger signals. Though inactivated vaccines are derived from a whole pathogen, the treatments to inactivate the pathogen, as well as its lack of infectivity, can reduce the number of PAMPs it contains. Thus, inactivated vaccines sometimes require addition of an adjuvant to supply extra danger signals and to generate a more potent immune response[14]. Adding adjuvants to inactivated vaccines also allows for dose sparing, making it so that less of the expensive inactivated pathogen is necessary to achieve the same level of protective response.

Subunit vaccines, because they only contain select antigens from pathogens, require adjuvants to supply danger signals[15]. Thus, both the vaccine antigen and the vaccine adjuvant are important; antigen selection determines what the immune system targets and adjuvant selection shapes the type of response against that antigen. The most common vaccine adjuvants—and until 2009 the only adjuvants found in Food and Drug Administration (FDA) approved vaccines—are aluminum salts, or alum[16]. Though the mechanisms of how alum elicits danger signals are still poorly understood, alum has nonetheless proven to be effective at strengthening the immune response and is contained in many vaccines[17,18]. Adding alum to vaccines causes development of a broader antibody repertoire following vaccination and increases the affinity of antibodies that are produced. Though alum is a useful adjuvant, developing adjuvants that more closely mimic the stimulation patterns of actual pathogens could lead to improved vaccine design[19–21].

Increased understanding of the innate immune system has led to a better understanding of pathogen recognition receptors (PRRs) in the innate immune system. PAMPS on pathogens stimulate different patterns of PRRs, leading to varied immune responses[22]. While most vaccines work primarily through eliciting neutralizing antibodies against an antigen, actual pathogens are cleared by both an antibody-based humoral response, as well as by a cellular response. There are many nuances associated with immune responses, but the body often responds to intracellular pathogen invasion by developing a T helper cell 1 (Th1) biased response[23]. When instead the body is infected with a parasite or affected by allergens, a Th2 biased response is more common. Th1 responses are characterized by a proinflammatory response, with high levels of IFNγ production. Th1 cells indirectly lead to activation of CD8+ T cells (cytotoxic T cells), which can then kill infected cells. Th1 cells also lead to activation of B cells, which ultimately differentiate into plasma cells and produce IgG antibodies that can both

neutralize pathogens and clear infected cells via antibody dependent cellular cytotoxicity (ADCC) and antibody mediated phagocytosis (AMP)[24,25]. While alum is able to elicit IgG neutralizing antibodies, the antibodies are not always able to elicit ADCC and AMP. In mice, IgG isotypes IgG2a and IgG2c (different mouse strains produce either IgG2a or IgG2c) contain Fc regions that interact with Fc receptors (FcR) on natural killer (NK) cells and macrophages, facilitating AMP and ADCC[26]. However, alum typically leads to higher levels of IgG1 than IgG2a/IgG2c, which can neutralize a pathogen, but does not trigger AMP and ADCC. Additionally, while vaccines using alum as an adjuvant can elicit B cell responses, they typically do not elicit cytotoxic T cell responses[27]. Creating vaccine adjuvants that elicit a Th1 biased response, complete with IgG2a or IgG2c antibodies and cytotoxic T cells, should help to create more effective vaccines that do a better job at preventing and clearing pathogen infection. Possibly, the lack of effective vaccines for certain diseases is due not to poor antigen selection, but rather to an ineffective immune response being mounted against that antigen.

Recently, the FDA has approved vaccines with more diverse adjuvants[28]. In 2009, Cervarix, a vaccine against cervical cancer produced by GlaxoSmithKline, received FDA approval[29]. Cervarix is comprised of proteins from HPV, which form a virus like particle (VLP), and uses the adjuvant system AS04. AS04 consists of alum as well as monophosphoryl lipid A (MPL)[30]. MPL is an agonist of PRR toll like receptor 4 (TLR4), which also is triggered in response to the common bacterial PAMP lipopolysaccharide (LPS). Unlike LPS, also known as endotoxin, MPL does not cause excessive inflammation and toxicity following injection. The mechanisms that cause MPL to have reduced toxicity in comparison to wild type bis-phosphorlyated lipid A remain an active area of research. It is hypothesized that MPL more strongly triggers the Myd88 independent TRIF pathway of TLR4, resulting in type 1 interferon

production, whereas wild type LPS triggers both the Myd88 independent and the Myd88 dependent proinflammatory pathway[31]. In addition to Cervarix, MPL is being explored as an adjuvant for many different vaccines[32–34]. In November 2015, the FDA approved the first seasonal influenza vaccine to contain an adjuvant, Fluad—produced by Novartis[35]. Fluad contains MF59, which is an oil in water emulsion of the biodegradable oil squalene[36]. Though its approval in the U.S. is recent, vaccines adjuvanted with MF59 have been approved in Europe since 1997. Similar to alum, it is not known why MF59 enhances the immune response, as it does not contain any specific PAMPSs. However, it is suspected that its triggering of inflammasome complexes plays a role in eliciting the response[37]. Also in 2015, the FDA approved the vaccine Bexerso for use in preventing meningitis B infection. Bexsero contains recombinant proteins from *Neisseria meningitidis,* and is adjuvanted with alum as well as outer membrane vesicles derived from *N. meningitidis*[38]. Outer membrane vesicles retain the PAMPs of the bacteria they are derived from, but are non-infectious, making them safe to use without further inactivation. The increase in FDA approved vaccines with diverse adjuvants highlights the impact that adjuvant choice can have on vaccine efficacy.

Outer membrane vesicles: a new class of adjuvants

The FDA approval of Bexsero marked the first time that a vaccine using outer membrane vesicles (OMVs) as an adjuvant was widely available. OMVs are classified as either 'native', where the OMVs are naturally shed off from bacterial membranes, or 'nonnative', where OMVs are synthetically created from bacterial membranes, commonly through sonication or detergent extraction[39,40]. Bexsero contains 'nonnative' OMVs, formed by using detergent to extract them from *N. meningitidis*[41]. Because nonnative OMVs are often formed by sonicating and shearing

bacteria, they contain proteins in their lumen from both the perisplasm and the cytoplasm of the bacteria from which they were derived[39,40]. While nonnative OMV production allows for high batch-to-batch conformity, nonnative OMVs require more downstream processing to produce than native OMVs, which are simply collected from the supernatant in which the bacteria were cultured. These 'native' OMVs, though more variable than nonnative OMVs, also hold potential as a vaccine adjuvant.

Currently, all gram-negative bacteria have been found to produce native OMVs. OMVs are nanoscale vesicles (~50-200 nm) that shed off from the outer membrane of bacteria, without disrupting the outer membrane integrity. Numerous reviews have explored why and how bacteria produce these vesicles[42–45]. OMV production has been found to be upregulated during periods of bacterial stress, such as when bacteria are exposed to increased temperatures, or when they are in the presence of antibiotics. One theory behind OMV production is that it is a method for exporting misfolded proteins; misfolded proteins accumulate in the periplasm prior to being exported within OMVs[46]. OMVs have also been shown to contribute to bacterial pathogenesis; OMVs can keep toxins concentrated over long distances, then penetrate other cells and deliver them. OMV secretion is also associated with the formation of biofilms. Finally, OMV secretion can be used as a method of bacterial quorum sensing. Though native OMV production occurs naturally, gene knockout can be used to increase OMV production. For example, knockout of the gene *new lipoprotein 1 (nlpI)* results in approximately 300x greater vesiculation rates[47]. While OMV production is useful to bacteria, it can also be exploited for use in vaccine production.

One approach to using OMVs in vaccine design is to simply collect native, or create nonnative, OMVs from the pathogen of interest, and then use them to supplement the vaccine

formulation. OMVs offer the advantage of naturally containing many PAMPS, and because OMVs are unable to replicate, there is no need to inactivate them or to treat them with chemicals. However, it should be noted that nonnative OMVs are sometimes produced using detergents and are often treated to remove LPS[48]. In addition to using *N. meningitidis* derived OMVs in a meningitis vaccine, *E. coli* derived OMVs have been explored as a method for generating a vaccine against sepsis and *E. coli* poisoning; *Vibrio cholerae* derived OMVs as a method for preventing cholera; and *Bordetella pertussis* OMVs as a method for preventing whooping cough[49–51]. Though Bexsero combines OMVs with recombinant proteins, theoretically, use of pure OMVs as a vaccine could obviate the need for protein production and purification. Instead, OMVs could just be collected and used without further components to immunize. However, producing OMVs still does require growing up pathogens to collect/produce the OMVs from. Recently though, researchers have begun to engineer OMVs to display recombinant proteins so that working with the actual pathogens is not necessary[52].

Recombinant outer membrane vesicles (rOMVs) use a transmembrane protein to display peptide and protein antigens on the surface of outer membrane vesicles[53]. Currently, rOMVs are primarily produced using different strains of *E. coli* to express and display exogenous antigens, though other strains of gram-negative bacteria could likely be used as well. *E. coli* strains that contain *nlpI* knockouts hypervesiculate, making them excellent candidates for production of native OMVs. Transformation of these hypervesiculating strains with a plasmid encoding a transmembrane protein, cytolysin A (ClyA), followed by an antigen of interest, results in the ClyA-antigen becoming embedded in the outer membrane of *E. coli* and subsequently shed in vesicles (**Figures 1A-C).** [54]. ClyA is a 34 kDa pore forming cytotoxin that is typically only expressed in pathogenic *E. coli* strains grown in anaerobic conditions. ClyA can be secreted in

OMVs, where it typically assembles into an 8 or 13 oligomeric pore complex, capable of causing hemolysis and cytotoxicity[55]. While the exact mechanism for how ClyA is translocated to the outer membrane remains unknown, it has been proven that ClyA does not need to be cytolytic in order to translocate. A cytotoxin-based vaccine platform might not seem like the safest vaccine option; however, Kim et al. demonstrated that genetically fusing an antigen to ClyA eliminated its cytotoxicity, perhaps by preventing oliogmerization into the pore complex from occurring[52]. Kim et al. also demonstrated that when ClyA was genetically fused to green fluorescent protein (GFP), rOMVs were produced that fluoresced, thus suggesting that ClyA could be used to display conformational epitopes on the outside of rOMVs as well as linear epitopes. The ease of DNA recombinant technology means that the plasmid containing ClyA can be quickly modified to insert different protein-based antigens for expression.

rOMVs offer the advantage of not requiring additional adjuvants to create a vaccine; simply suspending ClyA-GFP rOMVs in PBS results in high anti-GFP titers in BALB/c mice (**Figure 1D**)[54]. Unlike most subunit vaccine delivery systems, which require at a bare minimum two components to be mixed together (adjuvant and antigen), rOMVs couple antigen and adjuvant directly. Work in BALB/c mice comparing the immune response to ClyA-GFP rOMVs made in a common lab strain of *E. coli*, JC8031, to GFP adjuvanted with alum, showed that both elicited high levels of anti-GFP IgG antibodies that had approximately equivalent levels of IgG1 and IgG2a. When ClyA-GFP rOMVs were made from a probiotic strain of *E. coli*, *E. coli* Nissle 1917 (Nsl), a similar level of anti-GFP IgG antibodies was produced, but there were significantly more IgG2a antibodies than IgG1, indicating a useful Th1 bias[57]. Further investigation revealed that a cellular response was also elicited when mice were vaccinated with ClyA-GFP Nsl rOMVs. The high titers generated by both JC8031 and Nsl derived rOMVs

indicated that they would make good vaccine adjuvants, with the Th1 biased nature of the immune response to Nsl rOMVs making them a particularly intriguing vaccine platform. However, though the titers and cellular results were promising, GFP is an irrelevant antigen in preventing infectious disease. In order to determine whether rOMVs have potential as a vaccine platform, they need to be engineered to display a pathogen-derived antigen and tested in a challenge model.

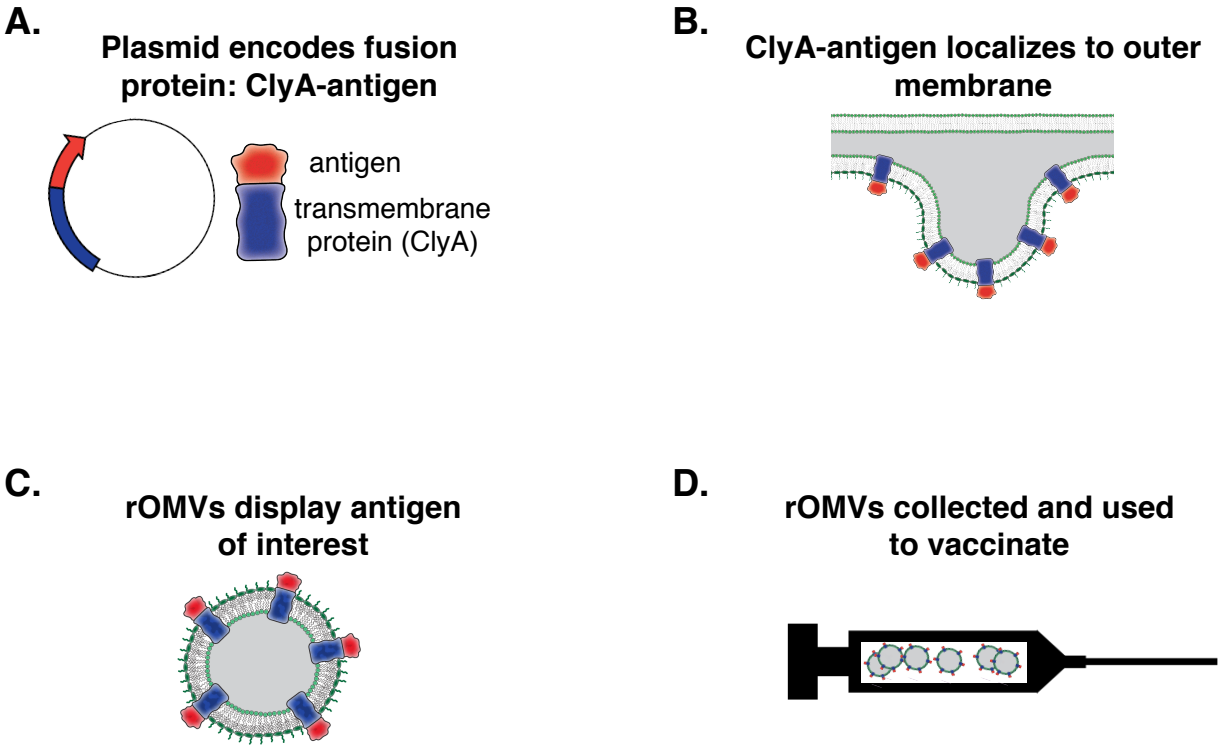

Figure 1:. Process of producing native rOMV vaccines. A.) *E. coli* are transformed with a plasmid encoding a transmembrane protein, ClyA, and an antigen of interest. B.) Transformed *E. coli* start to express ClyA-antigen protein, which translocates to the outer membrane of *E. coli*. The outer membrane of *E. coli* naturally buds off, forming rOMVs. C.) rOMVs are studded with ClyA-antigen. D). rOMVs are collected using a series of centrifugation steps, suspended in PBS, and used as a vaccine.

Influenza: a persisting global health challenge

Annually, 5-10% of adults and 20-30% of children will be infected with seasonal influenza, leading to about 3-5 million severe cases and 250,000-500,000 deaths worldwide[58]. Influenza pandemics can also occur, as happened in 1918, 1957, 1968, and 2009[59]. Though seasonal influenza vaccines exist, influenza's high mutation rate often renders them ineffective. Additionally, seasonal influenza vaccines are ineffective against pandemic strains of influenza. Influenza is a negative sense RNA virus that is a member of the Orthomyxoviridae family and can be divided into 4 types: A, B, C, and D[60]. While both influenza A and B are capable of producing severe disease in humans, only influenza A can cause pandemics.

Influenza A virus (IAV) is an approximately spherical virus (~ 80 -120 nm in diameter) comprised of a bilipid membrane studded with 3 proteins: hemagglutinin (HA), neuraminidase (NA), and transmembrane matrix protein 2 (M2) (**Figure 2**). The HA and NA proteins are used to divide IAV into different subtypes; currently, there are 18 different HA subtypes and 11 different NA subtypes[61]. Matrix 1 protein (M1) forms a layer underneath the lipid membrane to which IAV's ribonucleoproteins (RNP) associate. The RNP complexes are comprised of one of IAV's 8 RNA segments bound to the polymerase (P) proteins PA, PB1, and PB2, as well as to nucleoprotein (NP). Small amounts (130- 200 copies) of nuclear export protein (NEP, also known as NS2) are also located within the virion's core. In addition to these 9 proteins, influenza encodes non-structural protein 1 (NS1), which helps limit host interferon (INF) production, as well as several other proteins (PB1-N40, PA-X, PA-N155, PA-N182, M42, NS3) whose roles are still being defined[62].

IAV initiates cellular infection by binding HA to sialic-acid (SA) containing receptors on cell surfaces[63]. Following binding of HA (which must be cleaved to be infectious), the influenza

virion is endocytosed through receptor mediated endocytosis. The endosome decreases in pH as it progresses through the cell. The decreased endosomal pH activates the M2 ion channel, which starts pumping H^+ ions into the virion's core, causing the RNPs to dissociate from M1. When the endosome pH reaches about 5, HA (cleaved) undergoes a conformational change, allowing a fusion peptide to insert into the endosome's membrane. This results in the endosomal and viral membrane fusing together and the freeing of the viral RNPs. The RNPs travel to the nucleus where the vRNA is transcribed into positive sense mRNA for protein production and is also replicated to make more vRNA. The HA, NA, and M2 proteins are produced in the rough endoplasmic reticulum and then exported to the cell membrane, where they are joined by the cytoplasmically produced nonstructural proteins and vRNA. Complete viruses bud off with assistance from the NA protein, which cleaves SA from the cell's surface[64].

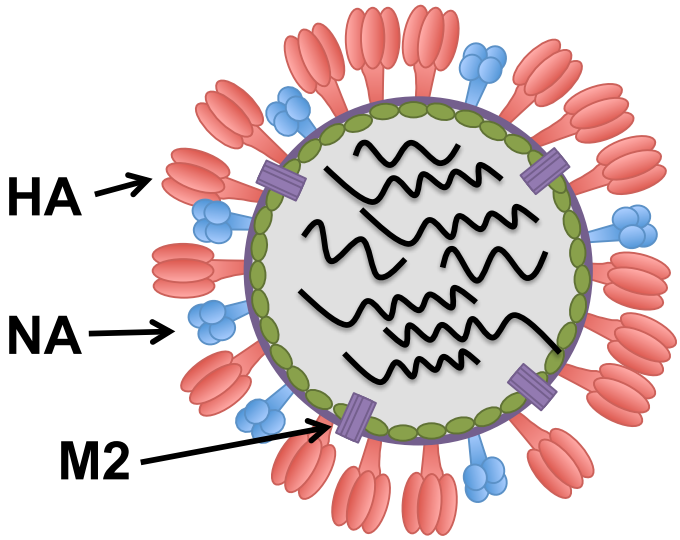

Figure 2: Schematic of influenza virion. Influenza is categorized into subtypes based on the hemagglutinin and neuraminidase type.

Influenza is a difficult pathogen to target through vaccination, due largely to its high mutation rate and ability to form new strains when two different strains co-infect (antigenic drift and shift)[65,66]. Current influenza vaccines work by forming antibodies against prominent external influenza proteins (hemagglutinin and—to a lesser extent—neuraminidase), preventing cellular entry. However, these antibodies are typically not cross strain protective and lose effectiveness as influenza evolves[67]. Thus, it is necessary to develop new influenza vaccines each year. It takes about 6 months to develop a new vaccine, necessitating scientists to predict which strains will be most prevalent before the flu season begins, resulting in vaccines that vary greatly in effectiveness from year to year. Live-attenuated, inactivated, and subunit influenza seasonal vaccines are typically available that are either trivalent (1 strain is influenza B) or quadrivalent (2 strains are influenza B). Some of the inactivated vaccines are mixed with an adjuvant to ensure a sufficient immune response. The live-attenuated influenza vaccine is cold-adapted, only replicating in the cooler nasal passages[66]. While improved adjuvant systems could lead to stronger immune responses being generated by the seasonal flu vaccine, the larger problem is that the antigens being targeted in the seasonal flu vaccine are so variable; even if a seasonal flu vaccine elicits a strong antibody response, that response is useless if it is directed against an irrelevant HA type.

The holy grail of influenza work is to create a 'universal' influenza A vaccine[68–70]. This vaccine would offer protection to both seasonal and pandemic strains of influenza, and would not require annual updates. Creating a single vaccine that protects against even unknown influenza strains requires directing the immune response against highly conserved influenza antigens. One approach has been to generate neutralizing antibodies against the stem of HA, as this portion is more conserved than the head region[71]. However, most of influenza's highly conserved proteins

are located internally, making neutralizing antibodies ineffective. Instead, the vaccine would need to elicit CD8+ T cells to kill the entire influenza infected cell. In humans, influenza specific T cells from one IAV subtype infection help to prevent influenza infection from a different IAV subtype infection[72]. However, anti-HA antibodies from one IAV subtype infection do not typically prevent influenza infection from a different IAV subtype infection. Current influenza vaccines do a poor job at generating cross-reactive T cells, thus, there is need for development of a vaccine that could elicit a T cell response, contributing to clearance of infected cells[73,74].

In addition to CD8+ T cells killing infected cells, ADCC and AMP can also lead to cell death[75]. In this case, the variable region (F_{ab}) of IgG antibodies binds to antigens on the infected cell surfaces and the crystalline region (F_c) binds to F_c receptors on immune cells, such as NK cells and macrophages, triggering cell death via cytokine secretion or phagocytosis. Proteins that are typically hidden on pathogens are sometimes exposed after the pathogen has infected a cell and begun to produce copies of itself. One such protein is the matrix 2 (M2) protein of IAV.

The tetrameric M2 protein of IAV is encoded on influenza's vRNA segment 7 and consists of an N-terminal ectodomain, transmembrane domain, and intracellular C domain[76]. The N-terminal ectodomain (amino acids 2-24) of M2 (M2e) is one of the most conserved regions in human influenza; between 1918 and 2008, nearly all circulating human influenza strains had the same sequence[77]. In 2009, the swine-origin influenza virus contained an avian vRNA 7 segment that encoded 4 amino acid changes in the M2e region, indicating that the region was not completely conserved[78]. Despite these differences, the M2 ectodomain has significantly less variation than HA. This lack of variation is likely due to M2e experiencing less evolutionary pressure (very few antibodies are generated against M2e during infection) and to M2e and M1

both being encoded on the same vRNA (M2 is formed from a spliced version of M1's mRNA). Though M2e is exposed on IAV's surface, it is highly inaccessible to neutralizing antibodies due to the overhanging HA and NA glycoproteins. However, when influenza infects a cell and starts exporting proteins, HA and NA cluster together in lipid rafts on the cell surface, whereas M2 is more dispersed, making it possible for antibodies to bind[79]. The high level of M2e conservation, as well as its exposure on infected cells, suggests it would make an excellent universal influenza vaccine target[77].

The concept to target influenza through M2e has been around for over a decade[80]. In 1999, Neirynck *et al.* demonstrated heterologous protection against mouse adapted influenza strains X47 (H3N2) and PR8 (H1N1) when vaccinating with M2e fused to a hepatitis B virus core protein (along with adjuvants). Since then, numerous animal studies involving M2e have been published, many of which were recently reviewed by Deng *et al*[77]. M2e has been delivered numerous ways using many different constructs. M2e conjugates have been formed using flagella, keyhole limpet protein (KHL), and *Neisseria meningitidis* outer membrane protein complex[81–84]. Additionally, influenza A DNA vaccines have been made that express M2e as well as whole M2. M2e-based vaccines have also been included in several clinical trials. The company Dynavax tested an influenza vaccine comprised of a proprietary TLR9 ligand fused to M2e and NP and found it resulted in strong anti-M2e titers with only mild side effects during a Phase I clinical trial initiated in 2010. However, Dynavax has not published any papers on the vaccine, nor made any press releases about it since then, suggesting that the project may be on hold. Another Phase I clinical trial involving an M2e-based vaccine (ACAM-FLU-A^{TM}), initially showed promising results, with anti-M2e seroconversion rates of 90%, but titers quickly

dropped after 45 days, resulting in Phase II clinical trials not being pursued[77]. Thus, while M2e vaccines show promise, there are still many aspects to be improved.

Possibly, an improved adjuvant system would allow for increased success of M2e-vaccines. The strong adjuvancy of rOMVs, and Th1 biased response of Nsl rOMVs, suggests that they would be a good platform for use in developing an M2e-based vaccine. Additionally, rOMVs naturally contain many of the TLR agonists that other M2e-based vaccines had to add separately, making rOMVs a simpler platform[85]. Finally, modifying the strains of *E. coli* used to produce the rOMVs to have less stimulatory LPS would both eliminate the need to do any post-processing of the rOMVs to remove endotoxin and minimize possible side effects following vaccination. During this dissertation, I will explore ways to use rOMVs to generate M2e-based influenza vaccines with heterosubtypic and long-lasting protection.

References

1. Moturi, EK, Porter, KA, Wassilak, SGF, Tangermann, RH, Diop, OM, Burns, CC, *et al.* (2014). Progress toward polio eradication—worldwide, 2013–2014. *MMWR Morb Mortal Wkly Rep* **63**: 468–472.

2. Hennessey, K, Schluter, WW, Wang, X, Boualam, L, Jee, Y, Mendoza-Aldana, J, *et al.* (2014). Are we there yet? Assessing achievement of vaccine-preventable disease goals in WHO's Western Pacific Region. *Vaccine* **32**: 4259–4266.

3. Hariri, S, Bennett, NM, Niccolai, LM, Schafer, S, Park, IU, Bloch, KC, *et al.* (2015). Reduction in HPV 16/18-associated high grade cervical lesions following HPV vaccine introduction in the United States–2008–2012. *Vaccine* **33**: 1608–1613.

4. Rappuoli, R, Pizza, M, Del Giudice, G and De Gregorio, E (2014). Vaccines, new opportunities for a new society. *Proc. Natl. Acad. Sci.* **111**: 12288–12293.

5. Takahashi, M, Okuno, Y, Otsuka, T, Osame, J and Takamizawa, A (1975). Development of a live attenuated varicella vaccine. *Biken J.* **18**: 25–33.

6. Zepp, F (2010). Principles of vaccine design—lessons from nature. *Vaccine* **28**: C14–C24.

7. Schiller, JT and Lowy, DR (2015). Raising expectations for subunit vaccine. *J. Infect. Dis.* **211**: 1373–1375.

8. Grimm, SK and Ackerman, ME (2013). Vaccine design: emerging concepts and renewed optimism. *Curr. Opin. Biotechnol.* **24**: 1078–1088.

9. Heinsbroek, E and Ruitenberg, EJ (2010). The global introduction of inactivated polio vaccine can circumvent the oral polio vaccine paradox. *Vaccine* **28**: 3778–3783.

10. Hansson, M and Nygren, P (2000). Design and production of recombinant subunit vaccines. *Biotechnol. Appl. Biochem.* **32**: 95–107.

11. Knudsen, NPH, Olsen, A, Buonsanti, C, Follmann, F, Zhang, Y, Coler, RN, *et al.* (2016). Different human vaccine adjuvants promote distinct antigen- independent immunological signatures tailored to different pathogens. *Sci. Rep.* **6**: 19570.

12. Awate, S, Babiuk, LA and Mutwiri, G (2013). Mechanisms of action of adjuvants. *Front. Immunol.* **4**.

13. Ozinsky, A, Underhill, DM, Fontenot, JD, Hajjar, AM, Smith, KD, Wilson, CB, *et al.* (2000). The repertoire for pattern recognition of pathogens by the innate immune system is defined by cooperation between toll-like receptors. *Proc. Natl. Acad. Sci.* **97**: 13766–

13771.

14. Marciani, DJ (2003). Vaccine adjuvants: role and mechanisms of action in vaccine immunogenicity. *Drug Discov. Today* **8**: 934–943.

15. Alving, CR, Peachman, KK, Rao, M and Reed, SG (2012). Adjuvants for human vaccines. *Curr. Opin. Immunol.* **24**: 310–315.

16. Baylor, NW, Egan, W and Richman, P (2002). Aluminum salts in vaccines—US perspective. *Vaccine* **20**: S18–S23.

17. Kool, M, Pétrilli, V, De Smedt, T, Rolaz, A, Hammad, H, van Nimwegen, M, *et al.* (2008). Cutting edge: alum adjuvant stimulates inflammatory dendritic cells through activation of the NALP3 inflammasome. *J. Immunol.* **181**: 3755–3759.

18. Eisenbarth, SC (2008). Crucial role for the Nalp3 inflammasome in the immunostimulatory properties of aluminium adjuvants. *Nature* **453**.

19. Wilson-Welder, JH, Torres, MP, Kipper, MJ, Mallapragada, SK, Wannemuehler, MJ and Narasimhan, B (2009). Vaccine Adjuvants : Current Challenges and Future Approaches. *J. Pharm. Sci.* **98**: 1278–1316.

20. Schijns, VEJC and Degen, WGJ (2007). Vaccine immunopotentiators of the future. *Clin. Pharmacol. Ther.* **82**: 750–5.

21. Del Giudice, G, Podda, A and Rappuoli, R (2001). What are the limits of adjuvanticity? *Vaccine* **20**: 39–42.

22. Blander, JM and Sander, LE (2012). Beyond pattern recognition: five immune checkpoints for scaling the microbial threat. *Nat. Rev. Immunol.* **12**: 215–225.

23. Mosmann, TR and Coffman, RL (1989). TH1 and TH2 cells: different patterns of lymphokine secretion lead to different functional properties. *Annu. Rev. Immunol.* **7**: 145–73.

24. Schwab, I and Nimmerjahn, F (2013). Intravenous immunoglobulin therapy: how does IgG modulate the immune system? *Nat. Rev. Immunol.* **13**: 176–189.

25. (2000). Science commentary: Th1 and Th2 responses: what are they? **321**: 5500.

26. He, W, Tan, GS, Mullarkey, CE, Lee, AJ, Lam, MMW, Krammer, F, *et al.* (2016). Epitope specificity plays a critical role in regulating antibody-dependent cell-mediated cytotoxicity against influenza A virus. *Proc. Natl. Acad. Sci.*: 201609316.

27. HogenEsch, H (2012). Mechanism of immunopotentiation and safety of aluminum adjuvants. *Front. Immunol.* **3**.

28. Vacchelli, E, Galluzzi, L, Eggermont, A, Fridman, WH, Galon, J, Sautès-Fridman, C, *et al.* (2012). Trial watch: FDA-approved Toll-like receptor agonists for cancer therapy. *Oncoimmunology* **1**: 894–907.

29. Hughes, B (2010). 2009 FDA drug approvals. *Nat. Rev. Drug Discov.* **9**: 89–92.

30. Garçon, N, Segal, L, Tavares, F and Van Mechelen, M (2011). The safety evaluation of adjuvants during vaccine development: The AS04 experience. *Vaccine* **29**: 4453–4459.

31. Needham, BD and Trent, MS (2013). Fortifying the barrier: the impact of lipid A remodelling on bacterial pathogenesis. *Nat. Rev. Microbiol.* **11**: 467–81.

32. Garçon, N and Van Mechelen, M (2011). Recent clinical experience with vaccines using MPL- and QS-21-containing adjuvant systems. *Expert Rev. Vaccines* **10**: 471–486.

33. Cluff, CW (2009). Monophosphoryl lipid a (MPL) as an adjuvant for anti-cancer vaccines: Clinical results. *Adv. Exp. Med. Biol.* **667**: 111–123.

34. Brunner, R, Jensen-Jarolim, E and Pali-Schöll, I (2010). The ABC of clinical and experimental adjuvants-A brief overview. *Immunol. Lett.* **128**: 29–35.

35. Fellner, C (2016). Pharmaceutical Approval Update. *Pharm. Ther.* **41**: 26.

36. O'Hagan, DT, Ott, GS, Nest, G Van, Rappuoli, R and Giudice, G Del (2013). The history of MF59 adjuvant: a phoenix that arose from the ashes. *Expert Rev. Vaccines* **12**: 13–30.

37. O'Hagan, DT, Ott, GS, De Gregorio, E and Seubert, A (2012). The mechanism of action of MF59–an innately attractive adjuvant formulation. *Vaccine* **30**: 4341–4348.

38. Carter, NJ (2013). Multicomponent meningococcal serogroup B vaccine (4CMenB; Bexsero®): a review of its use in primary and booster vaccination. *BioDrugs* **27**: 263–274.

39. Kulp, A and Kuehn, MJ (2010). Biological functions and biogenesis of secreted bacterial outer membrane vesicles. *Annu. Rev. Microbiol.* **64**: 163–84.

40. Tavano, R, Franzoso, S, Cecchini, P, Cartocci, E, Aricò, B and Papini, E (2009). The membrane expression of Neisseria meningitidis adhesin A (NadA) increases the proimmune effects of MenB OMVs on human macrophages, compared with NadA– OMVs, without further stimulating their proinflammatory activity on circulating monocytes. *J. Leukoc. Biol.* **86**: 143–153.

41. Frasch, CE, van Alphen, L, Holst, J, Poolman, JT and Rosenqvist, E (2001). Outer membrane protein vesicle vaccines for meningococcal disease. *Meningococcal vaccines methods Protoc.*: 81–107.

42. Kuehn, MJ and Kesty, NC (2005). Bacterial outer membrane vesicles and the host-pathogen interaction. *Genes Dev.* **19**: 2645–55.

43. MacDonald, IA and Kuehn, MJ (2012). Offense and defense: microbial membrane vesicles play both ways. *Res. Microbiol.* **163**: 607–618.

44. Manning, AJ and Kuehn, MJ (2011). Contribution of bacterial outer membrane vesicles to innate bacterial defense Contribution of bacterial outer membrane vesicles to innate bacterial defense **258**.

45. Ellis, TN and Kuehn, MJ (2010). Virulence and immunomodulatory roles of bacterial outer membrane vesicles. *Microbiol. Mol. Biol. Rev.* **74**: 81–94.

46. Bonnington, KE and Kuehn, MJ (2014). Protein selection and export via outer membrane vesicles. *Biochim. Biophys. Acta* **1843**: 1612–9.

47. Schwechheimer, C, Rodriguez, DL and Kuehn, MJ (2015). NlpI-mediated modulation of outer membrane vesicle production through peptidoglycan dynamics in Escherichia coli. *Microbiologyopen* **4**: 375–89.

48. Acevedo, R, Fernández, S, Zayas, C, Acosta, A, Sarmiento, ME, Ferro, VA, *et al.* (2014). Bacterial outer membrane vesicles and vaccine applications. *Front. Immunol.* **5**: 1–6.

49. Asensio, CJA, Gaillard, ME, Moreno, G, Bottero, D, Zurita, E, Rumbo, M, *et al.* (2011). Outer membrane vesicles obtained from Bordetella pertussis Tohama expressing the lipid A deacylase PagL as a novel acellular vaccine candidate. *Vaccine* **29**: 1649–1656.

50. Schild, S, Nelson, EJ and Camilli, A (2008). Immunization with Vibrio cholerae outer membrane vesicles induces protective immunity in mice. *Infect. Immun.* **76**: 4554–4563.

51. Kim, OY, Hong, BS, Park, KS, Yoon, YJ, Choi, SJ, Lee, WH, *et al.* (2013). Immunization with Escherichia coli outer membrane vesicles protects bacteria-induced lethality via Th1 and Th17 cell responses. *J. Immunol.* **190**: 4092–102.

52. Kim, JY, Doody, AM, Chen, DJ, Cremona, GH, Shuler, ML, Putnam, D, *et al.* (2008). Engineered bacterial outer membrane vesicles with enhanced functionality. *J. Mol. Biol.* **380**: 51–66.

53. Rosenthal, JA, Leung, T, DeLisa, M and Putnam, DA (2013). Low-dose recombinant

vaccine antigen delivery by engineered outer membrane vesicles. *Nano Life* **3**: e1342002.

54. Chen, DJ, Osterrieder, N, Metzger, SM, Buckles, E, Doody, AM, DeLisa, MP, *et al.* (2010). Delivery of foreign antigens by engineered outer membrane vesicle vaccines. *Proc. Natl. Acad. Sci. U. S. A.* **107**: 3099–104.

55. Wai, SN, Lindmark, B, Söderblom, T, Takade, A, Westermark, M, Oscarsson, J, *et al.* (2003). Vesicle-mediated export and assembly of pore-forming oligomers of the enterobacterial ClyA cytotoxin. *Cell* **115**: 25–35.

56. del Castillo, FJ, Moreno, F and del Castillo, I (2001). Secretion of the Escherichia coli K-12 SheA hemolysin is independent of its cytolytic activity. *FEMS Microbiol. Lett.* **204**: 281–285.

57. Rosenthal, JA, Huang, C, Doody, AM, Leung, T, Mineta, K, Feng, DD, *et al.* (2014). Mechanistic insight into the Th1-biased immune response to recombinant subunit vaccines delivered by probiotic bacteria-derived outer membrane vesicles. *PLoS One* **9**: e112802.

58. World Health Organization (2014). Seasonal Influenza Fact Sheetat <http://www.who.int/mediacentre/factsheets/fs211/en/>.

59. Centers for Disease Control and Prevention (U.S.) (2014). CDC Resources for Pandemic Fluat <http://www.cdc.gov/flu/pandemic-resources/index.htm>.

60. Ferguson, L, Eckard, L, Epperson, WB, Long, L-P, Smith, D, Huston, C, *et al.* (2015). Influenza D virus infection in Mississippi beef cattle. *Virology* **486**: 28–34.

61. Wu, Y, Wu, Y, Tefsen, B, Shi, Y and Gao, GF (2014). Bat-derived influenza-like viruses H17N10 and H18N11. *Trends Microbiol.* **22**: 183–191.

62. Vasin, a V, Temkina, O a, Egorov, V V, Klotchenko, S a, Plotnikova, M a and Kiselev, OI (2014). Molecular mechanisms enhancing the proteome of influenza A viruses: an overview of recently discovered proteins. *Virus Res.* **185**: 53–63.

63. Bender, BS and Small Jr, PA (1992). Influenza: pathogenesis and host defense. *Semin. Respir. Infect.* **7**: pp 38–45.

64. Compans, RW and Editors, MBAO. *Influenza Pathogenesis and Control - Volume I Current Topics in Microbiology* **I**.

65. Medina, RA and García-Sastre, A (2011). Influenza A viruses: new research developments. *Nat. Rev. Microbiol.* **9**: 590–603.

66. Demicheli, V, Jefferson, T, Al-Ansary, L, Ferroni, E, Rivetti, A and Di Pietrantonj, C

(2014). Vaccines for preventing influenza in healthy adults (Review). *Cochrane Libr.*: 1–263.

67. Lambert, L and Fauci, A (2010). Influenza vaccines for the future. *N. Engl. J. Med.* **363**: 2036–2044.

68. Wang, L, Zhang, H and Compans, RW (2013). Universal Influenza Vaccines - A Short Review: 13–17.

69. Fiers, W, De Filette, M, Birkett, A, Neirynck, S and Min Jou, W (2004). A "universal" human influenza A vaccine. *Virus Res.* **103**: 173–176.

70. Rudolph, W and Ben Yedidia, T (2011). A universal influenza vaccine: where are we in the pursuit of this "Holy Grail"? *Hum. Vaccin.* **7**: 10–11.

71. Krammer, F, Palese, P and Steel, J (2014). Advances in universal influenza virus vaccine design and antibody mediated therapies based on conserved regions of the hemagglutinin. *Influ. Pathog. Control. II*, Springer: pp 301–321.

72. Grant, EJ, Chen, L, Quiñones-parra, S, Pang, K, Kedzierska, K and Chen, W (2014). T-Cell Immunity to Influenza A Viruses. *Crit. Rev. Immunol.* **34**: 15–39.

73. Schotsaert, M, Ibañez, LI, Fiers, W and Saelens, X (2010). Controlling influenza by cytotoxic T-cells: calling for help from destroyers. *J. Biomed. Biotechnol.* **2010**: e863985.

74. Sridhar, S, Begom, S, Bermingham, A, Hoschler, K, Adamson, W, Carman, W, *et al.* (2013). Cellular immune correlates of protection against symptomatic pandemic influenza. *Nat. Med.* **19**: 1305–12.

75. Jegaskanda, S, Vandenberg, K, Laurie, KL, Loh, L, Kramski, M, Winnall, WR, *et al.* (2014). Cross-reactive influenza-specific antibody-dependent cellular cytotoxicity in intravenous immunoglobulin as a potential therapeutic against emerging influenza viruses. *J. Infect. Dis.* **210**: 1811–22.

76. Lamb, RA and Choppin, PW (1981). Identification of a second protein (M2) encoded by RNA segment 7 of influenza virus. *Virology* **112**: 729–737.

77. Deng, L, Cho, JK, Fiers, W and Saelens, X (2015). M2e-Based Universal Influenza A Vaccines. *Vaccines* **3**.

78. Zhou, C, Zhou, L and Chen, YH (2012). Immunization with high epitope density of M2e derived from 2009 pandemic H1N1 elicits protective immunity in mice. *Vaccine* **30**: 3463–3469.

79. Rossman, J and Lamb, R (2011). Influenza virus assembly and budding. *Virology* **411**: 229–236.

80. Neirynck, S, Deroo, T, Saelens, X, Vanlandschoot, P, Jou, WM and Fiers, W (1999). A universal influenza A vaccine based on the extracellular domain of the M2 protein. *Nat. Med.* **5**: 1157–1163.

81. De Filette, M, Ysenbaert, T, Roose, K, Schotsaert, M, Roels, S, Goossens, E, *et al.* (2011). Antiserum against the conserved nine amino acid N-terminal peptide of influenza a virus matrix protein 2 is not immunoprotective. *J. Gen. Virol.* **92**: 301–306.

82. Wibowo, N, Hughes, FK, Fairmaid, EJ, Lua, LHL, Brown, LE and Middelberg, APJ (2014). Protective efficacy of a bacterially produced modular capsomere presenting M2e from influenza: extending the potential of broadly cross-protecting epitopes. *Vaccine* **32**: 3651–5.

83. Turley, CB, Rupp, RE, Johnson, C, Taylor, DN, Wolfson, J, Tussey, L, *et al.* (2011). Safety and immunogenicity of a recombinant M2e-flagellin influenza vaccine (STF2.4xM2e) in healthy adults. *Vaccine* **29**: 5145–52.

84. Karpova, O, Nikitin, N, Chirkov, S, Trifonova, E, Sheveleva, A, Lazareva, E, *et al.* (2012). Immunogenic compositions assembled from tobacco mosaic virus-generated spherical particle platforms and foreign antigens. *J. Gen. Virol.* **93**: 400–407.

85. Kaparakis-Liaskos, M and Ferrero, RL (2015). Immune modulation by bacterial outer membrane vesicles. *Nat. Rev. Immunol.* **15**: 375–387.

CHAPTER 2

RECOMBINANT M2E OUTER MEMBRANE VESICLE VACCINES PROTECT AGAINST INFLUENZA A CHALLENGE IN BALB/C MICE

Introduction

Influenza remains a significant source of morbidity and mortality throughout the world, despite the availability of seasonal vaccines. Each year, 5-10% of adults and 20-30% of children are infected with seasonal influenza, leading to 3-5 million severe cases and 250,000-500,000 deaths worldwide [1]. Additionally, influenza A viruses have the potential to form pandemic strains via cross-species reassortment, as evidenced by the 1918 (Spanish flu), 1957 (Asian flu), 1968 (Hong Kong flu), and 2009 (swine-origin flu) pandemics, presenting a threat to global health [2]. Current influenza vaccines primarily target the immune response against the immunodominant—but hyper variable—glycoproteins hemagglutinin (HA), and to a lesser extent, neuraminidase (NA), necessitating annual development of strain-specific vaccines [3]. Accordingly, there is great public and scientific interest in the creation of a universal influenza A vaccine to obviate or reduce the need for yearly vaccination and to protect against pandemic strains [4,5].

One promising target antigen for a universal vaccine is M2e, the ectodomain of the influenza A matrix protein 2 (M2), a homotetrameric ion channel with roles in viral entry and budding, first explored as a vaccine target by Richardson et al. in 1985 [6]. M2e demonstrates remarkable conservation of its 23 amino acid sequence, especially among influenza A viruses of the same host restriction. This high conservation has been attributed to M2e's genetic relationship with M1–an integral structural protein–and the lack of selective pressure against M2e due to M2e's low virion presence and immunogenicity [7]. Although steric hindrance from HA and NA limits antibody recognition of M2e upon the virion surface, exposed M2e is

abundantly displayed on the membranes of infected epithelial cells [8]. Therefore, while anti-M2e antibodies are unable to neutralize the virus directly, they facilitate clearance of infected cells via antibody dependent cell-mediated cytotoxicity (ADCC) and phagocytosis (ADCP) [9,10].

During influenza infection, ADCC and ADCP are performed by alveolar macrophages and natural killer (NK) cells that recognize the Fc regions of antigen-bound antibodies and display selective efficacy with respect to antibody isotype [11]. It has been previously shown that IgG2a isotype antibody levels, associated with a Th1 type immune response in mice, correlate significantly with enhanced survival against influenza challenge for M2e-based vaccines [10,12]. Therefore, M2e-based vaccines have aimed to generate Th1-biased responses in an effort to improve protective efficacy. However, many methods that generate a Th1 bias require supplementation with viral components or cost-prohibitive adjuvants [13–16]. Here, we utilize a recently developed adjuvant system, recombinant outer membrane vesicles (OMVs), to elicit preferential production of IgG2a antibodies against M2e without addition of viral components or soluble adjuvant.

OMVs are nanoparticles naturally produced by gram-negative bacteria with complex adjuvant profiles that are parent strain dependent and can promote a robust Th1-biased response when designed accordingly [17,18]. Furthermore, OMVs can be engineered to display recombinant heterologous proteins by transforming hypervesiculating (*ΔnlpI*) strains of *E. coli* with a plasmid encoding the transmembrane protein ClyA followed by the antigen of interest [19,20]. Previously, we have shown that OMVs derived from the probiotic *E. coli* strain Nissle 1917 (EcN) carrying a model antigen, green fluorescent protein (GFP), promoted a Th1-biased response directed against GFP [18]. Here, we demonstrate that the display of M2e-based peptides on the surface of OMVs derived from EcN generate high levels of IgG2a antibodies—indicative of a Th1 bias—

and protect against a lethal challenge with influenza A virus. To ascertain the influence of the innate immune system on the observed response, the agonist activity of OMVs on toll like receptors (TLR) was quantified to help understand the mechanisms through which the OMVs function as an adjuvant.

Methods

Plasmid and expression vector design

M2e-based genetic sequences were cloned into a pBAD 18-CM plasmid containing transmembrane protein ClyA, as previously described [19]. Briefly, three M2e-based genetic sequences with a terminal histidine-tag were designed and codon optimized for *E. coli* (GeneArt service, LifeTechnologies, Waltham, U.S.) (**Figure 1BC, SI**). Gene blocks were inserted into a pBAD18-CM vector directly 3' terminal to the ClyA-encoding region.

OMV production and characterization

OMVs were prepared as previously described [18,20]. Briefly, *E. coli* Nissle 1917 ΔnlpI (EcN) cultures transformed with appropriate plasmid were grown overnight, subcultured to OD_{600} = 0.08 in Miller LB broth (ThermoFisher Scientific, Waltham, U.S.), grown to mid-log phase, then induced with 0.2% L-arabinose (Sigma-Aldrich, St. Louis, U.S.) (**Figure 1A**). Cultures were grown at 37˚C for 18 hours, centrifuged (5000x g, 4 °C, 15 min) to pellet bacteria, then sterile filtered (0.2 μM). OMVs were isolated from the filtrate by ultracentrifugation (26k rpm, 4 °C, 3h) and suspended in PBS. Total protein concentration was determined by Pierce BCA Protein Assay (ThermoFisher Scientific, Waltham, U.S.) and antigenic content was measured by Western Blot with anti-His6x primary antibody (Sigma-Aldrich, St. Louis, U.S.). Previous work provides detailed analyses of the proteins and sugars present within EcN OMVs [18].

Immunization

Female BALB/c mice (Jackson Laboratories, Bar Harbor, U.S.) were immunized subcutaneously with 100 μL of vaccine at age 8-weeks. Treatment groups M2e1xC-OMV (n=5), M2e1xS-OMV

(n=12), and M2e4xHet-OMV (n=12) received 40 μg total protein of OMVs containing ~0.2 μg total M2e antigen in PBS. Group M2e1xS with alum (n=12) received 1 μg M2e1xS peptide (NH2-SLLTEVETPIRNGSRSNDSSD-COOH, Lifetein, Somerset, U.S.) in PBS adsorbed to 2% Alhydrogel® (Invivogen, San Diego, U.S.) at a 1:1 [v/v] ratio. A sham vaccination group received only PBS (n=12). Prime and boost doses were administered 4 weeks apart. Blood was collected 1-2 days before the prime dose and every 2 weeks following. For passive transfer experiments, five 8-week old female BALB/c mice were immunized intraperitoneally (ip) with 100 μL pooled serum diluted to 500 μL in PBS collected 2 weeks prior to challenge from M2e4xHet-OMV (n=5), PR8 pre-exposed (n=5), or sham PBS (n=5) vaccinated mice. Blood was collected 24h post ip injection and analyzed via ELISA to ensure successful antibody transfer. All mouse work was conducted according to protocols approved by Cornell's Institutional Animal Care and Use Committee (IACUC).

Influenza challenge

A/Puerto Rico/8/1934 (PR8) virus (BEI Resources, Manassas, U.S) was diluted in PBS and administered via intranasal injection of 50 μL PBS under isofluorane anesthesia. Mice immunized via PR8 exposure (pre-exposed mice) were administered a sub lethal dose of 5 fluorescence forming units (FFU) PR8 virus at age 8 weeks. M2e1xC-OMV (n=5), M2e1xS-OMV (n=4), M2e4xHet-OMV (n=8), M2e1xS with alum (n=4), sham (PBS) vaccination (n=9), and pre-exposed (n=13) cohorts received a lethal dose (50 FFU) 10 weeks post initial exposure or vaccination. For passive transfer experiments, 8-wk old mice received 50 FFU PR8 24h post passive transfer. Weight loss greater than 30% or signs of severe distress were used as euthanasia criteria.

Viral load quantification via Fluorescence Forming Unit (FFU) assay

Day 6 following PR8 challenge, mice were sacrificed from sham, M2e4xHet-OMV, and pre-exposed groups (n=3/group) and their lungs and trachea isolated and homogenized. Homogenates were centrifuged at 5000x g for 10 minutes at 4˚C, filtered (0.2 μm), and stored at -80˚C. For FFU assay, sample aliquots were diluted into MEM media containing 0.2% BSA and activated with TPCK Trypsin at 37˚C (1 μg/ml) for 20 minutes then deactivated with soybean trypsin inhibitor (8.4 μg/ml) (Corning, Tewksbury, U.S.). Samples were serially diluted, 100 μL loaded into 96-well plates with confluent layers of MDCK cells, and incubated for 24 hours. Cells were stained with mouse anti-nucleoprotein from hybridoma H16-L10-495 (ATCC, Manassas, U.S.) and Hoechst (ThermoFisher Scientific, Waltham, U.S.) then imaged as described previously [21]. FFU/mL was back-calculated from the number of infected cells at the lowest infected dilution.

Enzyme-linked immunosorbent assay (ELISA)

ELISAs were conducted on serum samples as previously described, with the modification that plates were coated with 2 μg/mL M2e1xC peptide in PBS at 37 °C overnight [18]. Antibody titer was defined as the reciprocal of the greatest dilution at which the OD_{450} of vaccinated serum exceeded the OD_{450} of pre-vaccinated serum plus 3 standard deviations. The lowest titer detectable by ELISA was 1:500, owing to high background at higher concentrations.

Toll-like receptor (TLR) ligand activity assay

TLR panel using HEK-Blue KD-TLR 5 cells (Invivogen, San Diego, U.S.) was conducted as described for HEK293 cells [18]. Briefly, $1.5x10^5$ cells/well were seeded in 96-well plates and

transfected using TransIT-LT1 (Mirus, Madison, U.S.) with plasmids encoding human or mouse TLRs (TLR2, TLR3, TLR4 and MD2, TLR5, TLR7, TLR8, TLR9, mTLR2, mTLR3, mTLR4 and mMD2, mTLR9, mTLR11), CMV-β-galactosidase and 5xNF-κB-luciferase. After 24 h, cells were stimulated with 4xM2eHet-OMVs (10 ng/mL), positive control (TLR1/2: Pam3Cys, 1 μg/mL; TLR3: poly(I:C), 1 μg/mL; TLR4: LPS, 100 ng/mL; TLR5 and TLR11: flagellin from *S. typhimurium*, 100 ng/mL; TLR7: loxoribine, 100 μM, TLR9: CpG 10104, 3 μM (Invivogen, San Dieogo, U.S.) or PBS for 18h. Media was then removed, reporter lysis buffer, 100 μL/well, (Promega, Madison, U.S.) added, and cells mechanically lysed. Lysate (20 μL/well) was added to opaque 96-well plates and relative light units (RLUs) quantified using a Veritas luminometer (Promega, Madison, U.S.) through addition of 100 μL D-luciferin substrate per well. 4xM2eHet-OMV TLR5 stimulation was further confirmed using the same method with HEK293 cells (**Figure S1**).

Statistics

Antibody titers are reported as geomean titers (GMT) with error bars representing 95% confidence intervals. Comparisons between IgG1 and IgG2a titers use a paired 2-tailed t-test on log-transformed samples. Luciferase levels of PBS vs. M2e4xHet-stimulated cells in TLR panel are compared using a two-tailed t-test. Kaplan-Meier survival curves analyzed using log-rank test with Bonferroni-corrected alpha to account for multiple comparisons. Anti-M2e titer vs. percent weight loss was analyzed using a linear regression model in which the natural log of the titer was plotted against the maximum percent weight loss each mouse experienced during the challenge. All statistical analyses were conducted using Prism6 software (GraphPad software, La Jolla, U.S.).

Results

Production of OMVs containing M2e derived peptides

Three M2e-based OMV vaccines were designed and produced to determine the effect of antigen choice upon immunogenicity and protective efficacy (**Figure 1BC**). Here, we designed OMVs that display the most common human-type influenza A virus M2e antigen (M2e1xC-OMVs) as well as its serine analog (M2e1xS-OMVs). The native cysteines of M2e (C17 and C19) are frequently substituted with serines to prevent disulfide bond formation and aggregation, which may inhibit function or expression, though we did not encounter any difficulties in expression [22]. Additionally, while M2e is highly conserved amongst influenza A strains that infect a common host, M2e is divergent across host restrictions [23]. Recently, the Kang group showed improved immune recognition of broadly divergent influenza A strains by vaccination with a 5xM2e tandem construct containing heterologous host-restricted epitopes [24,25]. Therefore, a 4x multimeric construct (M2e4xHet-OMVs) consisting of the serine analogs of human, swine, and two avian influenza A restricted M2e variants—connected by flexible (G_3SG_3) linkers to provide epitope separation—was produced (**Figure 1BC**). Successful expression and localization of ClyA-M2e fusion proteins in OMVs was confirmed via Western blot of isolated vesicles (**Figure 1D**). TEM images of EcN-derived M2e-OMVs showed they were in the expected size range of 50-100 nm in diameter and consistent with native OMVs (**Figure 1E**).

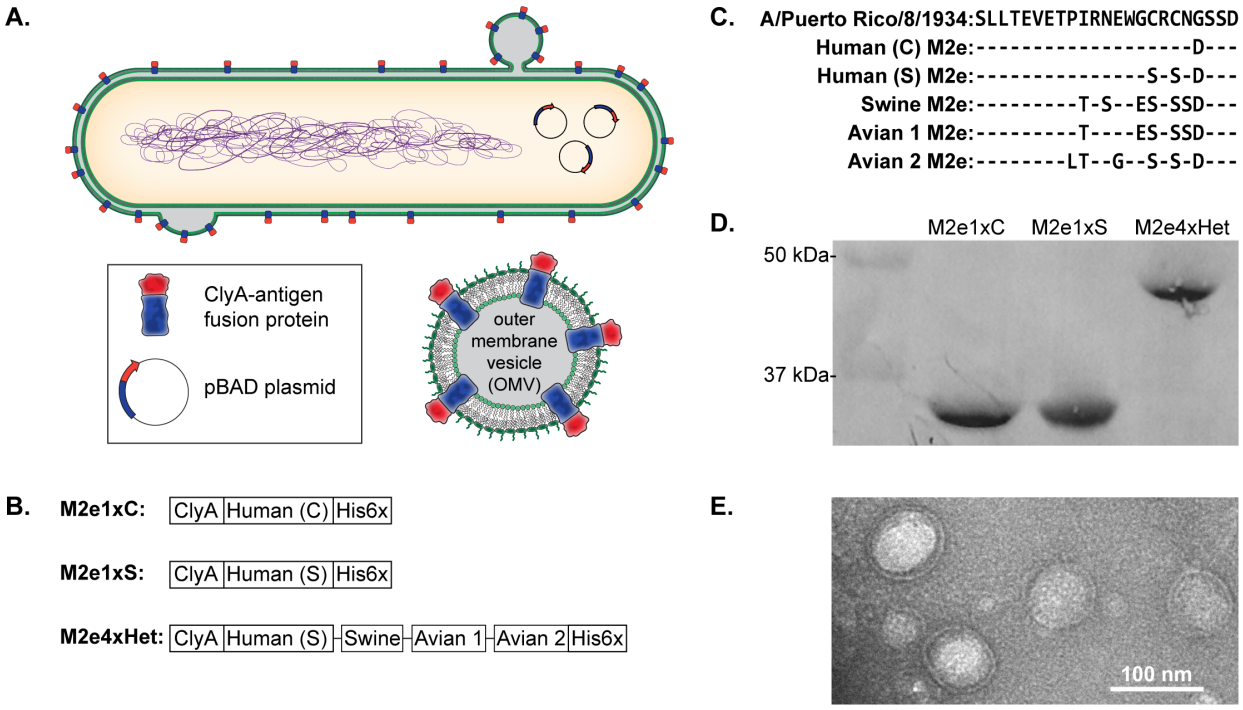

Figure 1: A: Hypervesiculating *E. coli* strain Nissle 1917 Δ*nlpI* was transformed with a pBAD plasmid that encodes transmembrane protein ClyA followed by an M2e-based antigen, resulting in production of outer membrane vesicles (OMVs) that display the desired antigen. **B.** Three ClyA-M2e constructs terminated by a 6x histidine-tag were expressed in *E. coli:* M2e1xC, M2e1xS, and M2e4xHet. M2e1xC contains a common human restriction M2e variant, M2e1xS contains the serine analog to M2e1xC, and M2e4xHet contains the serine analog to M2e1xC, along with the serine analogs to a common swine restricted M2e variant and two avian restricted variants. **C.** M2e contains several variants, largely dependent on host restriction. The sequence of M2e in the virus used for challenged, A/Puerto Rico/8/1934 (PR8), along with the sequences of M2e used to create M2e-based constructs (Human (C), Human (S), Swine, Avian (1), and Avian (2)) are listed. **D.** Western blot of M2e-OMV constructs demonstrates that M2e1xC, M2e1xS, and M2e4xHet are present in OMVs (5 μg total protein/well, anti-His antibody). **E.** Transmission electron microscopy (TEM) images of OMVs show polydispersed particles ranging approximately 50-100 nm in diameter (uranyl acetate staining).

M2e-OMV vaccination leads to high IgG titers

M2e1xC-OMV, M2e1xS-OMV, and M2e4xHet-OMV vaccinated mice all developed high and statistically equivalent anti-M2e IgG titers 8 weeks post initial vaccination that were all significantly higher than those of the M2e1xS alum cohort (**** $p<0.0001$) (**Figure 2A**). Mice that were pre-exposed to a low dose of PR8 also developed high titers that were significantly higher than the M2e1xS alum cohort (** $p<0.01$). Despite a 5x mole excess in M2e content compared to M2e1xS-OMVs, the M2e1xS peptide adsorbed to alum was unable to generate a robust immune response.

Serum from vaccinated mice was further assessed to compare the IgG2a:IgG1 ratio. IgG2a isotype antibodies, associated with a Th1 type immune response, are the proposed correlate of protection for M2e-based vaccines and are necessary and sufficient for protection [10,12]. All three M2e-OMV groups showed a significant elevation in IgG2a titers over IgG1 titers (* $p<0.05$) (**Figure 2B**), as did the cohort pre-exposed to PR8 (** $p<0.01$). This elevated IgG2a:IgG1 ratio is of particular significance as it occurred in BALB/c mice, which are naturally biased toward a Th2 response with higher IgG1 levels than IgG2a [26]. Additionally, no supplementation with additional extrinsic adjuvants, such as MPL or RNA and viral components, was required to generate this isotype distribution [27–29].

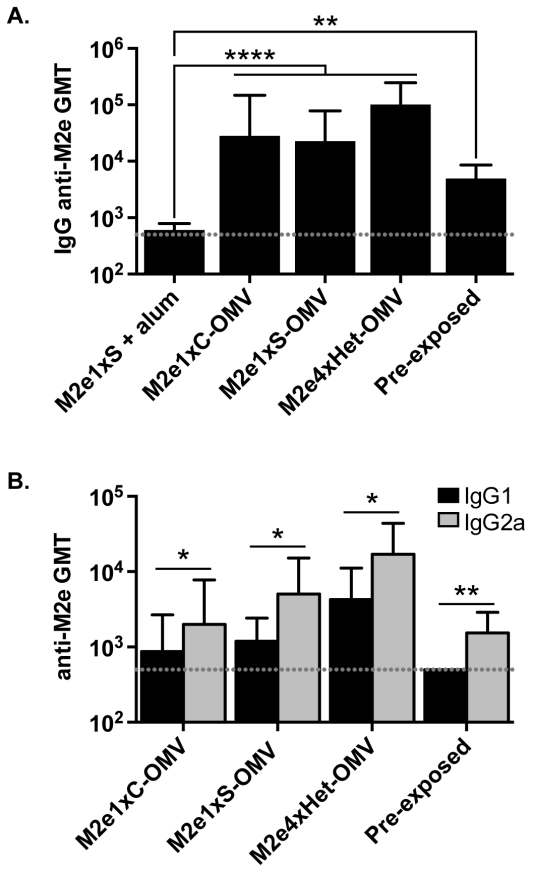

Figure 2: Mouse serum was analyzed for anti-M2e titers 8 weeks post initial vaccination. Dotted line represents lowest titer detectable above background. **A.** All three M2e-OMV vaccines yielded an IgG titer higher than that of M2e1xS peptide with alum (****$p<0.0001$). IgG titers from M2e1xC-OMVs, M2e1xS-OMVs, and M2e4xHet-OMVs did not have any statistical difference ($p>0.05$). Additionally, pre-exposed mice developed titers that were significantly higher than M2e1xS + alum (**$p<0.01$). Log transformed titers were analyzed using a one-way ANOVA followed by multiple comparisons that were corrected by Tukey's test. **B.** All M2e-OMV vaccines resulted in statistically elevated titers of IgG2a relative to IgG1, indicating a Th1 bias (*$p<0.05$). As expected the Th1 bias from mice pre-exposed to PR8 was especially robust (**$p<0.01$). The serum from mice vaccinated with M2e1xS with alum could not be analyzed for IgG1 vs. IgG2a titers as it was beneath the range of the ELISA assay. Log transformed IgG1 and IgG2a titers were compared in paired, 2-tailed t-tests. All graphs display geomean titers (GMT) with error bars that represent 95% confidence intervals. Data analyzed using Prism6 software.

M2e-OMV vaccines protect BALB/c mice from influenza A challenge

M2e4xHet-OMVs provided the best protection against PR8 with 100% survival post challenge (**Figure 3AB**). Additionally, the average lung and trachea viral titer of M2e4xHet-OMV vaccinated mice was approximately 10-fold lower than that of the sham (PBS) control at day 6 post challenge (**Figure 3C**). All sham (PBS) control mice succumbed to infection by day 10 post-challenge, confirming a lethal challenge dose. As titer data predicted, M2e1xS with alum mice fared poorly, with only 25% survival (1/4). Responses to vaccination with M2e1xC-OMVs and M2e1xS-OMVs were comparable, with 40% (2/5) survival and 50% survival (2/4) respectively. Survival analysis demonstrated that only M2e4xHet-OMVs provided better protection than that of the sham (PBS) vaccine ($p<0.01$) (**Figure 3B**).

M2e4xHet-OMV vaccinated mice showed the least morbidity of the vaccinated groups, with an average body weight loss of 14% (**Figure 3A**). Though the M2e4xHet mice showed greater weight loss than the pre-exposed mice, this result is expected, as M2e-based vaccines are infective permissive, requiring Fc-dependent clearance of infected cells by the innate immune system for protection [10]. Linear regression analysis of log transformed anti-M2e total IgG titers vs. the lowest percent original weight yielded a significant relationship ($r^2=0.403$, $p<0.05$) (**Figure 3D**). The literature suggests IgG2a is a correlate of protection for M2e; therefore, we next analyzed IgG2a vs. lowest percent original weight and found an even stronger relationship ($r^2= 0.477$, $p<0.01$) (**Figure 3F**), whereas IgG1 titers vs. lowest percent original weight did not have a significant relationship ($r^2=0.228$, $p>0.05$) (**Figure 3E**) [10,12,30].

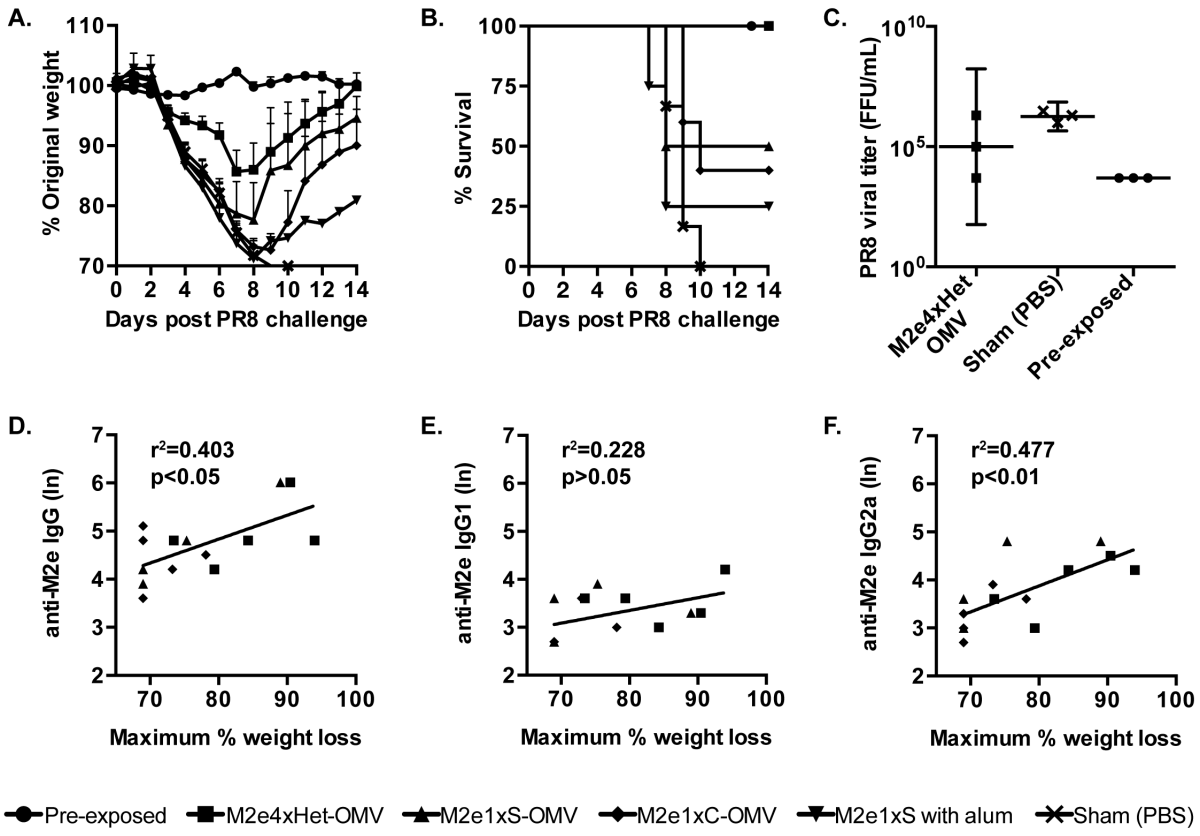

Figure 3: Mice were challenged with a lethal dose (50 FFU) of mouse adapted influenza A virus PR8 10 weeks after prime vaccine dose. Mortality (**A**) and morbidity (**B**) graphs show that different vaccines resulted in different levels of protection. As expected, all pre-exposed mice survived challenge and all sham vaccinated (PBS) mice died/required euthanasia. Mice that received the M2e4xHet-OMV vaccine fared best, with the highest survival rate (100%) and the least weight loss (apart from pre-exposed). Mice vaccinated with M2e1xS with alum fared worst, 25% survival, and M2e1xS-OMV and M2e1xC-OMV vaccinated mice fared intermediately, 50% and 40% survival respectively. Error bars represent standard error of the mean. **C.** PR8 viral titer from lungs and tracheas excised on day 6 of challenge for M2e4xHet-OMV, exposure-immunized, and sham PBS injection. **D-E.** Linear regression of anti-M2e IgG (**D**) IgG1 (**E**) and IgG2a (**F**) log transformed titers vs. minimum percent original weight of OMV-immunized mice during PR8 challenge. The highest significance was found for IgG2a, followed by that for IgG. IgG1 did not correlate significantly with weight loss.

M2e-OMVs stimulate multiple toll like receptors (TLRs)

Following the success of M2e4xHet-OMVs in PR8 challenge, their impact on TLR signaling was explored. TLR stimulation is important to drive an appropriate innate immune response against an antigen [31]. HEK293 TLR5 KD cells were transfected with human and murine TLRs and stimulated with M2e4xHet-OMVs. Comparable TLR stimulation patterns were found for both mouse and human TLRs, suggesting these OMVs would have similar adjuvant potency in humans and mice. The most predominantly activated TLRs were TLR1/2, mTLR1/2, TLR4, mTLR4, and TLR5 (**Figure 4**) (* $p<0.0001$). TLR9 and mTLR9 were activated to a lesser extent ($^{\#}$ $p<0.01$), suggesting a possible contribution to the innate immune response through these receptors. DNA is commonly found in OMVs, making it likely that the TLR9 stimulation was due to low levels of CpG DNA [32].

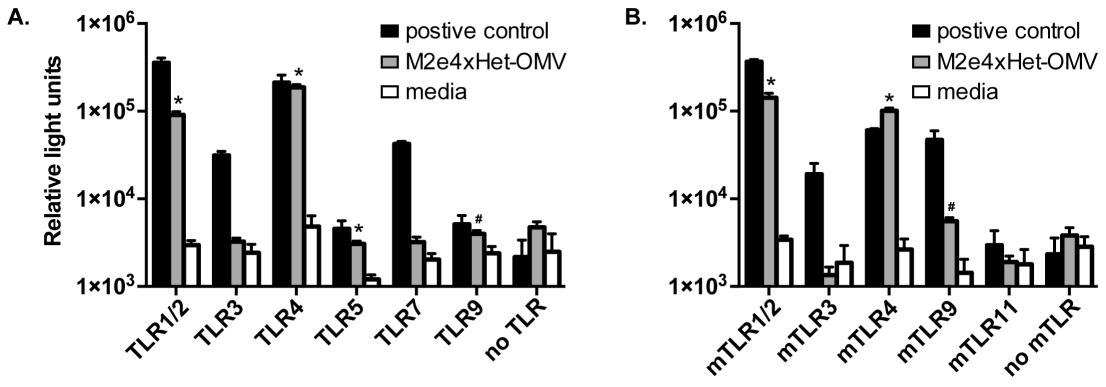

Figure 4: The toll like receptor (TLR) response to M2e4xHet-OMVs was analyzed using both human (**A**) and murine (**B)** TLRs. OMVs primarily stimulated TLR1/2, TLR4, TLR5, mTLR1/2 and mTLR4 (*$p<0.0001$), and to a lesser extent, TLR9 and mTLR9 ($^{\#}p<0.01$). Media vs. M2e4xHet-OMV stimulated luciferase production was compared using a 2-tailed t-test. Error bars represent standard deviation of the mean.

Passive transfer of serum protects against influenza A challenge

Consistent with previous reports of M2e mechanism of protection, passive transfer of serum from M2e4xHet-OMV vaccinated mice provided complete protection (100% survival) against subsequent lethal PR8 challenge (**Figure 5A**) [10,16,33,34]. However, greater weight loss—25% versus 14%—occurred in the passive transfer vaccinated mice vs. M2e4xHet-OMV vaccinated mice. This may be due to the reduced concentration of antibodies in passively immunized mice, which had an anti-M2e IgG GMT titer of 24,000, as opposed to 102,000 in M2e4xHet vaccinated mice, which is consistent with the anti-M2e IgG titer vs. percent weight loss correlation **(Figure 3D**).

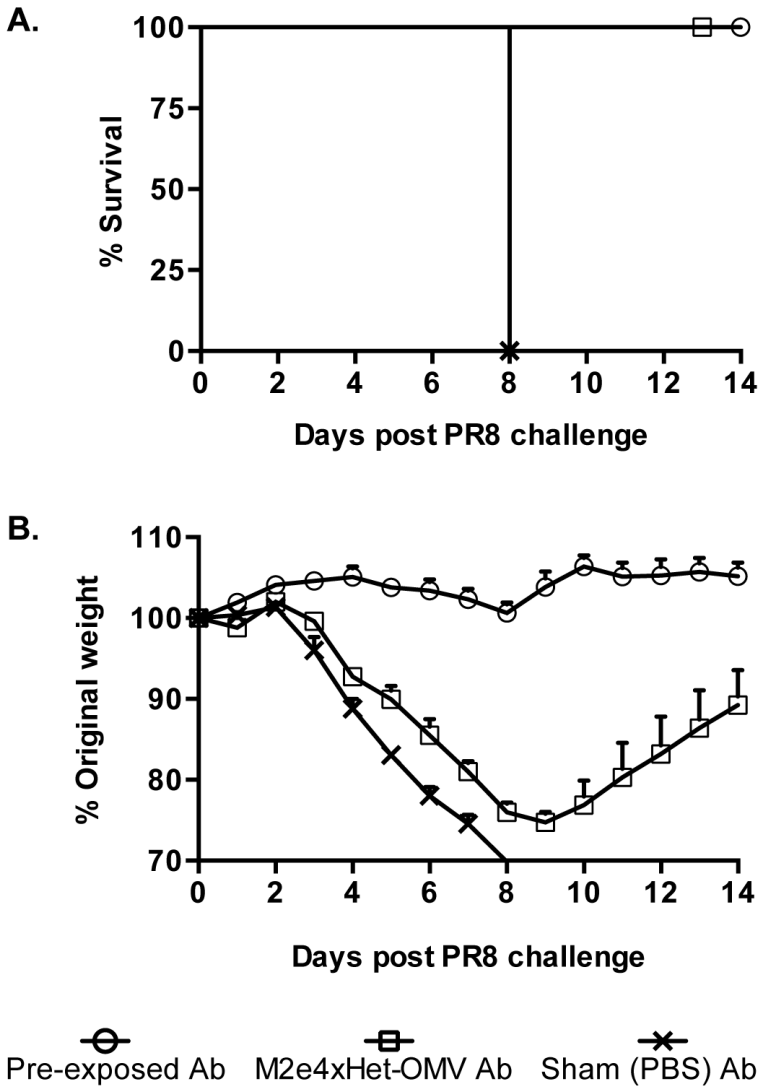

Figure 5: Mortality (**A**) and morbidity (**B**) of mice immunized through passive transfer of 100 µL of serum (Ab) from PR8 pre-exposed, M2e4xHet-OMV vaccinated, or sham vaccinated (PBS) mice 8 weeks following initial vaccination or exposure. Mice were vaccinated with serum 24h prior to challenge with 50 FFU of PR8. Cohorts that received serum from the pre-exposed or M2e4xHet-OMV vaccinated mice had 100% survival during challenge. All mice that received PBS serum died during challenge. Though all mice passively immunized with serum from donor M2e4xHet-OMV vaccinated mice survived, they showed higher levels of morbidity than the M2e4xHet-OMV vaccinated donor mice in equivalent PR8 challenge.

Discussion

The ectodomain of influenza A matrix protein 2 (M2e) is a popular target antigen for potential universal influenza A vaccines due to its remarkable conservation over time [35]. To overcome its low immunogenicity, M2e requires a potent adjuvant, and as we and others have demonstrated, peptide-adsorbed alum alone inadequately primes the immune response against influenza [27,36]. Subsequently, a range of subunit fusion vaccines that combine M2e with adjuvanting proteins, such as hepatitis B protein, keyhole limpet protein, and flagellin have been explored and developed, though many require supplementation by additional extrinsic adjuvants, such as incomplete Freund's adjuvant or MPL [16,37,38]. Here, we demonstrated that engineering EcN to display M2e peptides upon OMVs resulted in significantly elevated anti-M2e IgG2a titers vs. IgG1 titers and protection against influenza challenge without supplemental adjuvants. Additionally, the IgG2a:IgG1 ratio of 3:1 is comparable to that of M2e vaccines supplemented with viral components [25]. Future work will evaluate the ability of M2e-OMVs to give heterologous protection against multiple strains of influenza A virus, and thus better determine its potential as a universal influenza A vaccine.

The proposed mechanism of protection for M2e-based vaccines is clearance of infected cells through antibody dependent cell cytotoxicity and phagocytosis (ADCC and ADCP) and it has been shown that IgG2a antibodies are both necessary and sufficient to provide protection in mice [10,16,33,34]. Our results add further support to this proposed mechanism as we found that protection from weight loss during challenge most significantly correlated with IgG2a antibody levels. Furthermore, our minimum IgG2a antibody titer among passively immunized mice was 8,000, adding strength to the reported minimum protective IgG2a antibody titer of 10,000 previously suggested by Fiers et al. [30]. While only significant to $p<0.1$, M2e4xHet-OMV IgG2a

titers were higher than those of M2exC-OMV and M2eS-OMVs, perhaps contributing to the success of the M2e4xHet-OMV vaccine.

To further elucidate the potent adjuvant mechanisms of M2e-OMVs, we investigated the stimulation of the toll like receptor (TLR) family, as OMVs naturally contain a complex array of pathogen associated molecular patterns (PAMPS) [39]. The TLR panel indicated that M2e4xHet-OMVs trigger multiple bacteria-associated TLRs, predominantly TLR1/2, TLR4, and TLR5, and, to a lesser extent, TLR9. These TLRs signal through both the MyD88 (TLR1/2, TLR4, TLR5, TLR9) and TRIF/TRAF (TLR4) pathways, leading to NF-kβ activity and type I interferon production, which strongly promote a Th1 bias [40]. Previous work characterized the response of murine TLRs to EcN OMV stimulation, but the work was conducted in HEK293 cells that endogenously express TLR5 [18]. Here, we use HEK293 TLR5 KD cells to provide an enhanced perspective of OMV stimulation and to confirm that M2e4xHet-OMVs stimulate mouse and human TLRs similarly, suggesting translational possibilities. One current limitation of this platform is that while the bacterial components of OMVs elicit potent immune responses through high levels of TLR stimulation, these components also limit the maximum tolerable dose which may be administered. Lipopolysaccharide (LPS), a molecule present in bacterial outer membranes, is a strong TLR4 agonist, but also a causative agent of sepsis. M2e-OMV dose size was kept consistent with previous work involving OMV-based vaccines in which OMV LPS levels were measured and safe OMV dose sizes established [18,20]. However, further work in attenuating the LPS load in OMVs is ongoing and will permit larger does to be administered. Additionally, future work will explore other innate immune pathways, such as nucleotide-binding oligomerization domain containing protein 1 (NOD1) signaling, to develop a more nuanced perspective on the signaling mechanisms of OMVs [31].

In summary, M2e antigens presented on *E. coli* Nissle 1917 OMVs demonstrate protection against influenza A strain PR8. The three OMV vaccines tested, M2e1xC, M2e1xS, and M2e4xHet, all yielded high anti-M2e IgG titers with significantly elevated IgG2a:IgG1 ratios, and had improved survival over the peptide M2e1xS with alum formulation. The heterologous M2e4xHet vaccine was most protective, resulting in 100% survival following challenge. TLR studies demonstrated that the OMV adjuvancy could be partly attributed to the OMVs triggering TLR2, TLR4, TLR5, which was consistent for both human and mouse TLRs. Naïve mice that passively received antibodies from M2e4xHet-OMV vaccinated mice showed 100% survival following challenge. Overall, the data support the premise that OMVs represent a promising adjuvant platform for development of an M2e-based universal influenza vaccine.

Acknowledgements

This work published in Vaccine, 4 March 2016. Co-authors are C. Garrett Rappazzo, Cassandra M. Guarino, Annie Chau, Jody L. Lopez, Matthew P. DeLisa, Cynthia A. Leifer, Gary D. Whittaker, and David Putnam.

Research reported in this chapter was supported in part by the National Institute of Allergy and Infectious Diseases of the National Institutes of Health under Award Number 1R56AI114793-01. The content is solely the responsibility of the authors and does not necessarily represent the official views of the National Institutes of Health. This work made use of the Cornell Center for Materials Research Facilities supported by the National Science Foundation under Award Number DMR-1120296. This material is based upon work supported by the National Science Foundation Graduate Research Fellowship to H.C.W. We thank Michele Bialecki and Kelly Sams (Cornell College of Veterinary Medicine) for their guidance and assistance in virological preparations, procedures, and assays; David Topham and Mark Sangster (University of Rochester School of Medicine and Dentistry) for productive discussion of results and experimental suggestions; and the members of the Putnam and Whittaker groups for encouragement and comments.

References

1. World Health Organization (2014). Seasonal Influenza Fact Sheet <http://www.who.int/mediacentre/factsheets/fs211/en/>.

2. Centers for Disease Control and Prevention (U.S.) (2014). CDC Resources for Pandemic Fluat <http://www.cdc.gov/flu/pandemic-resources/index.htm>.

3. Treanor, JJ (2015). Prospects for broadly protective influenza vaccines. *Vaccine*: 1–7doi:10.1016/j.vaccine.2015.08.053.

4. Schotsaert, M and García-Sastre, A (2014). Influenza vaccines: a moving interdisciplinary field. *Viruses* **6**: 3809–3826.

5. Krammer, F and Palese, P (2015). Advances in the development of influenza virus vaccines. *Nat. Rev. Drug Discov.* **14**: 167–182.

6. Lamb, RA, Zebedee, SL and Richardson, CD (1985). Influenza virus M2 protein is an integral membrane protein expressed on the infected-cell surface. *Cell* **40**: 627–633.

7. Lamb, RA and Choppin, PW (1981). Identification of a second protein (M2) encoded by RNA segment 7 of influenza virus. *Virology* **112**: 729–737.

8. Leser, GP and Lamb, RA (2005). Influenza virus assembly and budding in raft-derived microdomains: A quantitative analysis of the surface distribution of HA, NA and M2 proteins. *Virology* **342**: 215–227.

9. Jegerlehner, A, Schmitz, N, Storni, T and Bachmann, MF (2004). Influenza A vaccine based on the extracellular domain of M2: weak protection mediated via antibody-dependent NK cell activity. *J. Immunol.* **172**: 5598–5605.

10. El Bakkouri, K, Descamps, F, De Filette, M, Smet, A, Festjens, E, Birkett, A, *et al.* (2011). Universal vaccine based on ectodomain of matrix protein 2 of influenza A: Fc receptors and alveolar macrophages mediate protection. *J. Immunol.* **186**: 1022–1031.

11. Guilliams, M, Bruhns, P, Saeys, Y, Hammad, H and Lambrecht, BN (2014). The function of Fcγ receptors in dendritic cells and macrophages. *Nat. Rev. Immunol.* **14**: 94–108.

12. Schmitz, N, Beerli, RR, Bauer, M, Jegerlehner, A, Dietmeier, K, Maudrich, M, *et al.* (2012). Universal vaccine against influenza virus: Linking TLR signaling to anti-viral protection. *Eur. J. Immunol.* **42**: 863–869.

13. De Filette, M, Ramne, A, Birkett, A, Lycke, N, Löwenadler, B, Min Jou, W, *et al.* (2006). The universal influenza vaccine M2e-HBc administered intranasally in combination with the adjuvant CTA1-DD provides complete protection. *Vaccine* **24**: 544–551.

14. Schotsaert, M, Ysenbaert, T, Neyt, K, Ibañez, LI, Bogaert, P, Schepens, B, *et al.* (2012). Natural and long-lasting cellular immune responses against influenza in the M2e-immune host. *Mucosal Immunol.* **6**: 276–87.

15. Tsybalova, LM, Stepanova, LA, Kuprianov, V, Blokhina, EA, Potapchuk, M, Korotkov, A, *et al.* (2015). Development of a candidate influenza vaccine based on virus-like particles displaying influenza M2e peptide into the immunodominant region of hepatitis B core antigen: Broad protective efficacy of particles carrying four copies of M2e. *Vaccine* **33**: 3398–3406.

16. Neirynck, S, Deroo, T, Saelens, X, Vanlandschoot, P, Jou, WM and Fiers, W (1999). A universal influenza A vaccine based on the extracellular domain of the M2 protein. *Nat. Med.* **5**: 1157–1163.

17. Kim, OY, Hong, BS, Park, KS, Yoon, YJ, Choi, SJ, Lee, WH, *et al.* (2013). Immunization with Escherichia coli outer membrane vesicles protects bacteria-induced lethality via Th1 and Th17 cell responses. *J. Immunol.* **190**: 4092–102.

18. Rosenthal, JA, Huang, C, Doody, AM, Leung, T, Mineta, K, Feng, DD, *et al.* (2014). Mechanistic insight into the Th1-biased immune response to recombinant subunit vaccines delivered by probiotic bacteria-derived outer membrane vesicles. *PLoS One* **9**: e112802.

19. Kim, JY, Doody, AM, Chen, DJ, Cremona, GH, Shuler, ML, Putnam, D, *et al.* (2008). Engineered bacterial outer membrane vesicles with enhanced functionality. *J. Mol. Biol.* **380**: 51–66.

20. Chen, DJ, Osterrieder, N, Metzger, SM, Buckles, E, Doody, AM, DeLisa, MP, *et al.* (2010). Delivery of foreign antigens by engineered outer membrane vesicle vaccines. *Proc. Natl. Acad. Sci. U. S. A.* **107**: 3099–104.

21. Hamilton, BS, Chung, C, Cyphers, SY, Rinaldi, VD, Marcano, VC and Whittaker, GR (2015). Inhibition of influenza virus infection and hemagglutinin cleavage by the protease inhibitor HAI-2 **450**: 1070–1075.

22. De Filette, M, Jou, WM, Birkett, A, Lyons, K, Schultz, B, Tonkyro, A, *et al.* (2005). Universal influenza A vaccine: optimization of M2-based constructs. *Virology* **337**: 149–161.

23. Liu, W, Zou, P, Ding, J, Lu, Y and Chen, YH (2005). Sequence comparison between the extracellular domain of M2 protein human and avian influenza A virus provides new information for bivalent influenza vaccine design. *Microbes Infect.* **7**: 171–177.

24. Kim, M-C, Lee, J-S, Kwon, Y-M, Eunju, O, Lee, Y-J, Choi, J-G, *et al.* (2013). Multiple heterologous M2 extracellular domains presented on virus-like particles confer broader and stronger M2 immunity than live influenza A virus infection. *Antiviral Res.* **99**: 328–335.

25. Kim, MC, Song, JM, Eunju, O, Kwon, YM, Lee, YJ, Compans, RW, *et al.* (2013). Virus-like particles containing multiple M2 extracellular domains confer improved cross-protection against various subtypes of influenza virus. *Mol. Ther.* **21**: 485–492.

26. Watanabe, H, Numata, K, Ito, T, Takagi, K and Matsukawa, A (2004). Innate immune response in Th1- and Th2-dominant mouse strains. *Shock* **22**: 460–466.

27. Lee, YN, Kim, MC, Lee, YT, Hwang, HS, Cho, MK, Lee, JS, *et al.* (2014). AS04-adjuvanted virus-like particles containing multiple M2 extracellular domains of influenza virus confer improved protection. *Vaccine* **32**: 4578–4585.

28. Ibañez, LI, Roose, K, De Filette, M, Schotsaert, M, De Sloovere, J, Roels, S, *et al.* (2013). M2e-displaying virus-like particles with associated RNA promote T helper 1 type adaptive immunity against influenza A. *PLoS One* **8**.

29. Kim, MC, Lee, YJYN, Ko, EJ, Lee, JS, Kwon, YM, Hwang, HS, *et al.* (2014). Supplementation of influenza split vaccines with conserved M2 ectodomains overcomes strain specificity and provides long-term cross protection. *Mol. Ther.* **22**: 1364–74.

30. Fiers, W, De Filette, M, Birkett, A, Neirynck, S and Min Jou, W (2004). A "universal" human influenza A vaccine. *Virus Res.* **103**: 173–176.

31. Maisonneuve, C, Bertholet, S, Philpott, DJ and De Gregorio, E (2014). Unleashing the potential of NOD- and Toll-like agonists as vaccine adjuvants. *Proc. Natl. Acad. Sci. U. S. A.* **111**: 1–6.

32. Kuehn, MJ and Kesty, NC (2005). Bacterial outer membrane vesicles and the host – pathogen interaction. *Genes Dev.*: 2645–2655doi:10.1101/gad.1299905.negative.

33. Adler-Moore, J, Munoz, M, Kim, H, Romero, J, Tumpey, T, Zeng, H, *et al.* (2011). Characterization of the murine Th2 response to immunization with liposomal M2e influenza vaccine. *Vaccine* **29**: 4460–4468.

34. Ernst, WA, Kim, HJ, Tumpey, TM, Jansen, ADA, Tai, W, Cramer, D V., *et al.* (2006). Protection against H1, H5, H6 and H9 influenza A infection with liposomal matrix 2 epitope vaccines. *Vaccine* **24**: 5158–5168.

35. Deng, L, Cho, JK, Fiers, W and Saelens, X (2015). M2e-Based Universal Influenza A Vaccines. *Vaccines* **3**.

36. Wu, F, Yuan, XY, Li, J and Chen, YH (2009). The co-administration of CpG-ODN influenced protective activity of influenza M2e vaccine. *Vaccine* **27**: 4320–4324.

37. Ravin, N, Blokhina, E, Kuprianov, V, Stepanova, L, Shaldjan, A, Kovaleva, A, *et al.* (2015). Development of a candidate influenza vaccine based on virus-like particles displaying influenza M2e peptide into the immunodominant loop region of hepatitis B core antigen: Insertion of multiple copies of M2e increases immunogenicity and protective effici. *Vaccine* **33**: 3392–3397.

38. Fan, J, Liang, X, Horton, MS, Perry, HC, Citron, MP, Heidecker, GJ, *et al.* (2004). Preclinical study of influenza virus a M2 peptide conjugate vaccines in mice, ferrets, and rhesus monkeys. *Vaccine* **22**: 2993–3003.

39. Kaparakis-Liaskos, M and Ferrero, RL (2015). Immune modulation by bacterial outer membrane vesicles. *Nat. Rev. Immunol.* **15**: 375–387.

40. Duthie, MS, Windish, HP, Fox, CB and Reed, SG (2011). Use of defined TLR ligands as adjuvants within human vaccines. *Immunol. Rev.* **239**: 178–196.

CHAPTER 3

INVESTIGATION OF LIPID IVA RECOMBINANT OUTER MEMBRANE VESICLES AS A SAFE AND EFFICACIOUS ADJUVANT PLATFORM

Introduction

There is high demand for tailored vaccine adjuvants that can elicit directed immune responses against protein-based antigens[1]. Traditionally, vaccines are made from inactivated or live attenuated pathogens. While inactivated and live attenuated vaccines often offer the longest immune memory and protection, they are not suitable for all pathogens due to safety concerns, such as the possibility of reversion and contraindications for use in immune-compromised patients. Recombinant subunit vaccines and virus like particles (VLP) are attractive alternative design choices, as they induce immunity to pathogen-derived antigens in the absence of the pathogen itself. However, unlike inactivated or live attenuated vaccines, which retain inherent immunogenicity from the pathogen, recombinant subunit vaccines often require an adjuvant to generate a sufficient immune response and to appropriately direct the immune system[2]. Recombinant *E. coli*-derived outer membrane vesicles (rOMVs) are a naturally self-adjuvanting and unique pathogen mimetic vaccine platform that represent a link between inactivated vaccines and subunit vaccines. rOMVs are shed from hypervesiculating strains of *E coli,* resulting in vesicles that contain pathogen associated molecular patterns (PAMPs), but are noninfectious[3,4]. The hypervesiculating *E. coli* strains are transformed with a plasmid encoding an antigen of interest genetically fused to a transmembrane protein, resulting in antigen transport to the outer membrane of *E. coli* and subsequent display on rOMVs[5]. Previously, rOMV vaccines proved capable of generating strong immune responses to antigens of interest displayed on their surface and in inducing protection against bacterial and viral pathogens, demonstrating their potential as

a vaccine platform[6–9].

While rOMV-based vaccine platforms shows significant promise, their lipopolysaccharide (LPS) content hampers clinical translation[10,11]. LPS is a potent adjuvant that stimulates through toll like receptor 4 (TLR4), but high levels can lead to fever, inflammation, and septic shock[12]. Modification to the lipid A region of LPS can greatly impact its ability to interact with TLR4 and increase the safety of LPS as an adjuvant. *lpxM* knockout *E. coli* strains, which produce pentacylated LPS instead of hexacylated LPS, were previously used to generate rOMVs with attenuated LPS toxicity[6,13]. However, rOMVs containing only the LPS precursor lipid IVa, which is a human TLR4 antagonist, have not yet been generated or reported. Unlike LPS, lipid IVa is an antagonist to human TLR4, though it does still retain some ability to stimulate murine TLR4[14]. The *E. coli* strain, BL21(DE3) (BL21), was recently engineered to contain only lipid IVa instead of full LPS. This strain, KPM404, sold as ClearColi® (CC), is marketed by Lucigen as an endotoxin-free *E. coli* strain for use in recombinant protein production[15]. Despite containing only lipid IVa, we hypothesized that CC-derived rOMVs would retain sufficient intrinsic PAMPs to generate equivalent immunity against displayed exogenous proteins, but with greatly reduced pyrogenicity and toxicity when compared to LPS unmodified rOMVs

Here, we report a retooling of the rOMV adjuvant platform that significantly reduces endotoxicity while maintaining adjuvant potential, thereby opening the opportunity of rOMVs to translate into the clinic. We engineered CC to hypervesiculate and compared the ability of CC rOMVs vs. the parent strain BL21- derived rOMVs to trigger immune responses both *in vivo* and *in vitro*. Additionally, we directly compared the immune responses of CC rOMVs to *E. coli* Nissle 1917 (Nsl) rOMVs, which previously demonstrated superior immunomodulatory

properties relative to rOMVs derived from *E. coli* K12 strains[6]. Finally, we evaluated the efficacy of CC rOMVs to protect against influenza challenge in mice of three genetic backgrounds (BALB/c, C57BL/6 and DBA/2J) as well as in the more clinically relevant ferret model against human pandemic H1N1 influenza. Collectively, our results demonstrate that CC rOMVs offer significantly improved safety over other rOMV *E. coli* source strains investigated herein, and maintain the rOMV benefits of potent immune responses.

Materials and methods

Strain engineering to induce hypervesiculation

Hypervesiculating, *nlpI* knockout *E. coli* strains were constructed using phage transduction and the KeiO collection as previously described[57,58]. Briefly, *E. coli* donor strain MC4100 Δ*nlpI* kan^r was subcultured 1:100, then infected with P1 phage for 6h. Phage was collected and used to infect ClearColi® (Lucigen, Middleton, WI) and BL21(DE3) (New England Biolabs, Ipswich, MA) for 1.5 h. Bacteria were centrifuged and plated on kanamycin (50 μg/mL) plates to select for *ΔnlpI* knockouts. Gene knockout was confirmed via PCR using primers nlpI-F and nlpI-R (**Table S1**) followed by sequencing and analysis using the Basic Local Alignment Search Tool (BLAST). To ensure strain contamination had not occurred during the knock out process, ClearColi® *ΔnlpI* was sequenced with gutQ-F and gutQ-R to verify absence of gene *gutQ* (**Table S1**)[15].

Recombinant OMV production and characterization

E. coli strains CC and BL21 were transformed with a pBAD plasmid expressing ClyA-GFP, as described by Kim et al[5]. *E. coli* strains CC and Nsl were transformed with a pBAD plasmid expressing ClyA-M2e4xHet, as described by Rappazzo et al[10]. Transformed strains were grown overnight (ON) in LB broth (Thermo Fisher Scientific, Waltham, MA) at 37° C then subcultured to OD_{600} = 0.08. Strains were induced with 2% L-arabinose (Sigma-Aldrich, St. Louis, MO) at OD_{600} = 0.55 and grown for 18 more hours. Subsequently, bacteria were centrifuged (4° C, 15 minutes, 5000 rcf) and passed through a 0.2 μm filter. The filtrate was ultracentrifuged (26k rpm, 4 °C, 3h) then decanted and the pellets suspended in sterile phosphate buffered saline (PBS). rOMV samples were aliquoted and stored at -20° C until use. rOMV surface protein

content was determined using a BCA assay (Thermo Fisher Pierce, Waltham, MA) and antigenic content determined via Western blot (WB). To detect ClyA-GFP, polyclonal anti-GFP antibody was used (Life Technologies, Carlsbad, CA) and to detect ClyA-M2e4xHet, anti-His (clone HIS-1) antibody (Sigma-Aldrich, St. Louis, MO) was used. Western blots (WB) were developed using chemiluminescence and imaged with ChemiDoc Touch Imaging System (Bio-Rad, Hercules, CA). Semi-quantitative analysis of WB demonstrated that 2% of total protein in Cly-GFP rOMVs was GFP and that ~6% of total protein in ClyA-M2e4xHet rOMVs was M2e4xHet (**Figure S1a,b**). TEM samples were prepared by negatively staining with 2% uranyl acetate on copper grids then imaged with a FEI T12 Spirit TEM.

Whole blood pyrogen testing

The protocol for the pyrogen test was adapted from Daneshian *et al*[18]. Donor blood was collected into a heparinized tube and rotated at room temperature until use (maximum time did not exceed 2h). Endotoxin-free 96 well tissue culture plates were filled with 200 µL of endotoxin-free saline, into which 20 µL of blood was added, along with 20 µL of rOMVs, 20 µL of lipid IVa (Carbosynth, Compton, UK), or 20 µL of E-toxate endotoxin standard (Sigma-Aldrich, St. Louis, MO). Endotoxin standard curve ranged from 10 EU/mL to 0.125 EU/mL. Lipid IVa and rOMV samples were serially diluted by 10 (from 10 µg/mL to 0.001 pg/mL), plated in quadruplicate, and incubated (37° C, 18h). Subsequently, samples were centrifuged (500 rcf, 5 minutes, RT) and supernatant collected. An IL-1β sandwich ELISA was performed on each supernatant, following the protocol from Biolegend (San Diego, CA). Plates were pre-coated with 2 µg/mL of anti IL-1β (clone H1b-27, Biolegend, San Diego, CA) in PBS overnight at 4° C. Plates were blocked (1% BSA, 1h, RT), incubated with 100 µL of supernatant per well

(2h, 37° C), coated with anti-IL-1β biotin (clone H1b-98, Biolegend, San Diego, CA) (1h, RT), coated with avidin-HRP (Sigma-Aldrich, St. Louis, MO) (30 min RT), then developed with 3,3,5,5-tetramethylbenzidine (TMB) in the dark for 20 minutes. The reaction was stopped with 4N H_2SO_4 and absorbance read at 450 nm. The plates were washed at least 3x with wash buffer (0.3% bovine serum albumin + 0.05% Tween-20 in PBS) between each step. A 4 parameter logistic curve was fitted to the log of the endotoxin standard vs. the standard absorbances using Prism6 software (GraphPad software, La Jolla, CA). All blood donors gave written, informed consent, and the protocol for blood collection and use was approved by Cornell University's Institutional Review Board.

In vitro pathogen recognition receptor studies

HEK-Blue^{TM} KD-TLR5 cells (InvivoGen, San Diego, CA), which lack expression of all TLRs except TLR1 and TLR6, were transfected with individual human or mouse TLRs and stimulated with TLR ligands overnight, as previously described[10]. Cells were grown in complete DMEM media comprised of the following: DMEM media (Corning, Corning, NY), supplemented with 10 mM HEPES, 1 mM sodium pyruvate, 2 mM L-glutamine, 50 U/mL penicillin, 50 U/mL streptomycin, and 10% heat inactivated low endotoxin fetal bovine serum (FBS) (VWR Life Science Seradigm, Radnor, PA). Subsequently, media was assayed for secreted alkaline phosphatase activity using Quanti-blue (InvivoGen, San Diego, CA). 20 µL of each sample was added to 200 µL of Quanti-blue, incubated (37° C, 3 h), and then read at absorbance of 630 nm. For sensitive chemiluminescence assay, cells were transfected with the following: 5xNF-kβ-luciferase reporter plasmid and either murine MD-2, murine CD14, and murine TLR4 plasmids (Invivogen, San Diego, CA) or human MD-2, human CD14, and human TLR4 plasmids

(Invivogen, San Diego, CA). Cells were stimulated with ligands overnight, and lysed (Reporter Lysis 5x Buffer, Promega, Madison, WI). Luciferase activity was quantified by addition of 100 µL D-luciferin substrate to 20 µL of lysate and read using a Veritas luminometer (Promega, Madison, WI). NOD signaling assays were carried out using HEK-Blue^{TM} mNOD1 and mNOD2 reporter cells (InvivoGen, San Diego, CA). Cells were plated at 0.28 x 10^6 cells/mL (NOD1) or 0.23 x 10^6 cells/mL (NOD2) and incubated (37° C, 48 h) with 10 µg/mL positive control (NOD1: γ-D-glutamyl-meso-diaminopilemic acid (iE-DAP), NOD2: muramyl dipeptide (MDP), Invivogen, San Diego, CA), negative control (PBS), and rOMVs (100 ng/mL). Supernatant was subsequently collected and analyzed using Quanti-blue (InvivoGen, San Diego, CA).

BMDC isolation and maturation

Methods for generating bone marrow-derived dendritic cells (BMDCs) were adapted from Lutz et al[59]. Femurs were harvested from three 12-week-old C57BL/6 mice and three 12-week-old BALB/c mice (Jackson Laboratories, Bar Harbor, ME) and subsequently kept separate throughout the culturing process. Femurs were flushed with RPMI 1640 media (Corning, Corning, NY) and the resulting cell suspension centrifuged (400 g, 5 min, 4° C) and resuspended 2x using RPMI 1640 media. Cells were cultured in Petri dishes (Corning, Corning, NY) at 1x10^6 cells/mL in RPMI 1640 media supplemented with 10% low endotoxin heat inactivated FBS, 2 mM L-glutamine, 50 U/mL penicillin, 50 U/mL streptomycin, 50 nM 2-mercaptoethanol, and 20 ng/mL of recombinant granulocyte macrophage colony-stimulating factor (GM-CSF, R&D Systems, Minneapolis, MN). Half of the media was removed and replaced with fresh media on days 3 and 6 post harvest. On day 7, all non-adherent and loosely adherent cells were harvested and plated in 6 well plates (Corning, Corning, NY) (2 mL/plate), then dosed with 100 ng/mL of

CC or Nsl rOMVs, or 100 ng/mL LPS. Cells were harvested for flow cytometry staining 24 h after dosing using 50 mM ethylenediaminetetraacetic acid (EDTA) in PBS. Cells were Fc blocked (Mouse BD Fc Block™, BD, Franklin Lakes, NJ) and stained for viability (Ghost Dye™ Violet 510 viability dye, Ex:405, Em:510) (15 min, 4° C, in dark). Next, cells were surface stained for CD11c (violetFluor™ 450, Ex:405, Em:450), CD86 (PE, Ex:496, Em:578), and MHCII (redFluor™ 710, Ex:633-647, Em:710) (Tonbo biosciences, San Diego, CA) (30 min, 4° C, in dark). Cells were then fixed (10% formaldehyde, 15 min, 4° C, in dark), resuspended in 1% FBS in PBS, and analyzed using flow cytometry. Data was collected using a LSR II flow cytometer and analyzed with FCS Express. DCs were gated on live, $CD11c^{Hi}$ cells. Mature DCs were identified as $MHCII^{Hi}$, $CD86^{Hi}$ cells. Concentration of cytokines IL-12p70, IL-10, TNF-α, and IL-6 in sample supernatants was determined by ELISA kits according to manufacturer instructions (R&D Systems, Minneapolis, MN). To determine the amount of type 1 IFN in supernatant, L929-ISRE cells were plated at $1x10^5$ cells/well in a 96 well plate using complete DMEM. Cells were allowed to settle overnight, then media was removed and replaced with 50 µL of either DC supernatant or complete DMEM with IFN standards. Cells were incubated with these samples for 4 hours, then supernatant removed, cells lysed (Reporter Lysis 5x Buffer, Promega, Madison, WI), and luminescence measured using same procedure as described above for the transfected HEK-Blue™ KD-TLR5 cells.

Mouse immunization

For the GFP trial, 10-week-old female BALB/c mice bred at Cornell University were subcutaneously injected with a prime dose of 20 µg ClyA-GFP CC rOMVs (n=5), 20 µg ClyA-GFP BL21 rOMVs (n=5), or 100 µL phosphate buffered saline (PBS) (n=3). All mice received a

boost dose of the same composition as the prime dose 4 weeks later. For the influenza trials, 7-week-old female BALB/c, C57BL/6, and DBA/2J mice (Jackson Laboratories, Bar Harbor, ME) were subcutaneously injected with 40 μg (total surface protein) ClyA-M2e4xHet CC rOMVs in 100 μL PBS (n=11 BALB/c, n=10 C57BL/6, n=5 DBA/2J), 40 μg (total surface protein) ClyA-M2e4xHet Nsl rOMVs in 100 μL PBS (n=12 BALB/c), or 100 μL PBS (n=16 BALB/c, n=10 C57BL/6, n=5 DBA/2J). Four weeks post prime injection, a boost dose of the same composition was administered. All mice were weighed and observed daily following the prime (BALB/c, C57BL/6) and boost (BALB/c) injections. An additional cohort of mice, referred to as 'pre-exposed', was immunized at age 8 weeks via intranasal injection of 5 FFU of influenza A/PR8 (n=9 BALB/c, n=8 C57BL/6) to give them immunity to the PR8 virus and allow them to serve as a positive vaccination control. All mouse work was approved by Cornell's Institutional Animal Care and Use Committee.

Enzyme-linked immunosorbent assay (ELISA)

ELISAs were performed as previously described[6,10]. Briefly, Nunc Maxisorp plates (Nalge Nunc, Rochester, NY) were coated (2 μg/mL GFP, 12h, 4° C or 2 μg/mL M2e peptide (SLLTEVETPIRNEWGSRSNDSSD) (LifeTein, Somerset, NJ), 12h, 37° C), blocked (5% milk in PBS, 1h, 25° C), then incubated with 2-fold serial dilutions of serum plated in triplicate (2h, 37°C). Plates were subsequently incubated with biotin-conjugated antibody (1:10000 dilution, IgG, IgG1, or IgG2a) (eBiosciences, San Diego, CA) (1h, 37° C), incubated with HRP-avidin (1:10000 dilution, 0.5h, 37° C), developed in the dark for 20 minutes with TMB (Thermo Fisher Scientific, Waltham, MA), then stopped with 4N H_2SO_4 and absorbance read at 450 nm. The plates were washed at least 3x with wash buffer (0.3% bovine serum albumin + 0.05% Tween-20

in PBS) between each step. Titers were determined as the highest dilution in which the sample gave a signal greater than the average of naïve serum at the same dilution plus three times the standard deviation of the naïve serum.

Mouse influenza challenge

Influenza A/Puerto Rico/8/1934 (PR8) virus (BEI Resources, Manassas, VA) was used to challenge BALB/c and C57BL/6 mice in the influenza vaccine trial. Previously, the PR8 stock was titered via fluorescent forming units (FFU) assay[10]. PR8 was diluted in PBS for use in exposure vaccination of the pre-exposed positive control mice and for use in the lethal challenges. All mice were challenged 10 weeks post their prime vaccination (for both subcutaneously injected and pre-exposed mice). Mice were administered 50 μL via intranasal injection of diluted PR8 while under isofluorane anesthesia (5 FFU for exposure vaccination of BALB/c and C57BL/6, 50 FFU for lethal challenge of BALB/c (~2.5x LD_{50}), 100 FFU for lethal challenge of C57BL/6 (~2.5x LD_{50}). 100 FFU was selected for lethal challenge of C57BL/6 mice, as preliminary dosing studies indicated C57BL/6 mice were less sensitive than BALB/c to PR8. Influenza A virus reassortant X-47 (A/Victoria/3/1975 (HA, NA) x A/Puerto Rico/8/193 (H3N2)) (BEI Resources, Manassas, VA) was used to challenge DBA/2J mice. Virus was grown in embryonated eggs, then collected and titered via plaque forming unit (PFU) assay, as previously described[60]. Mice were weighed daily and observed twice daily following influenza infection. Any mouse with more than 30% weight loss, or exhibiting signs of severe distress, was humanely euthanized. All mouse work was approved by Cornell's Institutional Animal Care and Use Committee.

Ferret immunization and challenge

Three groups of 6 male Fitch ferrets (Triple F Farms, Sayre, PA) that were 7 months of age and serologically negative by hemagglutination inhibition (HI) for currently circulating influenza viruses were used for this study. Ferrets were housed in a Duo-Flo Bioclean Unit (Lab Products Incorporated, Seaford, DE) throughout the study and were intramuscularly vaccinated twice with either 500 µL (1.5 mg total surface protein) of ClyA-M2e4xHet CC rOMV, 500 µL (1.5 mg total surface protein) of CC rOMV that did not contain the pBAD plasmid (Mock-rOMV) or 500 µL of Fluvirin (2015-2016 formula, Norvartis Vaccines and Diagnostics Limited, Cambridge, MA) at four week intervals for primary and boost vaccinations. Body temperature and local inflammation at the injection site (biceps femoris of caudal thigh) were monitored daily for 3 days post vaccination. Serum samples were collected on day 28 (pre-boost) and on day 56 (pre-challenge) after primary vaccination for antibody titer determination. Ferrets were intranasally challenged 35 days after the boost vaccination with 1 mL of 10^6 PFU of A/California/7/2009 virus (pdmH1N1) virus diluted in PBS following anesthesia with ketamine-xylazine-atropine cocktail injection. Three ferrets from each group were observed daily for clinical signs of disease, weight loss and lethargy as described previously[61]. The remaining three ferrets were euthanized on day 3 p.c. so that nasal washes and respiratory tissues (nasal turbinate, trachea and lung) could be collected to evaluate viral replicative ability in the respiratory tract of ferrets by titrating samples in eggs. All animal experiments were performed under the guidance of the Centers for Disease Control and Prevention's Institutional Animal Care and Use Committee in an Association for Assessment and Accreditation of Laboratory Animal Care International-accredited facility.

Statistics

Groups in the pyrogenicity assay were compared with the Kruskal-Wallis test, followed by Mann-Whitney between pairs, using Bonferroni method to account for multiple comparisons. TLR/NOD signaling data, dendritic cell maturation marker data, cytokine production data, and mouse weight loss data were analyzed using an ANOVA, followed by multiple comparisons with respect to control using Dunnett's method of correction. Average titer values were calculated by taking the geometric mean of the titers in each cohort. IgG ELISA titer data were compared between two groups using a two-sided Student's t-test on log-transformed data. IgG1 and IgG2a/IgG2c titer data was analyzed using a paired two-sided Student's t-test on log-transformed data. Kaplan-Meier survival curves were analyzed with a log-rank test using a Bonferroni-corrected alpha to account for multiple comparisons. All statistical analyses were conducted using Prism6 software (GraphPad software, La Jolla, CA).

Results

Antigen expressing ClearColi® and BL21(DE3) rOMVs produce and display equivalent in vivo immunogenicity

ClearColi® (CC) and its parent strain, BL21(DE3), were engineered to hypervesiculate through knock out of *nlpI,* which is known to induce increased vesiculation in laboratory strains of *E. coli*[16,17]. rOMVs were imaged using transmission electron microscopy (TEM) and demonstrated similar morphology and size (50-100 nm) to rOMVs produced by the previously reported *E. coli* strain Nissle 1917 (Nsl) (**Figure 1A-C**)[10]. CC and BL21 were further modified by transformation with plasmids carrying the gene for transmembrane protein cytolysin A (ClyA) fused to GFP[5]. Western blot confirmed that the rOMVs contained ClyA-GFP (**Figure S1a**).

To provide a direct assessment of the role LPS plays in eliciting a humoral response against rOMV displayed proteins, 10-week-old BALB/c mice were injected with 20 μg ClyA-GFP displaying rOMVs derived from either CC (n=5) or BL21 (n=5), then given an equivalent boost dose 4 weeks later. Humoral immune response to the rOMV vaccines was evaluated using serum from 8 weeks post prime injection and measuring the anti-GFP titers of total IgG and IgG isotypes. Both CC and BL21 ClyA-GFP rOMV vaccinated mice developed high total IgG titers, and the geometric mean of anti-GFP titers elicited by CC did not vary significantly from those elicited by BL21 ($p>0.05$) (**Figure 1d**). The serum was further analyzed for IgG1 and IgG2a isotype titers to assess immune system bias and found a balanced IgG1:IgG2a ratio generated by both CC and BL21 rOMVs (**Figure 1e**). Therefore, although the CC rOMVs contained only lipid IVa, they were able to elicit a strong anti-GFP humoral immune response that was equivalent to that of their parent strain, BL21, which contained unmodified LPS.

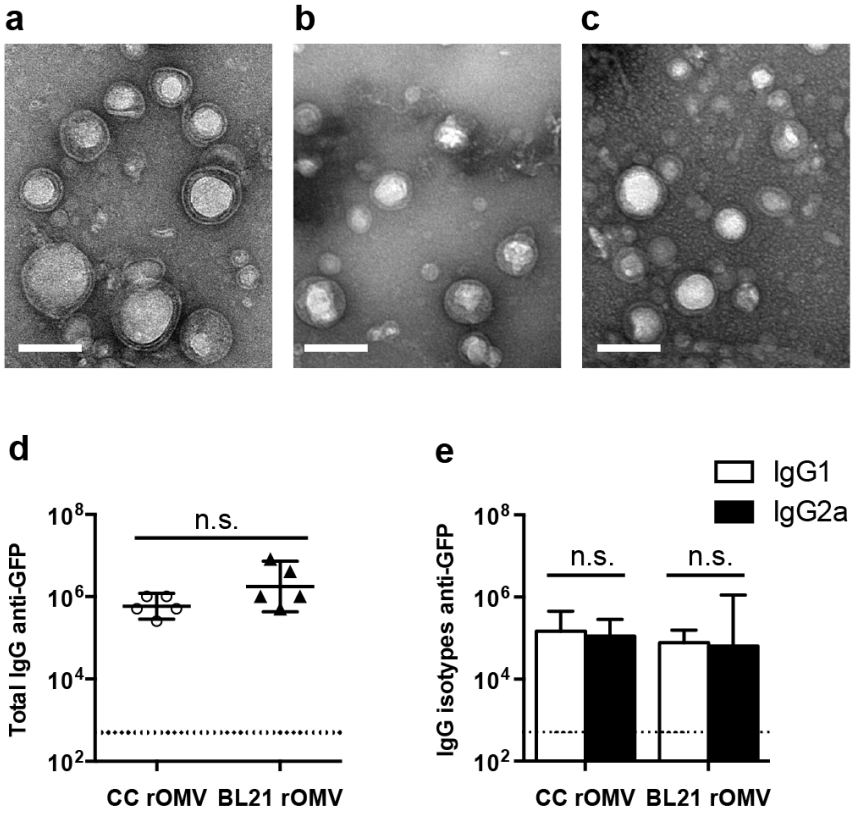

Figure 1. rOMVs produced from 3 different *E. coli* strains are structurally comparable. (**a**-**c**) TEM images of rOMVs stained with uranyl acetate: CC rOMVs (**a**), BL21 rOMVs (**b**), Nsl rOMVs (**c**). Scale bar represents 100 nm. (**d, e**) Total IgG (**d**) and isotypes IgG1 and IgG2a (**e**) anti-GFP titers from BALB/c mice 8 weeks post prime dose of ClyA-GFP expressing CC or BL21 rOMVs. Titer error bars represent 95% confidence intervals (C.I.) of geometric mean. Log-transformed data analyzed using an unpaired Student's t-test to compare CC vs. BL21 rOMV anti-GFP IgG levels and using a paired Student's t-test to compare IgG1:IgG2a levels for each rOMV type. Dotted line indicates titer of sera from mice pre-vaccination.

ClearColi® derived rOMVs have greatly reduced pyrogenicity than parent strain rOMVs

The investigational aim for CC rOMVs was to reduce the toxicity associated with high doses of rOMVs, while retaining the benefits of a pathogen mimetic particle. As CC rOMVs displayed equivalent capability to BL21 in generating anti-GFP titers, we sought to determine whether CC rOMVs had significantly reduced pyrogenicity relative to rOMVs derived from BL21 or Nsl strains using a whole blood pyrogenicity test. In this test, the response of blood monocyte interactions with pyrogens is quantified by IL-1β release, which is then related to a standard endotoxin curve[18]. Thus, the readout for the whole blood pyrogen test is endotoxin units (EU), though the test measures all pyrogens present and not just endotoxin (LPS). This test is performed using human blood, as humans have enhanced endotoxin and pyrogen sensitivity relative to mice[19]. CC rOMVs generated a response that was 10^5 - 10^6 fold lower than BL21 rOMVs and Nsl rOMVs, highlighting the impact that lipid IVa, as opposed to full LPS, has on reducing the overall toxicity (**Figure 2a**). Pure lipid IVa at a concentration of 10 μg/mL generated a response that was beneath detection by the IL-1β ELISA, confirming that it alone is not pyrogenic. The assay highlights that while CC rOMVs have significantly reduced pyrogenicity compared to other OMV types, they are not completely pyrogen free.

ClearColi® rOMVs stimulate through TLR2

The ability of CC rOMVs to generate equivalent immune titers as BL21 rOMVs led us to investigate their ability to trigger pathogen recognition receptors (PRRs) other than toll-like receptor 4 (TLR4), of which LPS is a known agonist. First, rOMVs were used to stimulate a panel of TLR transfected reporter cells, leading to NF-kβ activation; cells transfected with TLR4 were also always transfected with species specific MD-2 and CD14. Both murine (m) and human

TLRs were tested (**Figures 2b,c; S2a-c**). As expected, Nsl rOMVs signaled predominantly through murine and human TLR2 and TLR4, human TLR5, and murine TLR11, as was previously described[10]. BL21 rOMVs also stimulated TLR2 and TLR4; however, BL21 lack flagellin and thus did not stimulate TLR5 (**Figures 2b,c; S2a-c**)[20]. Similar to BL21, CC also does not make flagellin and lacks activity against TLR5 (**S2c**). Unlike Nissle and BL21, CC showed no activity for human TLR4 (**Figures 2c**). CC did stimulate murine TLR4, though to a level significantly lower than either the BL21 or Nsl rOMVs. This is unsurprising, as it is reported that lipid IVa is a moderate agonist of murine TLR4, but an antagonist of human TLR4 [21,22]. CC exhibited activity against both murine and human TLR2, indicating TLR2 stimulation might contribute to CC pyrogenicity **(Figures 2 b**). None of the rOMVs showed activity against any of the other tested murine or human TLRs (**Figures S2a-b**). Nucleotide-binding oligomerization domain (NOD) receptors are intracellular sensors of bacteria, which detect motifs found in peptidoglycan[23]. Neither CC nor BL21 rOMVs caused a response in NOD1 or NOD2 reporter cells (**S2d,e**). While Nsl rOMVs did stimulate NOD1 and NOD2, the NOD1 and NOD2 reporter cell lines endogenously express TLR5, indicating that flagellin was likely responsible for their activation. While possible that CC rOMVs stimulate PRRs that were not tested, the data suggests that the immunogenicity of CC rOMVs is likely driven primarily by their TLR2 agonist activity.

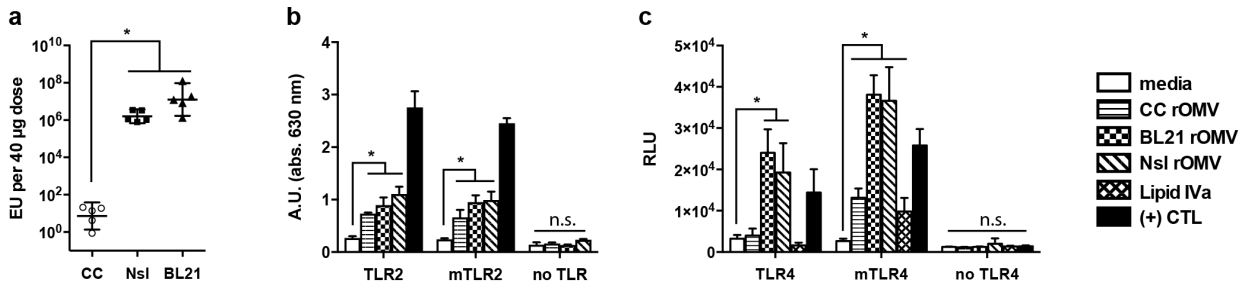

Figure 2. (**a**) Pyrogenicity (measured in endotoxin units, EU) of CC, Nsl, and BL21 rOMVS determined using whole blood pyrogenicity test. Groups were compared with Kruskal-Wallis test, followed by Mann-Whitney between pairs, using Bonferroni method to account for multiple comparisons (* $p<0.01$). Error bars represent 95% CI of geometric mean (n=5 blood donors). (**b**) HEK-Blue^{TM} KD-TLR5 cells transfected with human TLR2 or mTLR2 were stimulated with rOMVs (100 ng/mL) or Pam3Cys (1 µg/mL, (+) CTL) for 16 h. (**c**) HEK-Blue^{TM} KD-TLR5 cells transfected with 5xNF-kβ-luciferase reporter and TLR4/MD-2/CD14 or mTLR4/mMD-2/mCD14 were stimulated with rOMVs (100 ng/mL), lipid IVa (100 ng/mL), or LPS (100 ng/mL, (+) CTL) for 16 h. Samples analyzed by ANOVA followed by multiple comparisons against media using Dunnett method of correction (* $p<0.0001$). Error bars represent standard deviation (n=4).

ClearColi® rOMVs promote dendritic cell maturation

Dendritic cells (DCs) play a key role in directing the immune system and help to facilitate bias towards a Th1 or Th2 type response[24]. Production of IL-12p70 by DCs triggers production of IFN-γ by Th1 cells, cytotoxic T cells, and NK cells[25]. It is well established that LPS matures DCs and promotes a Th1 bias; therefore, we next asked if the outer membrane composition of the lipid IVa-containing CC rOMVs could lead to maturation of DCs[26]. We compared the cytokines produced from bone marrow-derived dendritic cells (BMDCs) stimulated by CC and Nsl rOMVs to determine if one rOMV type was more prone to eliciting a Th1 bias. We focused our comparison on CC rOMVs vs. Nsl rOMVs, as there is precedent for Nsl rOMVs being used in

protective rOMV vaccines[6,10]. Immature BMDCs from BALB/c or C57BL/6 mice were incubated with CC rOMVs, Nsl rOMVs, LPS (positive control) or PBS (negative control) for 24 h or 48h. Both CC rOMVs and Nsl rOMVs resulted in significant and equivalent BMDC maturation in both BALB/c and C57BL/6 mice, as indicated by upregulation of maturation markers CD86 and MHCII (**Figures 3a-c**). Supernatants from the stimulated and unstimulated BMDCs were collected and measured for IL-10, IL-12p70, Type 1 IFN, IL-6, and TNF-α (**Figures 3d-h, S3a-f**). Production of IL-12p70 is associated with a Th1 biased inflammatory response, whereas production of IL-10 is associated with a suppressive immune response[27]. Treating BMDCs with rOMVs did not increase IL-10 production relative to the control PBS treated cells, except in the 24h time point of BALB/c BMDCs treated with CC rOMVs. However, by 48h, the difference in IL-10 levels between PBS and CC rOMV treated BALB/c BMDCs was no longer significant (**Figure S3a**). This observed decrease in IL-10 production suggests sustained BMDC activation at 48h, as mature BMDCs lose sensitivity to IL-10 signaling, which is known to stimulate IL-10 production[28]. IL-12p70 levels were significantly elevated after treatment with both CC and Nsl rOMVs in BALB/c mice, but were significantly elevated only after treatment with Nsl rOMVs in C57BL/6 mice. CC rOMV treatment of C57BL/6 BMDCs did result in an increase in IL-12p70 production, but the difference was not significant. As expected, treatment with LPS led to significant production of IL-12p70 in BMDCs from both mouse strains. Analysis of type1 IFN, IL-6, and TNF-α at 24h post stimulation showed significant increases occurred after treatment with both CC rOMVs and Nsl rOMVs in both BALB/c and C57BL/6 mouse strains (**Figures 3f-h)**. The presence of type 1 IFN and TNF-α provide further confirmation of BMDC maturation, as type 1 IFNs have an activating effect on immature, committed dendritic cells by stimulating the upregulation of cell surface

proteins MHCII and CD86[29]. Additionally, autocrine TNF-α has been shown to be necessary for the activation of BMDCs and survival of matured BMDCs.[30,31] While the inflammatory properties of IL-6 are context-dependent, IL-6 is known to have a significant role in promoting and directing the adaptive immune response. IL-6 induces B-cell maturation into antibody-secreting cells and promotes the proliferation and survival of $CD4^+$ T-cells[32]. Overall, the equivalent levels of BMDC maturation and increased levels of IL-12p70, IL-6, type I IFN, and TNF-α production, indicate potent immune activation. Only subtle differences were seen between mouse strains, indicating that rOMV vaccines should activate DCs in both Th2 biased BALB/c mice as well as Th1 biased C57BL/6 mice. Furthermore, the presence of lipid IVa instead of full LPS in CC rOMVs did not impair their ability to mature and activate dendritic cells.

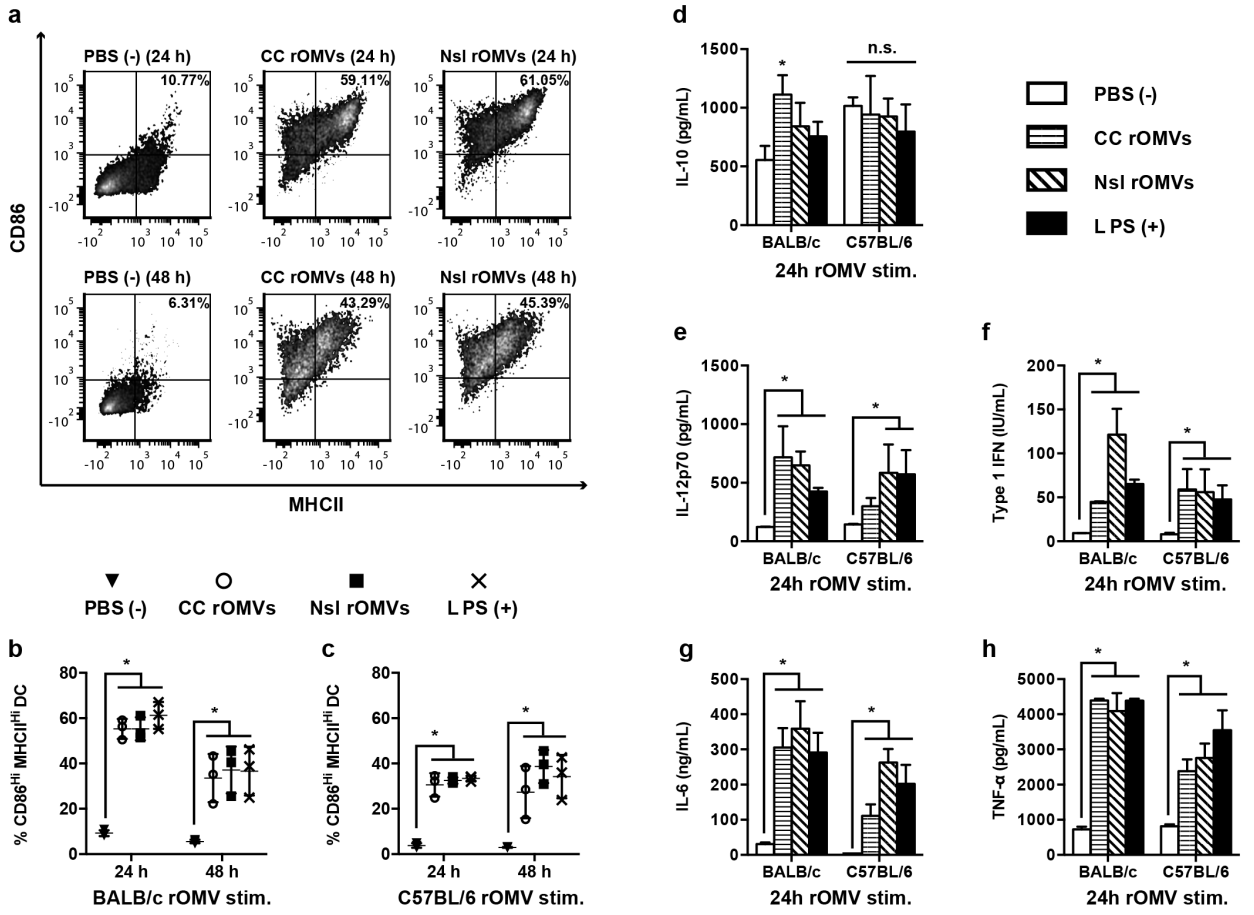

Figure 3. Murine bone marrow-derived dendritic cells (BMDCs) from BALB/c and C57BL/6 mice were stimulated with NsI rOMVs (100 ng/mL), CC rOMVs (ng/mL), LPS (100 ng/mL), or PBS for 0, 24, or 48 hr, then supernatants collected for cytokine analysis, and cells stained for DC maturation markers (stains: viability, CD11c, CD86, MHCII). Flow cytometry was used to determine percent mature dendritic cells (DCs) ($CD86^{Hi}$, $MHCII^{Hi}$) out of the total DC population (gated on viability, $CD11c^{Hi}$). (**a**). Representative density plots of BMDCs isolated from a BALB/c mouse. (**b**) Percent mature DCs from BALB/c mice. (**c**) Percent mature DCs from C57BL/6 mice. (**d**) IL-10 concentration after 24 h stimulation. (**e**) IL-12p70 conc. after 24 h stimulation. (**f**) Type 1 IFN conc. after 24 h stimulation. (**g**) IL-6 conc. after 24 h stimulation. (**h**) TNF-α conc. after 24 h stim. Cytokine stimulation is shown for both C57BL/6 and BALB/c mice. Error bars represent standard deviation. Samples analyzed via ANOVA followed by Holm multiple comparison test * $p<0.05$ (n=3 mice).

ClearColi® rOMVs expressing influenza A antigen M2e4xHet elicit high titers without side effects

The CC rOMVs containing model antigen GFP demonstrated the ability to elicit high total IgG anti-GFP titers and *in vitro* work showed this was likely due to TLR2 stimulation, leading to DC maturation and immune-directive cytokine secretion. With these promising results, we sought to test the protective efficacy of the CC rOMV platform by creating CC rOMVs that displayed an influenza A-based peptide, M2e4xHet, fused to ClyA. The antigen M2e4xHet contains four variants of the influenza A virus matrix 2 protein separated by glycine/serine linkers (peptide sequence:SLLTEVETPIRNEWGSRSNDSSDgggsgggSLLTEVETPTRSEWESRSSDSSDgggsg ggSLLTEVETPTRNEWESRSSDSSDgggsgggSLLTEVETLTRNGWGSRSSDSSD)[10]. Western blot confirmed that the rOMVs contained the ClyA-M2e4xHet protein (**Figure S1b**). Previously, Nsl rOMVs displaying ClyA-M2e4xHet led to 100% protection from challenge with influenza A/Puerto Rico/8/1934 (PR8) (H1N1)[10]. Thus, by comparing Nsl and CC M2e4xHet rOMVs it is possible to determine whether CC rOMVs are as effective as an established rOMV vaccine in eliciting titers and providing influenza protection.

Seven-week-old BALB/c mice were immunized with CC M2e4xHet rOMVs, Nsl M2e4xHet rOMVs, or PBS. Following prime and boost immunization, mice were weighed daily for one week to determine whether the pyrogenicity of the rOMVs was causing negative side effects leading to weight loss (**Figures 4 a,b**). Twenty four hours post vaccination, marked differences were seen between mice vaccinated with Nsl rOMV and CC rOMVs; Nsl rOMV vaccinated mice exhibited anorexia, lethargy, and piloerection, whereas CC rOMV vaccinated mice maintained normal activity and appearance. Mice vaccinated with Nsl rOMVs lost a similar amount of weight after both prime (**Figure 4a**) and boost (**Figure 4b**) doses, whereas mice

vaccinated with CC rOMVs experienced no weight loss after either dose, and had an equivalent response to mice receiving sham PBS injections. The lack of negative side effects in CC rOMV vaccinated mice vs. Nsl rOMV vaccinated mice emphasizes the increased safety profile of the CC rOMV vaccine.

Eight weeks following the prime vaccine dose, anti-M2e titers were measured to assess humoral vaccine response. Both CC and Nsl rOMVs generated high and equivalent total IgG anti-M2e titers ($p>0.05$), indicating potential for both to be used as vaccine adjuvants (**Fig. 4c**). Nsl rOMVs had slight, but significant ($p<0.05$), elevation of IgG2a over IgG1 titers, whereas CC rOMVs resulted in a more balanced IgG2a:IgG1 response (**Fig 4d**). Though CC rOMVs did not lead to elevated IgG2a:IgG1 ratio, the geometric mean IgG2a titer of CC rOMV vaccinated mice was not significantly different from that of Nsl rOMV vaccinated mice ($p>0.05$). The equivalent anti-M2e total IgG titers generated by Nsl and CC rOMVs once again demonstrate that full LPS is not necessary for CC rOMVs to cause a robust humoral immune response.

ClearColi® M2e4xHet rOMVs protect against lethal influenza A challenge in BALB/c mice

Ten weeks post prime immunization, mice were challenged with a lethal dose (50 FFU) of influenza A strain PR8. In addition to the rOMV vaccinated groups and the negative control group, which was administered phosphate buffered saline (PBS), a positive control group of pre-exposed mice was included. The pre-exposed mice were given a low dose (5 FFU) of PR8 virus 8 weeks prior to the lethal (50 FFU) dose, to allow them to develop a protective immune response against PR8. As expected, 100% of pre-exposed mice survived (5/5) and 0% of PBS vaccinated mice survived (0/5) (**Figure 4e**). Mice immunized with rOMVs from both Nsl and CC were equally protected; 80% of mice vaccinated with Nsl M2e4xHet rOMVs survived (4/5),

and 100% of mice vaccinated with CC M2e4xHet rOMVs survived (5/5) (**Figure 4e**). Though one mouse in the Nsl rOMV group required euthanasia due to weight loss exceeding 30% original body weight, the survival of mice vaccinated with Nsl and CC rOMVs was statistically equivalent. The CC rOMV vaccinated mice showed reduced morbidity with respect to the PBS negative control group and had weight loss that was statistically equivalent to the weight loss of the pre-exposed mice throughout the duration of the trial (**Figure 4f**). While the literature suggests a Th1 bias is preferred for M2e-based vaccines, as IgG2a antibodies are a correlate of protection, the balanced CC rOMV vaccine response generated sufficient IgG2a to elicit full protection from challenge[33,34]. The 100% survival of BALB/c mice vaccinated with CC M2e4xHet rOMVs demonstrates that the immune response CC rOMVs elicit is protective against lethal influenza challenge.

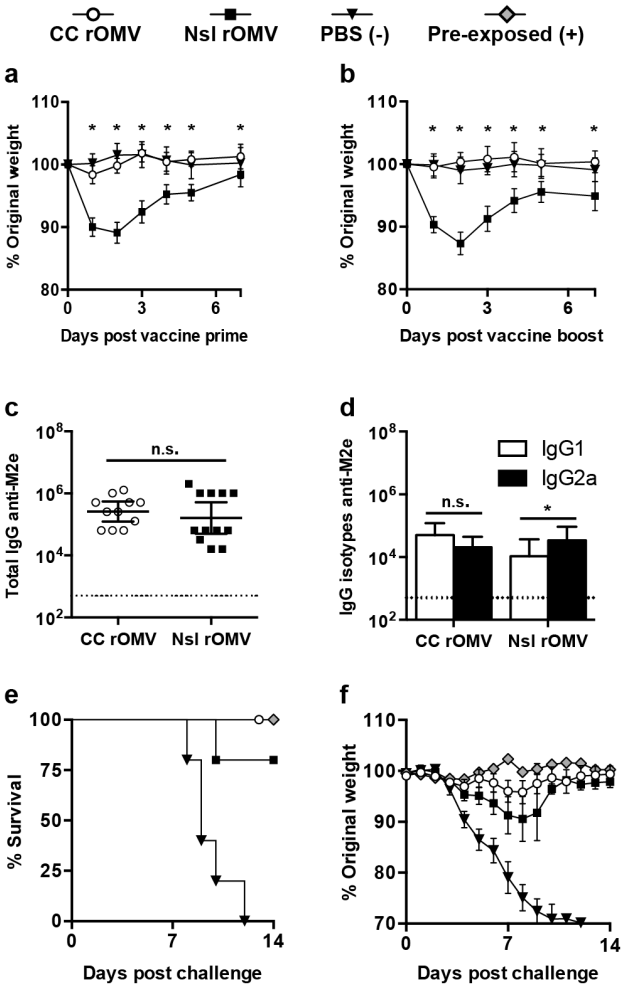

Figure 4. (**a**,**b**) Mice were weighed daily for one week post prime (**a**) and boost (**b**) immunization. Analyzed using ANOVA followed by multiple comparisons using Dunnett method of correction. Error bars represent standard deviation of mean (* $p < 0.001$). (**c,d**) Total IgG (**c**) and IgG isotypes IgG1 and IgG2a (**d**) anti-M2e titers of BALB/c mice 8 weeks post prime rOMV immunization. Dotted line indicates lowest titer detectable above background (serum from PBS vaccinated mice). Log transformed IgG1 and IgG2a anti-M2e titers compared using paired t-test. Error bars indicate 95% CI of geometric mean (* $p < 0.05$) (n=11 CC rOMV vaccinated mice, n=12 Nsl rOMV vaccinated mice, n=16 PBS vaccinated mice). (**e,f**) Mortality (**e**) and morbidity (**f**) of mice challenged with a lethal dose (50 FFU) of influenza A/PR8 (n=5 CC rOMV vaccinated, n=5 Nsl rOMV vaccinated, n=5 PBS vaccinated, n=5 pre-exposed). Kaplan-Meier survival curves were analyzed with a log-rank test using the Bonferroni method to account for multiple comparisons. Error bars on morbidity curves represent SEM.

ClearColi® M2e4xHet rOMVs elicit Th1 bias in C57BL/6 mice and protect against influenza

While previous studies have demonstrated protection against influenza using M2e-based antigens in BALB/c mice, fewer have assessed M2e-based antigens in C57BL/6 mice[35–37]. When Misplon et al. directly compared the response of BALB/c and C57BL/6 mice to M2e based vaccines, they found significantly lower antibody and T-cell responses in C57BL/6 mice[38]. Thus, to determine the robustness of the M2e4xHet antigen, and ability of CC rOMVs to adjuvant in varied mouse strains, 10 C57BL/6 mice were given prime and boost doses of CC rOMVs containing the M2e4xHet antigen. Mouse weight was tracked for three days post injection, but no weight loss or other side effects (lethargy, piloerection) were noted. Four weeks post boost injection, blood was collected and anti-M2e titers assessed. The anti-M2e total IgG titers were high and statistically equivalent to those developed by the BALB/c vaccinated mice (**Figure 5a**). In contrast to the BALB/c mice, which developed a balanced IgG2a: IgG1 ratio, the C57BL/6 mice had significantly higher IgG2c titers than IgG1—several of the mice even had IgG1 levels that were beneath the limit of detection of the ELISA assay (**Figure 5a**). IgG2c levels were measured instead of IgG2a, as C57BL/6 mice do not produce IgG2a and instead produce IgG2c[39]. The mice were challenged at 10 weeks post prime dose with a lethal dose of PR8 (100 FFU), which resulted in 100% survival of vaccinated mice and 0% survival of unvaccinated mice (**Figure 5b**). Though all CC rOMV vaccinated mice survived, they did have significant weight loss compared to the positive control pre-exposed mice, which were exposed to a sublethal dose of PR8 (5 FFU) prior to receiving a lethal dose of PR8 (**Figure 5c**). The 100% protection of C57BL/6 mice from challenge demonstrates the versatility of the CC M2e4xHet rOMV vaccine in protecting mice of different genetic background from influenza A/PR8.

ClearColi® M2e4xHet rOMVs elicit anti-M2e IgG titers and protect DBA/2J mice in lethal influenza A/X-47 (H3N2) challenge

M2e is highly conserved amongst different influenza strains; thus, mice immunized with M2e4xHet rOMVs should be protected from subtypes of influenza other than influenza A/PR8 (H1N1). To test the robustness of the M2e rOMV antigen, DBA/2J mice were immunized with CC M2e4xHet rOMVs or given a PBS sham injection. DBA/2J mice are Th2 biased and share the same $H2^d$ major histocompatibility complex (MHC) as BALB/c mice, but are significantly more susceptible to many influenza types, allowing a lethal challenged to be performed using influenza A/X-47 (H3N2), which is typically only sublethal in BALB/c and C57BL/6 mice[40,41]. DBA/2J mice vaccinated with CC M2e4xHet rOMVs developed high levels of anti-M2e IgG titers and had a balanced IgG2a:IgG1 titer ratio, just as occurred in CC M2e4xHet rOMV immunized BALB/c mice (**Figure 5d**). Following challenge with 5000 PFU influenza A/X-47, 100% (5/5) of M2e4xHet rOMV vaccinated DBA/2J mice survived and 100% (5/5) of PBS sham injected mice required euthanasia (**Figure 5e,f)**. Thus, the survival of mice in X-47 challenge demonstrates that M2e4xHet rOMVs are effective at immunizing mice against influenza A strains of different subtypes.

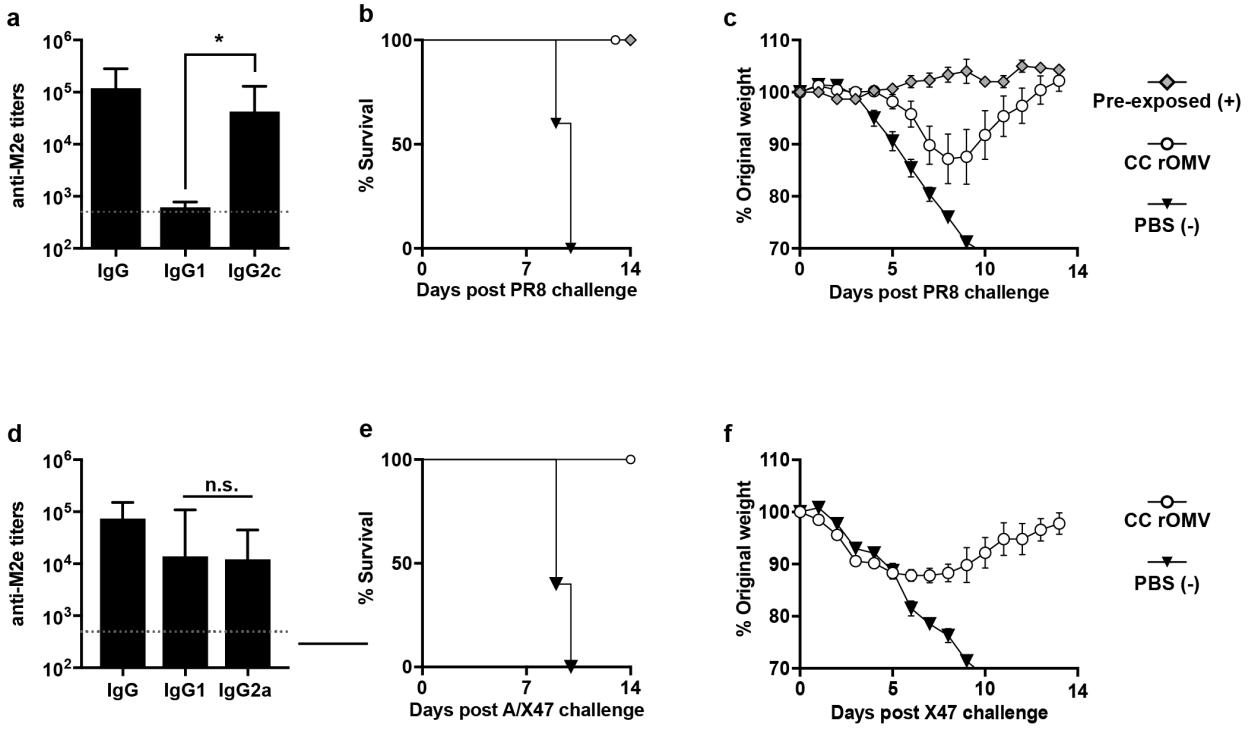

Figure 5. (**a**) Total IgG and isotypes IgG1 and IgG2c titers of C57BL/6 mice 8 weeks post prime rOMV vaccination. Dotted line indicates lowest titer detectable above background. Log transformed IgG1 and IgG2c titers compared using paired t-test. Error bars indicate 95% C.I. of geometric mean (n=10 CC rOMV vaccinated mice) (* $p<0.0001$). (**b, c**) Mortality (**b**) and morbidity (**c**) of mice challenged with a lethal dose (100 FFU) of influenza A/PR8 (n=5 CC rOMV vaccinated, n=5 PBS vaccinated, n=5 pre-exposed). Kaplan-Meier survival curves were analyzed with a log-rank test. Error bars on morbidity curves represent standard error of mean. (**d**) Total IgG and isotypes IgG1 and IgG2a titers of DBA/2J mice 8 weeks post prime rOMV vaccination. Dotted line indicates lowest titer detectable above background. Log transformed IgG1 and IgG2c titers compared using paired t-test. Error bars indicate 95% C.I. of geometric mean (n=5 CC rOMV vaccinated mice) (* $p<0.0001$). (**e, f**) Mortality (**e**) and morbidity (**f**) of mice challenged with a lethal dose (500 PFU) of influenza A/X-47 (n=5 CC rOMV vaccinated, n=5 PBS vaccinated). Kaplan-Meier survival curves were analyzed with a log-rank test. Error bars on morbidity curves represent standard error of mean.

ClearColi® M2e4xHet rOMVs elicit anti-M2e IgG titers in ferrets and reduce virus load in lungs

The mouse studies indicated that M2e4xHet CC rOMVs showed promise as an influenza vaccine, thus the vaccine was next evaluated in a more clinically relevant influenza animal model: ferrets. Unlike mice, which typically require influenza strains to be mouse adapted, ferrets are naturally susceptible to both human and avian influenza viruses. Additionally, ferrets infected with influenza present with fever, sneezing, and nasal discharge in addition to weight loss, more closely mimicking a human infection[42]. Three cohorts of 6 ferrets were immunized with either CC M2e4xHet rOMVs, CC 'mock' rOMVs (produced from *E. coli* that did not contain the pBAD ClyA-M2e4xHet encoding plasmid), or Fluvirin (an FDA-approved seasonal hemagglutinin subunit influenza vaccine). Similar to the mouse experiments, the prime and boost doses were given 4 weeks apart and blood was collected 4 weeks post the boost dose. Following each round of vaccinations, ferret body temperature was recorded to watch for fever and injection sites were monitored for inflammation. None of the ferrets experienced any elevated temperature or injection site inflammation following the prime round of vaccination. Day 1 following the boost dose, 6/6 ferrets receiving the mock rOMV vaccine and 6/6 ferrets receiving the M2e4xHet rOMV vaccine exhibited slight to moderate inflammation, as indicated by redness and swelling at the injection site. By day 3 post boost dose, the injection sites had recovered to normal in 6/6 ferrets in the mock rOMV group and 5/6 ferrets in the M2e4xHet rOMV group. None of the ferrets in the Fluvirin group experienced any inflammation. None of the ferrets in any cohort exhibited elevated temperatures, except 1 ferret in the M2e4xHet rOMV group. This one ferret's body temperature rose from a baseline temperature of 39 °C prior to vaccination to 40 °C 1 day post vaccination. While these side effects are not desirable, all were

transient and none caused the ferrets severe distress. IgG anti-M2e titers were assessed 8 weeks post prime vaccination and showed that all M2e4xHet rOMV immunized ferrets developed high titers, whereas mock rOMV and Fluvirin immunized ferrets had anti-M2e titers that were indistinguishable from pre-vaccination sera (**Figure 6a**). Fluvirin is a subunit hemagglutinin vaccine and was not expected to elicit anti-M2e titers. Ferrets were challenged with pandemic A/California/7/2009 virus (pdmH1N1) 9 weeks post initial vaccination and their body temperature and weight monitored. Day three post challenge, 3 ferrets from each group were euthanized and lungs removed to assess viral titers. Ferrets vaccinated with M2e4xHet rOMVs showed a significant ($p<0.01$) 2-log reduction in lung viral titer compared to ferrets vaccinated with mock rOMVs (**Figure 6b**). Nasal turbinates and tracheas were also excised and assessed for lung viral titers, but neither the M2e4xHet nor Fluvirin vaccinated mice had titers that were significantly reduced from mock rOMV vaccinated mice (**Figure S4a**). Ferrets in the Fluvirin group lost less weight than ferrets in the mock rOMV group and M2e4xHet rOMV groups, but the difference was not significant (**Figure S4b**). None of the groups of ferrets showed significant changes in temperature (**Figure S4c**). Overall, the mild side effects, high antibody titers, and low viral lung titers that resulted from M2e4xHet rOMV ferret immunization provide further evidence that CC rOMVs are a viable adjuvant platform.

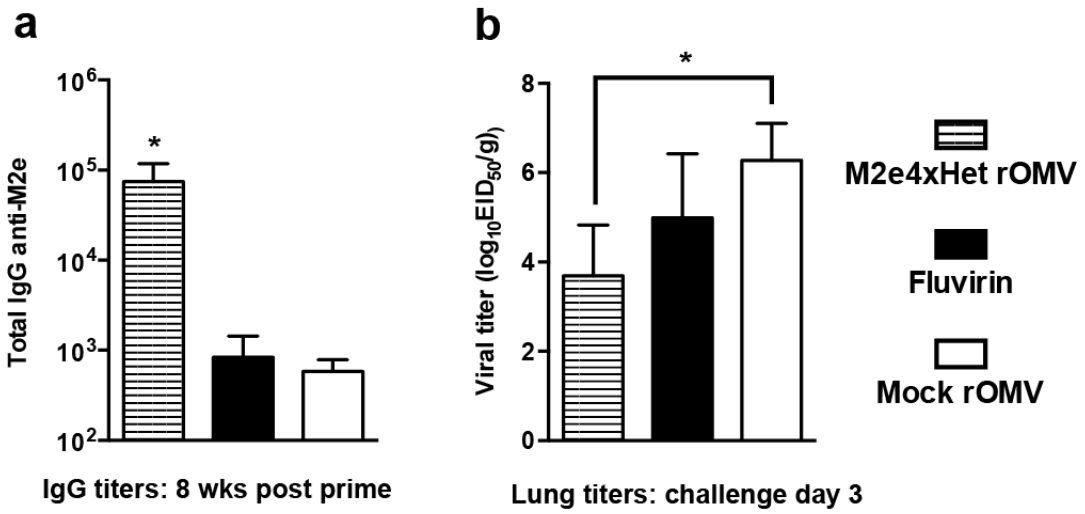

Figure 6: (**a**) Total IgG anti-M2e titers of ferrets 8 weeks post prime vaccination. Error bars indicate 95% C.I. of geometric mean (n=6 CC rOMV vaccinated ferrets) (* $p<0.01$). (**b**) Lung viral titers of ferrets 3 days post challenge with influenza strain pdmH1N1. Lung titers compared using ANOVA followed by comparison to mock CC rOMVs using Bonferroni method of correction (n=3). Error bars indicate standard deviation of log transformed egg infectious dose (EID_{50}) per gram lung tissue (* $p<0.01$).

Discussion

Lipid IVa containing *E. coli* strain ClearColi® was successfully engineered through genetic knockout to increase rOMV production. The CC derived rOMVs offer a clear advantage over Nsl rOMVs in terms of their safety profile, as indicated by their reduced pyrogenicity *in vitro* and substantial attenuation of negative side effects *in vivo*. Although CC was developed to simplify the process of producing endotoxin-free proteins, CC rOMVs are still sufficiently immunogenic to serve as a potent adjuvant platform. Furthermore, the ability of CC rOMVs to adjuvant the immune response is applicable to both peptide-scale antigens, such as M2e4xHet (11.5 kDa), and protein-scale antigens, such as GFP (27 kda). Both constructs led to high IgG titers that were equivalent to those generated by GFP in BL21-derived rOMVs. This work highlights the improved safety and versatility of the CC rOMV platform, greatly increasing its potential for use in larger animal systems.

One metric used to assess the safety of the CC rOMV platform was a pyrogenicity analysis using human whole blood. Traditionally, a limulus amebocyte lysate (LAL) assay is used to assess endotoxin in samples; however, this assay is not sensitive to the reduced toxicity of different lipid A acylation patterns, or to pyrogens other than endotoxin, making it unsuitable for assessing CC rOMV-associated toxicity[43]. The rabbit endotoxicity test is also standard, but for these translationally-minded studies it was deemed more clinically relevant to use human blood samples in lieu of rabbits. The United States Pharmacopoeia recommends a maximum endotoxin level of 5 EU/kg for most drugs, which is the highest dose of endotoxin that does not elicit fever in humans or rabbits; however, vaccines are exempt from this clause[44]. The EU levels associated with specific vaccines are not widely reported, though one paper has extrapolated EU/mL levels of vaccines to show that some vaccines exceed this threshold; the typhus vaccine

has about 800 EU/kg and the typhoid vaccine has 8000 EU/kg[45]. The BALB/c mice weighed approximately 20 g when given their prime vaccination, which, given the data in Figure 2a, corresponds to ~600 EU/kg, or of 120 EU/mL for a 40 μg CC rOMV dose. Thus, though the vaccines do contain significantly more endotoxin than allowable for a traditional drug, they are lower than several vaccines currently used in humans. Future testing will identify the minimal CC rOMV dose needed to elicit a protective effect in murine models, as well as other relevant animal models of infectious disease.

The TLR agonist analysis indicated that CC rOMVs strongly stimulated TLR2, suggesting that it is critical to the immunogenicity of CC rOMVs. Additionally, the TLR4 data highlighted that CC rOMVs stimulate murine TLR4, but not human TLR4. While this ability of CC rOMVs to stimulate mTLR4 indicates that the mouse studies should be interpreted with some caution, the lack of weight loss following vaccination with CC rOMVS indicates that the TLR4 agonism is significantly reduced compared to that caused by the wild type LPS in Nsl. Follow up studies using a humanized TLR4 mouse model could perhaps better ascertain the impact of TLR4 signaling on the immune response to CC rOMVs, though the current humanized TLR4 mouse model is on the Th1 biased C57BL/6 background[46]. Further work using murine TLR2, TLR4, and TLR2/4 knockout models will help to better define the mechanisms of adjuvant activity by CC rOMVs. Also interesting was that neither NOD1 nor NOD2, which both detect PAMPS located in peptidoglycan, were stimulated by CC rOMVs. Thus, though rOMVs derived from some pathogens, such as *H. pylori*, strongly stimulate NOD1, none of the *E. coli* derived rOMVs tested relied on NOD signaling to generate a response[47]. Overall, CC rOMVS appear to stimulate primarily through TLR2 stimulation, though future work can help to address other—and perhaps synergistic—signaling that may be occurring.

BALB/c, C57BL/6, and DBA/2J mice generated high IgG titers when vaccinated with CC rOMVs. That BALB/c mice vaccinated with CC rOMVs developed equivalent total IgG anti-M2e titers to Nsl rOMV vaccinated mice is somewhat surprising, given the attenuated mTLR4 signaling and lack of TLR5 signaling from the CC rOMVs. However, previous work has demonstrated that TLR2 stimulation alone is sufficient to drive high anti-M2e titers in mice[48]. Additionally, the *in vitro* DC work reported here demonstrated that similar levels of mature DCs are produced following CC or Nsl rOMV stimulation. Thus, though CC rOMVs contain a slightly less diverse PRR profile than Nsl rOMVs, they still are effective at generating high IgG titers.

All BALB/c and C57BL/6 CC rOMV immunized mice survived PR8 challenge, though the C57BL/6 mice experienced greater weight loss than the BALB/c vaccinated mice after exposure to PR8. While the IgG2c titers developed by C57BL/6 mice were equivalent to the IgG2a titers developed by BALB/c mice, C57BL/6 mice had significantly lower IgG1 titers. It is possible that the higher dose of influenza required for the C57BL/6 mice affected the response, or that there was a difference in T cell response. Wolf et al. produced multi-antigenic peptide influenza vaccines comprised of four M2e peptides and two T helper cell epitopes adjuvanted with either CpG DNA or cholera toxin that elicited a robust antibody response in BALB/c mice, but not C57BL/6 mice, which they attributed to a lack of T cell responsiveness[49]. While some controversy remains, C57BL/6 mice should be capable of generating potent anti-M2e antibodies; Rosendahl Huber et al. demonstrated the capability of C57BL/6 mice to develop weak titers against M2e when vaccinated using a M2e-based peptide vaccine adjuvanted with incomplete Freund's adjuvant and CpG DNA, though there was no difference in weight loss between vaccinated and non-vaccinated mice when challenged with influenza A virus X31[50]. Lee et al.

found that M2e VLP particles supplemented with AS04 were sufficient to elicit protection in C57BL/6 mice against PR8 challenge, but that supplementation with monophosphoryl lipid A (MPL) or alum was not sufficient[51]. Using the CC rOMV vaccine, protection against PR8 influenza challenge in BALB/c and C57BL/6 mice and X-47 influenza challenge in DBA/2J mice was elicited without addition of any supplemental adjuvants (i.e. alum, CpG DNA). X-47 is a reassortant virus comprised of the hemagglutinin and neuraminidase from A/Victoria/3/1975 and all other proteins from PR8; thus, the M2 protein is the same in both X-47 and PR8 virions, making it unsurprising that the CC M2e4xHet rOMV vaccine was effective against both X-47 and PR8[52]. Future work will further investigate the ability of CC M2e4xHet rOMVs to protect against influenza A strains with more divergent M2e peptides. Overall, the ability of CC rOMVs to protect mice of different genetic backgrounds from different influenza subtypes highlights the robustness of the CC rOMV adjuvant platform.

The ferret study further demonstrates that CC rOMVs remain immunogenic, even when used in a different animal model. Though the ferret model is frequently used for influenza vaccine trials, no literature to our knowledge has yet examined the interaction of lipid IVa with ferret TLR4, making it difficult to determine the degree to which TLR4 signaling is playing a role in the immune response to CC rOMVs. The literature further emphasizes the variability of lipid IVa signaling by species—it is a weak agonist of equine TLR4, but an antagonist in canine TLR4[53]. Further studies into the response of ferrets to lipid IVa will help us to better evaluate the immunogenicity of CC rOMVs in humans.

The ferrets that received the CC M2e4xHet rOMVs had statistically significant reduced viral lung titers compared to CC mock rOMVs, while ferrets the received Fluvirin had reduced—but not statistically significantly reduced—viral lung titers compared to CC mock rOMVs. This

result is of especial interest because one of the three HA variants that Fluvirin contains, derived from virus A/Christchurch/16/2010, is extremely similar to the HA in pdmH1N1, and leads to neutralizing antibodies being formed that are effective against pdmH1N1[54]. Thus, the M2e4xHet CC rOMV vaccine did a better job at controlling influenza infection at day three post challenge than the FDA approved Fluvirin vaccine designed to generate neutralizing titers against the challenge pdmH1N1 virus. While the ferrets that received CC rOMVs had reduced viral lung titers, they did exhibit weight loss in response to influenza challenge. Because antibodies against M2e are believed to drive protection through antibody dependent cellular cytotoxity, not viral neutralization, as Fluvirin does, some weight loss is unsurprising[33,55]. Further work challenging ferrets with different flu subtypes will provide a better assessment of CC-rOMVs as a pandemic influenza vaccine. Additionally, a dosing study is necessary to determine the optimal CC M2e4xHet rOMV dose size for the ferrets. In another recent study involving an M2e-VLP platform, Music et al. found no difference in weight loss or in nasal viral titers between M2e-VLP vaccinated ferrets and naïve ferrets; however, they did not check the viral titers of the lungs, precluding a direct comparison to our results[56]. Interestingly, when Music et al. then supplemented their M2e-VLPs with a seasonal flu vaccine, this combination led to a reduction in both weight loss and viral titers following challenge. Thus, future work could examine the possibility of combining M2e CC-rOMVs with other influenza vaccines. Overall, the reduction of viral lung titers in CC rOMV vaccinated ferrets indicates that the CC-rOMVs warrant further investigation as an influenza vaccine platform.

CC rOMVs represent a viable new adjuvant platform that offers benefits to current rOMV platforms. CC rOMVs retain the positive aspects of the rOMV vaccine platform—simple to produce, inexpensive, highly pathogen mimetic—but contain only the lipid IVa portion of

LPS, giving them significantly greater translational potential than other available rOMV platforms. Even without a strong Th1 bias, CC rOMVs still elicit a robust humoral response. Furthermore, vaccination with CC M2e4xHet-rOMVs garnered complete protection to mice in a lethal influenza challenge against mouse strains with different MHC haplotypes and reduced lung viral titers in ferrets challenged with human pdmH1N1 influenza. While CC rOMVs certainly hold promise in influenza vaccine development, this versatile platform has the potential for use in vaccines against a range of pathogens, and offers a viable alternative to alum-based adjuvants.

Acknowledgments

This work is being prepared for submission to the journal Molecular Therapy. Contributing authors are C. Garrett Rappazzo, Jaclyn S. Higgins, Xiangjie Sun, Nicole Brock, Annie Chau, Aditya Misra, Joseph P. B. Cannizzo, Michael R. King, Taronna R. Maines, Cynthia A. Leifer, Gary R. Whittaker, Matthew P. DeLisa, David Putnam. .

Funding for this work was provided through NIH grant 1R56AI114793-01. This work made use of the Cornell Center for Materials Research Shared Facilities, which are supported through the NSF MRSEC program (DMR-1120296). Hannah Watkins (Cornell University) was partially supported by a National Science Foundation Graduate Research Fellowship. Thank you to Jody Lopez (Cornell University College of Veterinary Medicine) for maintenance of the HEK-293 cell lines, Jeff Mattison (Cornell University) for blood collection, Dorian LaTocha (Cornell University College of Veterinary Medicine) for assistance with flow cytometry, Dr. Erika Gruber (Cornell University College of Veterinary Medicine) for training in BMDC isolation, John Grazul (Cornell University) for assistance with TEM, Dr. Marco Straus (Cornell University College of Veterinary Medicine) for his assistance with the plaque formation unit assay, and Dr. Linxiao Chen and Dr. Jenny Baker (Cornell University) for their early discussions on the potential of ClearColi® as a method for rOMV detoxification.

References

1. Reed, SG, Orr, MT and Fox, CB (2013). Key roles of adjuvants in modern vaccines. *Nat. Med.* **19**: 1597–608.

2. Azmi, F, Fuaad, AAHA, Skwarczynski, M and Toth, I (2014). Recent progress in adjuvant discovery for peptide-based subunit vaccines. *Hum. Vaccines Immunother.* **10**: 778–796.

3. Kuehn, MJ and Kesty, NC (2005). Bacterial outer membrane vesicles and the host-pathogen interaction. *Genes Dev.* **19**: 2645–55.

4. Macdonald, IA and Kuehn, MJ (2012). Offense and defense: microbial membrane vesicles play both ways. *Res. Microbiol.* **163**: 607–618.

5. Kim, JY, Doody, AM, Chen, DJ, Cremona, GH, Shuler, ML, Putnam, D, *et al.* (2008). Engineered bacterial outer membrane vesicles with enhanced functionality. *J. Mol. Biol.* **380**: 51–66.

6. Rosenthal, JA, Huang, C, Doody, AM, Leung, T, Mineta, K, Feng, DD, *et al.* (2014). Mechanistic insight into the Th1-biased immune response to recombinant subunit vaccines delivered by probiotic bacteria-derived outer membrane vesicles. *PLoS One* **9**: e112802.

7. Chen, DJ, Osterrieder, N, Metzger, SM, Buckles, E, Doody, AM, DeLisa, MP, *et al.* (2010). Delivery of foreign antigens by engineered outer membrane vesicle vaccines. *Proc. Natl. Acad. Sci. U. S. A.* **107**: 3099–104.

8. Baker, JL, Chen, L, Rosenthal, JA, Putnam, D and DeLisa, MP (2014). Microbial biosynthesis of designer outer membrane vesicles. *Curr. Opin. Biotechnol.* **29**: 76–84.

9. Kaparakis-Liaskos, M and Ferrero, RL (2015). Immune modulation by bacterial outer membrane vesicles. *Nat. Rev. Immunol.* **15**: 375–387.

10. Rappazzo, CG, Watkins, HC, Guarino, CM, Chau, A, Lopez, JL, DeLisa, MP, *et al.* (2016). Recombinant M2e outer membrane vesicle vaccines protect against lethal influenza A challenge in BALB/c mice. *Vaccine* **34**: 1252–1258.

11. Kim, OY, Hong, BS, Park, KS, Yoon, YJ, Choi, SJ, Lee, WH, *et al.* (2013). Immunization with Escherichia coli outer membrane vesicles protects bacteria-induced lethality via Th1 and Th17 cell responses. *J. Immunol.* **190**: 4092–102.

12. Copeland, S, Warren, HS, Lowry, SF, Calvano, SE and Remick, D (2005). Acute inflammatory response to endotoxin in mice and humans. *Clin. Diagn. Lab. Immunol.* **12**: 60–67.

13. Kim, SH, Kim, KS, Lee, SR, Kim, E, Kim, MS, Lee, EY, *et al.* (2009). Structural modifications of outer membrane vesicles to refine them as vaccine delivery vehicles. *Biochim. Biophys. Acta* **1788**: 2150–9.

14. Hajjar, AM, Ernst, RK, Tsai, JH, Wilson, CB and Miller, SI (2002). Human Toll-like receptor 4 recognizes host-specific LPS modifications. *Nat Immunol* **3**: 354–359.

15. Mamat, U, Wilke, K, Bramhill, D, Schromm, AB, Lindner, B, Kohl, TA, *et al.* (2015). Detoxifying Escherichia coli for endotoxin-free production of recombinant proteins. *Microb. Cell Fact.* **14**: 1–15.

16. Schwechheimer, C, Rodriguez, DL and Kuehn, MJ (2015). NlpI-mediated modulation of outer membrane vesicle production through peptidoglycan dynamics in Escherichia coli. *Microbiologyopen* **4**: 375–89.

17. McBroom, AJ, Johnson, AP, Vemulapalli, S and Kuehn, MJ (2006). Outer membrane vesicle production by Escherichia coli is independent of membrane instability. *J. Bacteriol.* **188**: 5385–5392.

18. Daneshian, M, von Aulock, S and Hartung, T (2009). Assessment of pyrogenic contaminations with validated human whole-blood assay. *Nat. Protoc.* **4**: 1709–1721.

19. Kajiwara, Y, Schiff, T, Voloudakis, G, Gama Sosa, MA, Elder, G, Bozdagi, O, *et al.* (2014). A critical role for human caspase-4 in endotoxin sensitivity. *J. Immunol.* **193**: 335–343.

20. Yoon, SH, Han, MJ, Jeong, H, Lee, CH, Xia, XX, Lee, DH, *et al.* (2012). Comparative multi-omics systems analysis of Escherichia coli strains B and K-12. *Genome Biol.* **13**: R37.

21. Oblak, A and Jerala, R (2015). The molecular mechanism of species-specific recognition of lipopolysaccharides by the MD-2/TLR4 receptor complex. *Mol. Immunol.* **63**: 134–142.

22. Maeshima, N and Fernandez, RC (2013). Recognition of lipid A variants by the TLR4-MD-2 receptor complex. *Front. Cell. Infect. Microbiol.* **3**: 3.

23. Franchi, L, McDonald, C, Kanneganti, TD, Amer, A and Nunez, G (2006). Nucleotide-binding oligomerization domain-like receptors: intracellular pattern recognition molecules for pathogen detection and host defense. *J. Immunol.* **177**: 3507–3513.

24. Banchereau, J and Steinman, RM (1998). Dendritic cells and the control of immunity. *Nature* **392**: 245–252.

25. Krummen, M, Balkow, S, Shen, L, Heinz, S, Loquai, C, Probst, H-C, *et al.* (2010). Release of IL-12 by dendritic cells activated by TLR ligation is dependent on MyD88 signaling, whereas TRIF signaling is indispensable for TLR synergy. *J. Leukoc. Biol.* **88**: 189–199.

26. Netea, MG, Vad der Meer, JWM, Sutmuller, RP, Adema, GJ and Kullberg, B (2005). From the Th1 / Th2 paradigm towards a toll-like receptor/T-helper bias. *Antimicrob. Agents Chemother.* **49**: 3991–3996.

27. Trinchieri, G (2003). Interleukin-12 and the regulation of innate resistance and adaptive

immunity. *Nat. Rev. Immunol.* **3**: 133–46.

28. Corinti, S, Albanesi, C, la Sala, A, Pastore, S and Girolomoni, G (2001). Regulatory activity of autocrine IL-10 on dendritic cell functions. *J. Immunol.* **166**: 4312–4318.

29. McNab, F, Mayer-Barber, K, Sher, A, Wack, A and O'Garra, A (2015). Type I interferons in infectious disease. *Nat Rev Immunol* **15**: 87–103.

30. Trevejo, JM, Marino, MW, Philpott, N, Josien, R, Richards, EC, Elkon, KB, *et al.* (2001). TNF-α-dependent maturation of local dendritic cells is critical for activating the adaptive immune response to virus infection. *Proc. Natl. Acad. Sci.* **98**: 12162–12167.

31. Lehner, M, Kellert, B, Proff, J, Martina, A, Diessenbacher, P, Ensser, A, *et al.* (2016). Autocrine TNF Is Critical for the Survival of Human Dendritic Cells by Regulating BAK, BCL-2, and FLIP Ldoi:10.4049/jimmunol.1101610.

32. Hunter, CA and Jones, SA (2015). IL-6 as a keystone cytokine in health and disease. *Nat Immunol* **16**: 448–457.

33. El Bakkouri, K, Descamps, F, De Filette, M, Smet, A, Festjens, E, Birkett, A, *et al.* (2011). Universal vaccine based on ectodomain of matrix protein 2 of influenza A: Fc receptors and alveolar macrophages mediate protection. *J. Immunol.* **186**: 1022–1031.

34. Schmitz, N, Beerli, RR, Bauer, M, Jegerlehner, A, Dietmeier, K, Maudrich, M, *et al.* (2012). Universal vaccine against influenza virus: Linking TLR signaling to anti-viral protection. *Eur. J. Immunol.* **42**: 863–869.

35. Schotsaert, M, Ysenbaert, T, Neyt, K, Ibañez, LI, Bogaert, P, Schepens, B, *et al.* (2012). Natural and long-lasting cellular immune responses against influenza in the M2e-immune host. *Mucosal Immunol.* **6**: 276–87.

36. Kim, MC, Song, JM, Eunju, O, Kwon, YM, Lee, YJ, Compans, RW, *et al.* (2013). Virus-like particles containing multiple M2 extracellular domains confer improved cross-protection against various subtypes of influenza virus. *Mol. Ther.* **21**: 485–492.

37. Zhou, D, Wu, TL, Lasaro, MO, Latimer, BP, Parzych, EM, Bian, A, *et al.* (2010). A universal influenza A vaccine based on adenovirus expressing matrix-2 ectodomain and nucleoprotein protects mice from lethal challenge. *Mol. Ther.* **18**: 2182–9.

38. Misplon, J a, Lo, C-Y, Gabbard, JD, Tompkins, SM and Epstein, SL (2010). Genetic control of immune responses to influenza A matrix 2 protein (M2). *Vaccine* **28**: 5817–5827.

39. Martin, RM, Brady, JL and Lew, AM (1998). The need for IgG2c specific antiserum when isotyping antibodies from C57BL/6 and NOD mice. *J. Immunol. Methods* **212**: 187–192.

40. Sellers, RS, Clifford, CB, Treuting, PM and Brayton, C (2012). Immunological Variation Between Inbred Laboratory Mouse Strains Points to Consider in Phenotyping Genetically Immunomodified Mice. *Vet. Pathol. Online* **49**: 32–43.

41. Pica, N, Iyer, A, Ramos, I, Bouvier, NM, Fernandez-Sesma, A, García-Sastre, A, *et al.* (2011). The DBA.2 mouse is susceptible to disease following infection with a broad, but limited, range of influenza A and B viruses. *J. Virol.* **85**: 12825–12829.

42. Belser, JA, Katz, JM and Tumpey, TM (2011). The ferret as a model organism to study influenza A virus infection. *Dis. Model. & Mech.* **4**: 575 LP-579.

43. Gutsmann, T, Howe, J, Zähringer, U, Garidel, P, Schromm, AB, Koch, MHJ, *et al.* (2010). Structural prerequisites for endotoxic activity in the Limulus test as compared to cytokine production in mononuclear cells. *Innate Immun.* **16**: 39–47.

44. Food, And, Drug and Administration (2012). *Guidance for industry pyrogen and endotoxins testing: questions and answers.* Compliance Report, June 2012.

45. Brito, LA and Singh, M (2011). Acceptable levels of endotoxin in vaccine formulations during preclinical research. *J. Pharm. Sci.* **100**: 34–37.

46. Hajjar, AM, Ernst, RK, Fortuno III, ES, Brasfield, AS, Yam, CS, Newlon, LA, *et al.* (2012). Humanized TLR4/MD-2 mice reveal LPS recognition differentially impacts susceptibility to Yersinia pestis and Salmonella enterica. *PLoS Pathog* **8**: e1002963.

47. Irving, AT, Mimuro, H, Kufer, TA, Lo, C, Wheeler, R, Turner, LJ, *et al.* (2014). The immune receptor NOD1 and kinase RIP2 interact with bacterial peptidoglycan on early endosomes to promote autophagy and inflammatory signaling. *Cell Host Microbe* **15**: 623–635.

48. Zeng, W, Tan, ACL, Horrocks, K and Jackson, DC (2015). A lipidated form of the extracellular domain of influenza M2 protein as a self-adjuvanting vaccine candidate. *Vaccine* **33**: 3526–3532.

49. Wolf, AI, Mozdzanowska, K, Williams, KL, Singer, D, Richter, M, Hoffmann, R, *et al.* (2011). Vaccination with M2e-based multiple antigenic peptides: characterization of the B cell response and protection efficacy in inbred and outbred mice. *PLoS One* **6**.

50. Rosendahl Huber, SK, Camps, MGM, Jacobi, RHJ, Mouthaan, J, van Dijken, H, van Beek, J, *et al.* (2015). Synthetic long peptide influenza vaccine containing conserved T and B cell epitopes reduces viral load in lungs of mice and ferrets. *PLoS One* **10**.

51. Lee, YN, Kim, MC, Lee, YT, Hwang, HS, Cho, MK, Lee, JS, *et al.* (2014). AS04-adjuvanted virus-like particles containing multiple M2 extracellular domains of influenza virus confer improved protection. *Vaccine* **32**: 4578–4585.

52. Baez, M, Palese, P and Kilbourne, ED (1980). Gene composition of high-yielding influenza vaccine strains obtained by recombination. *J. Infect. Dis.* **141**: 362–365.

53. Scior, T, Alexander, C and Zaehringer, U (2013). Reviewing and identifying amino acids of human, murine, canine and equine TLR4 / MD-2 receptor complexes conferring endotoxic innate immunity activation by LPS/lipid A, or antagonistic effects by Eritoran,

in contrast to species-dependent modulation by li. *Comput. Struct. Biotechnol. J.* **5**: e201302012.

54. (2011). Community Network of Reference Laboratories (CNRL) for Human Influenza in Europe. Influenza virus characterisation: Summary Europe, July 2011.

55. Jegerlehner, A, Schmitz, N, Storni, T and Bachmann, MF (2004). Influenza A vaccine based on the extracellular domain of M2: weak protection mediated via antibody-dependent NK cell activity. *J. Immunol.* **172**: 5598–5605.

56. Music, N, Reber, AJ, Kim, M-C, York, IA and Kang, S-M (2016). Supplementation of H1N1pdm09 split vaccine with heterologous tandem repeat M2e5x virus-like particles confers improved cross-protection in ferrets. *Vaccine* **34**: 466–473.

57. Baba, T, Ara, T, Hasegawa, M, Takai, Y, Okumura, Y, Baba, M, *et al.* (2006). Construction of Escherichia coli K-12 in-frame, single-gene knockout mutants: the Keio collection. *Mol. Syst. Biol.* **2**.

58. Thomason, LC, Costantino, N and Court, DL (2001). *E. coli Genome Manipulation by P1 Transduction*. *Curr. Protoc. Mol. Biol.*, John Wiley & Sons, Inc.doi:10.1002/0471142727.mb0117s79.

59. Lutz, MB, Kukutsch, N, Ogilvie, ALJ, Rößner, S, Koch, F, Romani, N, *et al.* (1999). An advanced culture method for generating large quantities of highly pure dendritic cells from mouse bone marrow. *J. Immunol. Methods* **223**: 77–92.

60. Costello, DA, Whittaker, GR and Daniel, S (2015). Variations in pH sensitivity, acid stability, and fusogenicity of three influenza virus H3 subtypes. *J. Virol.* **89**: 350–360.

61. Reuman, PD, Keely, S and Schiff, GM (1989). Assessment of signs of influenza illness in the ferret model. *J. Virol. Methods* **24**: 27–34.

CHPATER 4

SINGLE DOSE, PLGA ENCAPSULATED M2E RECOMBINANT OUTER MEMBRANE VESICLE VACCINE ELICITS ROBUST, LONG-TERM PROTECTION AGAINST INFLUENZA A VIRUS IN BALB/C MICE

Introduction

Single dose vaccines offer numerous benefits over a traditional vaccine regimen, which typically requires a prime dose followed by one or more boost doses. Vaccines that require just a single dose for efficacy have the potential to increase vaccine coverage, reduce costs, and save time, as patients would require only one healthcare visit[1]. Additionally, in a pandemic setting, it is desirable to generate a protective response as rapidly as possible, yet many inactivated vaccines require a boost dose to be protective. Thus, there is great interest in development of a controlled-release vaccine formulation that elicits rapid and long lasting protection.

Poly(lactic-co-glycolide) (PLGA), a Food and Drug Administration (FDA) approved biodegradable polymer, has been employed numerous times for drug delivery applications, as is extensively reviewed[2–4]. Through use of emulsion techniques, PLGA microparticles (μP) can be used to encapsulate and slowly release peptides and proteins, which has resulted in many FDA approved products[5,6]. Controlled release vaccine formulations using PLGA μP to encapsulate subunit proteins and adjuvants have demonstrated moderate degrees of success, though none are yet commercially available[7]. In addition to providing a tunable method for controlling antigen release, PLGA μP can be formulated into sizes that facilitate their uptake by macrophages and dendritic cells, both of which are professional antigen presenting cells[8,9]. While PLGA μP have

been studied for use in protein subunit—and even DNA—vaccine delivery systems, significantly less work has investigated their ability to release liposomes, or other small vesicles[10].

Recently, *E. coli* derived recombinant outer membrane vesicles (rOMVs) demonstrated potential as a safe and effective vaccine platform that directly couples adjuvant with antigen[11,12]. Transformation of hypervesiculating strains of *E. coli* with a plasmid that contains a transmembrane protein, cytolysin A (ClyA) followed by an antigen of interest, results in the shedding of outer membrane vesicles (diameter: 50-200 nm) that display the antigen of interest on their surface[13,14]. These rOMVs can then be collected, suspended in phosphate buffered saline (PBS), and used as a vaccine, without need for further protein purification or addition of supplemental adjuvants. In particular, rOMVs displaying the antigen M2e4xHet, derived from the highly conserved matrix 2 protein ectodomain, have demonstrated the ability to protect against different influenza A subtypes, making M2e4xHet rOMVs a candidate for a pandemic influenza A vaccine[11]. Thus, using M2e4xHet rOMVs, we sought to (1.) determine the feasibility of encapsulating rOMVs in PLGA μP (2.) create a single dose vaccine that would elicit equivalent protection to a typical prime/boost rOMV regimen, and (3.) assess the longevity of a single dose rOMV formulation vs. typical prime/boost regimen.

Materials and Methods

M2e-rOMV generation and characterization

Recombinant OMVs were prepared as previously described[11,15]. Briefly, *E. coli* strain ClearColi® Δ*nlpI* (CC) was transformed with a pBAD plasmid containing transmembrane protein cytolysin A (ClyA) followed by an antigen (M2e4xHet) derived from the ectodomain of the matrix 2 protein (M2e) of influenza A virus. M2e4xHet has previously been expressed on rOMVs and is comprised of four M2e variants separated by glycine-serine linkers and ending in a His-tag[11]. Bacteria were inoculated in terrific broth (TB) (ThermoFisher Scientific, Waltham, U.S.), grown overnight, then sub-cultured to OD_{600} = 0.08. When bacteria reached mid-log phase growth, ClyA-M2e production was induced by addition of L-arabinose to a final concentration of 0.2%. 18 h post induction, bacteria were centrifuged (5000 rcf, 10 min, 4° C) and supernatant passed through a 0.2 μm filter. Filtrate was further centrifuged (130,000 rcf, 3 h, 4° C), then supernatant decanted and remaining rOMV pellet suspended in sterile phosphate buffered saline (PBS), aliquoted, and stored at -20° C until use. Total protein concentration in rOMV samples was measured using a Pierce BCA Protein Assay kit according to the manufacturer's instructions (ThermoFisher Scientific, Waltham, U.S.). M2e4xHet content was assessed via Western Blot using an anti-His6x primary antibody (Sigma-Aldrich, St. Louis, U.S.).

Synthesis of M2e4xHet rOMV loaded PLGA microparticles

Microparticles loaded with rOMVs were formulated via a water-in-oil-in-water double emulsion (w/o/w). 250 mg of poly(lactic-co-glycolide) (PLGA) (38-54 kD) with a 50:50 ratio of lactide to glycolide ratio (Sigma-Aldrich, St. Louis, U.S.) was dissolved in 4 mL of dichloromethane (DCM) (VWR, Radnor, U.S.) . A water-in-oil (w/o) emulsion was then prepared by adding 400

μL of rOMVs at a concentration of 20 mg/mL dropwise to the surface of DCM/PLGA solution. Emulsification was produced by homogenization at 26,000 rpm with a small sawtooth dispersion head for 30s. The resulting solution was added drop-wise into 60 mL of a 1.3% polyvinylalcohol (PVA) (31-50 kD) (Sigma-Aldrich, St. Louis, U.S.) solution and homogenized for 5 min with a large dispersion head at a speed of 3000 rpm to form the double emulsion (w/o/w). The PVA-PLGA-rOMV solution was then poured into 200 mL of a 0.3% PVA solution. The solution was stirred uncovered in a fume hood for 7 h to facilitate DCM evaporation. Subsequently, PLGA micrparticles were washed 3x by centrifugation (4000 rcf, 4° C, 10 min) followed by resuspension in 40 mL of sterile water. After the third wash, microparticles were resuspended in 13 mL of sterile water, aliquoted, lyophilized, then stored at -20° C until use.

Characterization of protein loading of PLGA microparticles

PLGA μP were sputter coated with Au/Pd, then imaged on a Tescan MIRA3 scanning electron microscope (SEM). Total encapsulated rOMV protein was determined by dissolving a known mass of rOMV loaded PLGA microparticles (μP) in 0.5mL of 0.1M NaOH containing 0.5% sodium dodecyl sulfate (SDS) (Sigma-Aldrich, St. Louis, U.S.) and incubating under continuous rotation at 37°C for 24hr (n=4 samples). The solution was then neutralized with 0.5mL 0.1M HCl in PBS and protein concentration of released rOMVs measured using a Pierce BCA Protein Assay (ThermoFisher Scientific, Waltham, U.S.). Total encapsulated rOMV protein was divided by mass of PLGA μP to determine percent protein encapsulation. Encapsulation efficiency was calculated as percent μP encapsulated protein out of total protein added during μP formulation.

In vitro release profile of rOMV-loaded PLGA microparticles

In vitro release profiles were generated by suspending particles in 0.5 mL of PBS and incubating at 37℃ under continuous rotation (n=4 samples). Every other day for 30 days and then once weekly, particles in solutions were centrifuged (5000 rcf, 20° C, 5 min), then 250 µL of supernatant was collected and replaced by an equal volume of PBS. Protein concentration was quantified using the FluoroProfile Protein Quantification Kit (Sigma-Aldrich, St. Louis, U.S.). Assay was stopped upon microparticle degradation and adsorption to tube, as well as stabilization of protein release (Day 51).

Mouse immunization and study design

Three groups (n=15 per group) of seven-week-old female BALB/c mice (Jackson Laboratories, Bar Harbor, U.S.) were immunized subcutaneously (s.c.) with 200 µL of the appropriate vaccine. The 3 vaccine regimens were as follows: (1) a single dose of PLGA microparticles loaded with 40 µg of M2e4xHet rOMVs suspended in a PBS solution that contained an additional 40 µg of non-encapsulated (free) M2e4xHet rOMVs (group PLGA µP), (2) a prime dose of 40 µg of free M2e4xHet rOMVs in PBS and a boost dose of the same composition 4 weeks later (group free rOMVs), (3) a prime (sham) vaccination of PBS followed by a boost does of PBS 4 weeks later (group PBS (sham)). Approximately 5% of total rOMV protein is M2e4xHet, resulting in 40 µg of rOMVs containing ~2 µg of M2e4xHet antigen. Each of these vaccination groups of 15 mice was further divided down into 3 cohorts: cohorts 1 and 2 were challenged at 10 weeks post prime vaccination, cohort 2 was euthanized 6 days post challenge, and cohort 3 was challenged at 26 weeks (~6 months) post prime vaccination (**Figure 1C**). Sub-mandibular blood collection was performed at weeks 0, 4, 6, 8, 10, 14, 18, 22, and 26 post prime vaccination. All mouse work was

conducted according to protocols approved by Cornell's Institutional Animal Care and Use Committee (IACUC).

M2e enzyme linked immunosorbent assay (ELISA)

ELISAs to determine anti-M2e IgG, IgG1, and IgG2a titers were performed as previously described[11]. Briefly, 96 well Nunc Maxisorp plates (Thermofisher Scientific, Waltham, U.S.) were coated with M2e peptide (SLLTEVETPIRNEWGCRCNDSSD) (Lifetein, Hillsborough, U.S.) at 2 µg/mL in PBS and incubated at 37° C overnight. Plates were washed 2x using wash buffer (PBS with 0.3% bovine serum albumin (BSA) and 0.05% Tween20), then blocked in PBS with 5% milk (Biorad) (20° C, 1h). Plates were washed 3x, then 2-fold serial dilutions of sera added (n=3 technical replicates, 1 PBS sham control sera sample included per plate) and incubated (37° C, 2 h). Plates were washed 3x, then incubated with appropriate biotin-conjugated secondary antibody (IgG, IgG1, IgG2a) (eBiosciences, San Diego, U.S.) (37° C, 1 h). Plates were washed 3x, then incubated with avidin-horse radish peroxidase (Sigma-Aldrich, St. Louis, U.S.) (37° C, 30 min). Plates were washed 5x, then developed in the dark with TMB (3,3',5,5'-Tetramethylbenzidine) (20° C, 20 min). Reaction was stopped through addition of 4N H_2SO_4 and absorbance read at OD450 and background absorbance read at OD570. ELISAs were analyzed by first subtracting background OD570 absorbance from OD450 absorbance. Next, the average plus 3 standard deviations of the control sera OD was calculated for each dilution. These control sera values were subtracted from the vaccinated sera samples and the titer was called as the highest dilution that was still positive.

Influenza challenge

Mice were challenged with a lethal dose of mouse-adapted H1N1 influenza strain A/Puerto Rico/8/1934 (PR8) (BEI Resources, Manassas, U.S) as previously described[11]. Briefly, PR8 stock was thawed on ice, then diluted to a concentration of 1 fluorescent forming unit (FFU)/ μL in sterile PBS. 50 μL of this solution (50 FFU of PR8) was administered intranasally to mice under isoflurane anesthesia. Mice were checked on twice daily and weighed once daily to assess response to influenza. Mice were euthanized if weight dropped more than 30% from original weight, or if they displayed signs of severe distress.

Enzyme-linked Immunospot (ELISPOT) assay

Day 5 post challenge, ELISPOT plates (EMD Millipore, Billerica, U.S.) were coated with anti-IFNγ or anti-IL-4 (R&D Systems, Minneapolis, U.S.) and placed at 4° C overnight. Day 6 post challenge, mice in cohort 2 were euthanized and spleens ascetically removed and placed in complete RPMI media (RPMI media, 10% heat inactivated fetal bovine serum (FBS), 50 U/mL penicillin, 50 U/mL streptomycin) (Thermofisher Scientific, Waltham, U.S.) on ice. Spleens were subsequently mashed into petri dishes using 10 mL complete RPMI media, then filtered through a 70 μm sterile screen. Splenocytes were centrifuged (500 rcf, 5 min, 4° C), then suspended in 1 mL of red blood cell (RBC) lysis buffer (Sigma-Aldrich, St. Louis, U.S.). One minute after addition of RBC lysis buffer, 10 mL of complete RPMI media was added and cells spun down (500 rcf, 5 min, 4° C) and washed 2x. Cells were subsequently diluted to a concentration of $1x10^6$ cells/mL. The ELISPOT plates were blocked with complete RPMI media for 1h, then 200 μL of splenoctyes were added per well (5 spleens per cohort, with 3 technical replicates performed from each spleen for each condition). Cells were stimulated with M2e

peptide (5 μg/mL), PBS, or cell stimulation cocktail (positive control) (eBiosciences, San Diego, U.S.). Plates were incubated at 37° C with 5% CO_2 for either 24 h (IFNγ) or 48 h (IL-4). Plates were then washed using wash buffer (as described for ELISA) and incubated with anti-IFN or anti-IL-4 (37° C, 1h). Plates were washed 3x, then incubated with avidin-HRP (37° C, 30 min). Plates were washed 3x with wash buffer and 2x with plain PBS, then developed using 3-Amino-9-ethylcarbazole (AEC) (BD Biosciences, San Jose, U.S.) and monitored in the dark until spots appeared, then reaction stopped through addition of tap water. Plates were dried then sent to ZellNet for reading and spot enumeration (ZellNet Consulting, Inc., Fort Lee, U.S.).

Statistics

ELISAs were analyzed using n=3 technical replicates per sample per mouse. Titers were averaged using a geometric average and graphed with 95% confidence intervals. IgG titers were compared between the PLGA μP and free rOMVs groups by using a Mann-Whitney test. IgG1: IgG2a titers were compared using a Wilcoxon matched-pairs sign test. Mouse morbidity data was compared using a two-way ANOVA followed by Sidak's test to allow for multiple comparisons between the vaccine groups. Mouse mortality data was analyzed using a log-rank test followed by Bonferoni method of correction between groups. ELISPOT data was analyzed by averaging the technical replicates (n=3) for each spleen, then comparing data from the PLGA μP vaccinated mice spleens and free rOMVs vaccinated mice spleens to the PBS vaccinated mice spleens using an ANOVA followed by using Dunnett's method to allow for multiple comparisons. Statistics were calculated using Graphpad Prism7 (La Jolla, U.S).

Results

rOMV loaded PLGA microparticles with first order release profile synthesized and characterized

Poly(lactic-co-glycolide) microparitlces (PLGA μP) loaded with M2e-rOMVs were synthesized using standard PLGA μP production techniques. Size of rOMV loaded PLGA μPs was assessed using scanning electron microscopy (SEM); μPs were fairly polydispered, with an average diameter and standard deviation of 4.22 +/-2.8 μm (**Figure 1A**). M2e rOMVs ranged in size from ~50-200 nm, indicating that multiple rOMVs could be contained within each PLGA μP[11,15]. Encapsulation efficiency of total rOMVs (measured in total protein content) added to PLGA solution to percent protein PLGA polymers encapsulated was 37.6%. PLGA μP contained 2.18% rOMVs/ PLGA mass (w/w). *In vitro* analysis for rOMV release from PLGA μPs shows a first order release profile that stabilized after 40 days (**Figure 1B**). Previously, prime and boost rOMV vaccinations administered 4 weeks apart resulted in development of high anti-M2e titers and subsequent protection from influenza challenge[11]. Thus, the degradation time period of 40 days—which is likely accelerated *in vivo*—seemed appropriate for delivery of a vaccine dose. Overall, the ability of rOMV loaded PLGA microparticles to be formed with a long-term *in vitro* release profile indicated that there was potential for their use as a single dose vaccine.

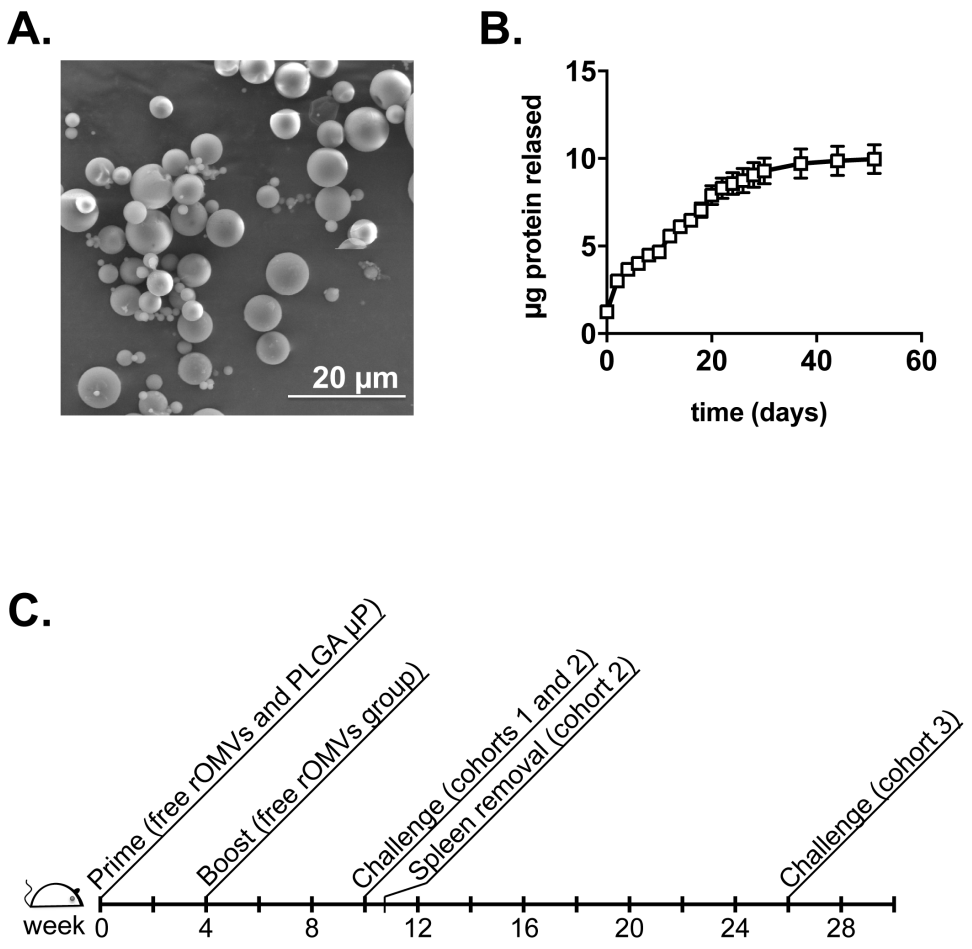

Figure 1: (**A**) SEM image of M2e4xHet rOMV loaded PLGA microparticles. (**B**) *In vitro* release profile of M2e4xHet rOMV loaded PLGA microparticles in PBS at 37° C (n=4 samples). (**C**) Experimental timeline.

PLGA rOMV vaccination leads to high anit-M2e titers

Rapid production of high IgG titers is useful for the creation of a pandemic vaccine, where it is desirable to generate a protective response as quickly as possible. Mice were given either a single dose of PLGA µP containing 40 µg encapsulated rOMVs and 40 µg free rOMVs in PBS or two doses (a prime and a boost doses separated by four weeks) of 40 µg of free rOMVs

(**Figure 1C**). An additional control group of mice received only phosphate buffered saline (PBS) in their vaccines. Blood was collected from the mice every 2-4 weeks to assess the humoral response to the vaccine. Mice vaccinated with free rOMVs generated an anti-M2e geometric mean titer of 1,800 4 weeks post prime dose, whereas mice vaccinated with rOMV loaded PLGA μPs had a geometric mean titer of 53,200 (**Figure 2A**). By 6 weeks post prime vaccination (and 2 weeks post boost vaccination of the free rOMVs group) there was no significant difference in anti-M2e IgG levels between the PLGA μP vaccinated group and the free rOMVs group. Titers remained high and were statistically equivalent at week 8. In addition to total anti-M2e IgG levels, anti-M2e IgG1 and anti-M2e IgG2a levels were also measured. Elevated IgG2a: IgG1 ratios are associated with a Th1 biased immune response, useful for clearance of viral infections, such as influenza infection. At week 4, both IgG1 and IgG2a anti-M2e titers were barely above those of naïve sera (dotted line) in the free rOMVs group (**Figure 2B**). Mice in the PLGA μP group had high and statistically equivalent levels of both IgG1 and IgG2a anti-M2e antibodies. By week 8, the free rOMVs group of mice also had high and statistically equivalent IgG1 and IgG2a anti-2e antibody levels (**Figure 2C**). Somewhat surprisingly, at week 8, the PLGA μP vaccinated mice had slightly elevated IgG1 titers relative to IgG2a (* $p<0.05$). Despite this slightly skewed Th2-biased response, the high anti-M2e IgG titers indicated that PLGA μP encapsulated rOMVs were still capable of eliciting a robust humoral response.

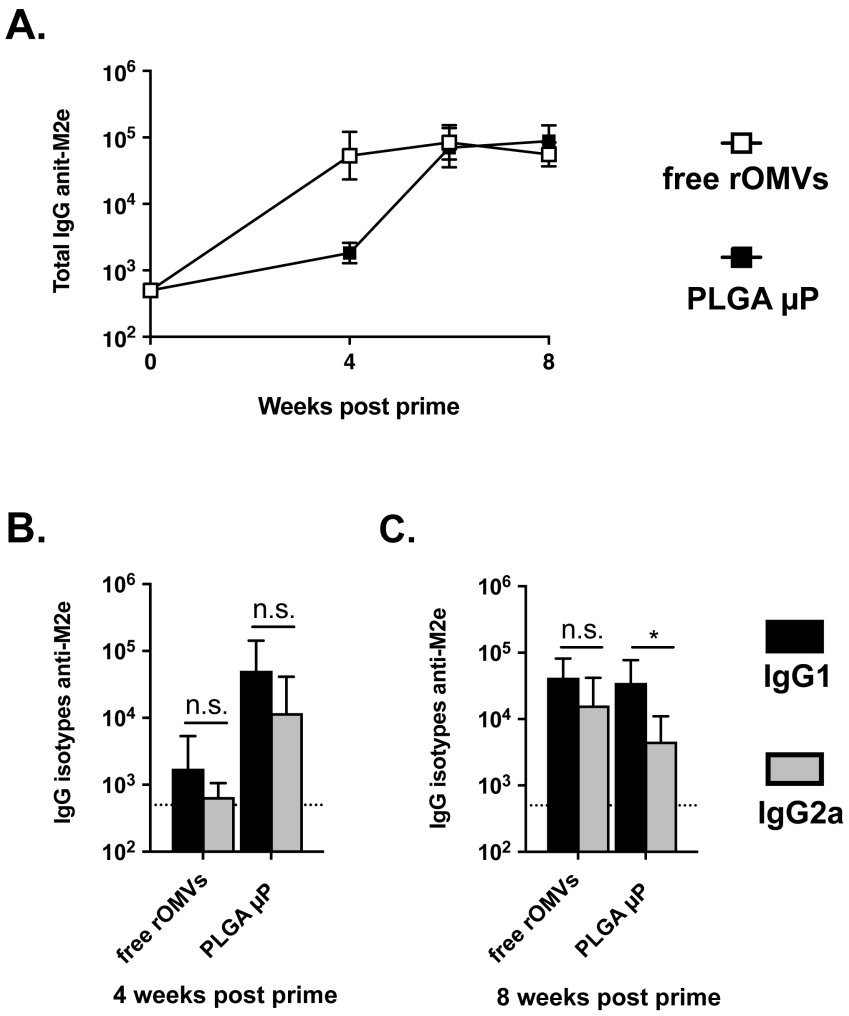

Figure 2: (**A**) Anti-M2e IgG titers elicited by PLGA µP and free rOMVs. (**B,C**) Anti-M2e IgG1 and IgG2a titers at 4 weeks (**B**) and 8 weeks (**C**) post prime. Titers display geomean average (n=15 mice) with 95% confidence intervals (* $p < 0.05$).

PLGA rOMV single dose vaccine protects BALB/c mice in influenza A challenge and elicits cellular response

To assess the ability of a PLGA µP rOMV vaccine to protect mice from influenza challenge, mice were exposed to a lethal dose of mouse adapted influenza virus A/Puerto Rico/8/1934

(PR8). PBS vaccinated mice all lost more than 30% of their original body weight, necessitating euthanasia. Both PLGA μP vaccinated mice and free rOMVs vaccinated mice had 100% survival following challenge (**Figure 3A**). There was no significant difference in weight loss between mice that received the PLGA μP vaccine and mice that received the free rOMVs vaccine (**Figure 3B**). Thus, the μP PLGA vaccine demonstrated that it was possible to create a single dose rOMV vaccine that was as effective as the traditional prime/boost rOMV vaccine.

On day 6 of the challenge, 5 mice (cohort 2) from each of the vaccine groups were euthanized and their spleens excised. Splenocytes were subsequently cultured in the presence of M2e peptide or plain PBS and the IFNγ and IL-4 cytokines produced in response to the stimulation analyzed via an ELISPOT assay. IFNγ is associated with a Th1 biased response, whereas IL-4 is associated with a Th2 biased response[16]. Splenocytes from both PLGA μP and free rOMVs vaccinated mice produced significant levels of IFNγ relative to splenoycytes from PBS vaccinated mice when stimulated with M2e peptide (**Figure 3C**). Mice vaccinated with PLGA μP had especially high levels of IFNγ relative to splenocytes from PBS vaccinated mice, indicating the μP were causing a Th1 bias, despite the elevated IgG1: IgG2a anti-M2e antibody ratio. Splenocytes from both PLGA μP and free rOMVs vaccinated mice produced significantly more IL-4 than PBS vaccinated mice when stimulated with M2e peptide (**Figure 3D**). Unlike in IFNγ production, PLGA μP and free rOMVs vaccination resulted in similar amounts IL-4 production. The presence of IL-4 as well as IFNγ indicates that the rOMVs generate a fairly balanced immune response, which matches the balanced IgG1:IgG2a anti-M2e ratio the free rOMVs vaccinated mouse group displayed. There was no difference in IFNγ or IL-4 production between vaccine groups when splenocytes were treated with plain PBS instead of M2e peptide.

Overall, the complete protection elicited by the PLGA μP vaccine indicates that it is a feasible way to formulate a pandemic influenza A vaccine.

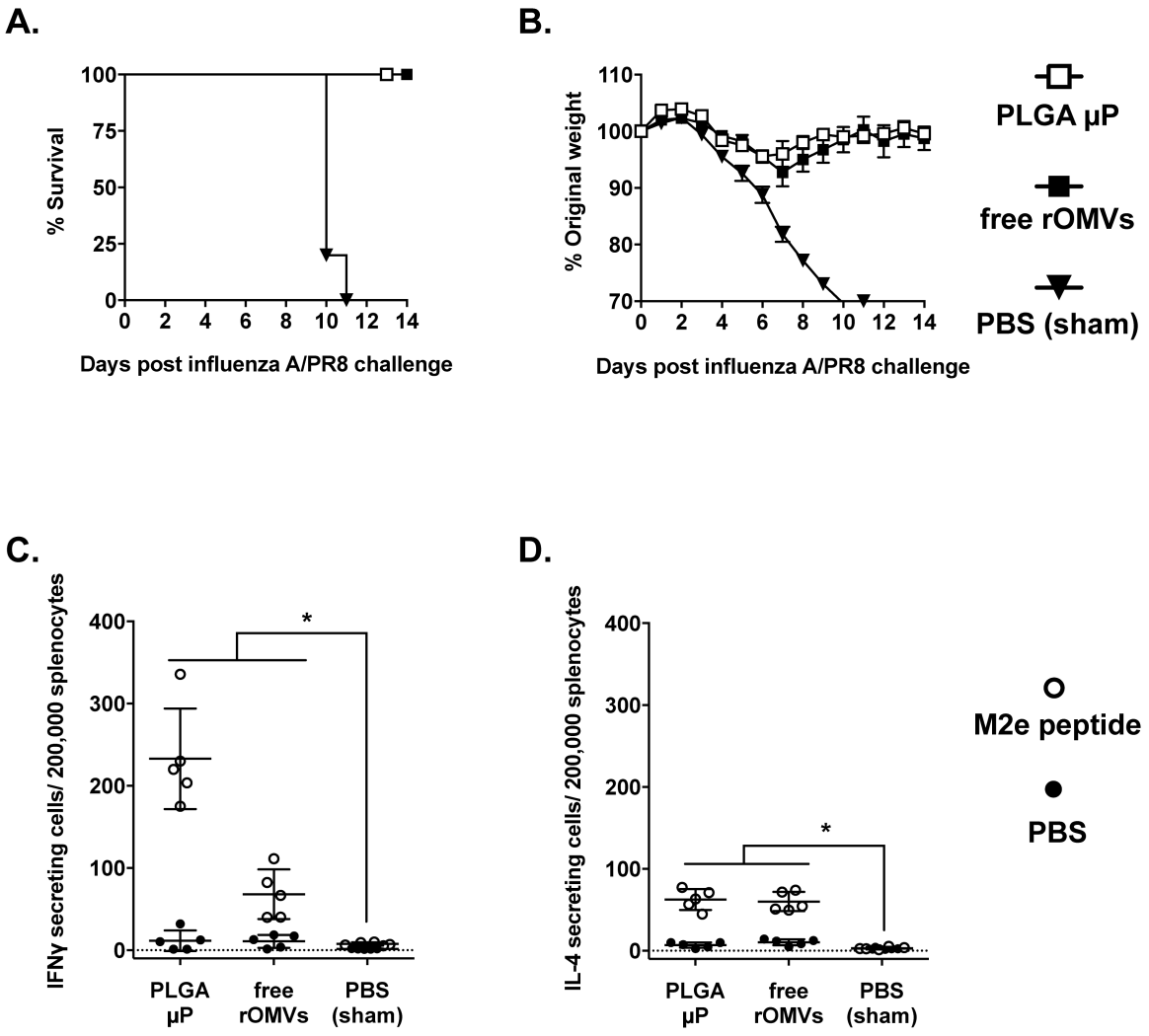

Figure 3: (A,B) Mortality (A) and morbidity (B) of mice challenged with influenza A/PR8 at 10 weeks post prime vaccination (n=5 mice). Error bars represent standard error of the mean. (C,D) Production of cytokines IFNγ (C) and IL-4 (D) 6 days post influenza A/PR8 challenge in PLGA μP, free rOMVs, and PBS vaccinated mice (n=5 mice). Error bars represent standard deviation of average (* $p < 0.05$).

Long term anti-M2e titers result from both PLGA rOMV encapsulated and free rOMV vaccination

Five mice from each of the vaccine groups were not challenged; instead, their anti-M2e IgG levels continued to be monitored every 4 weeks to determine the level of antibody attrition that occurred with time (**Figure 4A**). At 10 weeks post prime vaccination, both the PLGA μP and free rOMVs vaccine groups had statistically equivalent anti-M2e IgG titers. The titers remained statistically equivalent over the next 16 weeks, though the average anti-M2e IgG titer was lower in the PLGA μP group than in the free rOMVs group. At 26 weeks post prime vaccination, both the PLGA μP group and free rOMV group had balanced, statistically equivalent anti-M2e IgG1 and IgG2a antibody titers (**Figure 4B).** The geometric average of IgG1 and IgG2a anti-M2e titers at 26 weeks was lower than the geometric average of IgG1 and IgG2a anti-M2e titers at 8 weeks in both the PLGA μP and free rOMVs vaccinated groups; however, the differences were not significant. The maintenance of high anti-M2e IgG titers for 26 weeks post the prime vaccination indicates that the PLGA μP and free rOMVs vaccines elicit a long-lasting humoral response.

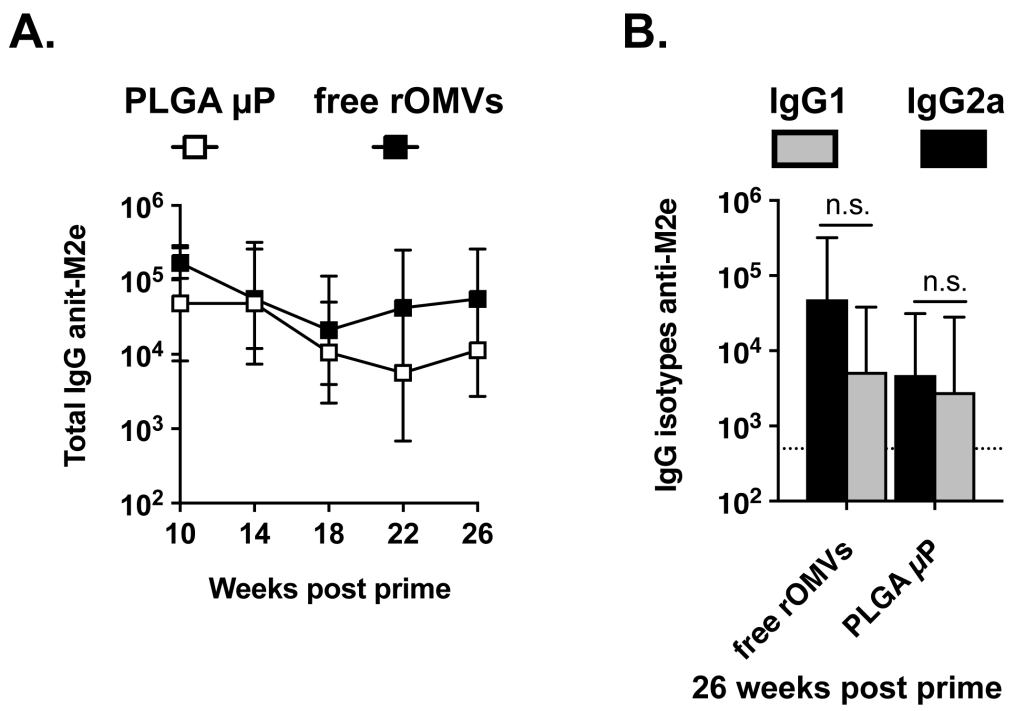

Figure 4: (A) Anti-M2e IgG titers from week 10 post prime vaccination to week 26. (B) Anti-M2e IgG1 and IgG2a titers at 26 weeks post prime vaccination. Error bars represent 95% confidence intervals of geometric mean (n=5 mice, except week 26 group PLGA μP n=4).

PLGA rOMV vaccine protects BALB/c mice from influenza A challenge 6 months post vaccination

Mice in cohort 3 were challenged with mouse adapted influenza A/PR8 at 26 weeks post their prime vaccination. Just as in the challenge that took place at 10 weeks post prime vaccination, mice in the PLGA μP group, free rOMVs group, and PBS (sham) vaccination group all received a lethal dose of PR8. Following challenge, 100% (n=4/4) of PLGA μP vaccinated mice, 100% (n=5/5) of free rOMVs vaccinated mice, and 0% (n=0/5) PBS vaccinated mice survived (**Figure 5A**). The number of mice in the PLGA μP cohort was 4 not 5, as one mouse developed a

recurring abscess and required euthanasia at week 24 post prime vaccination. Though both PLGA μP vaccinated mice and free rOMVs vaccinated mice survived, the PLGA μP vaccinated mice experienced significantly more weight loss than the PLGA μP vaccinated mice on days six through ten of challenge (**Figure 5B**). The weight loss experienced by the PLGA μP vaccinated mice was still significantly less than that experienced by the PBS (sham) vaccinated mice. Overall, the ability of the PLGA μP vaccine to still protect mice from challenge 6 months after it was administered highlights its potential as a single dose vaccine. That the free rOMVs showed such robust challenge protection is also promising, though that vaccine strategy does require both a prime and boost dose to be administered.

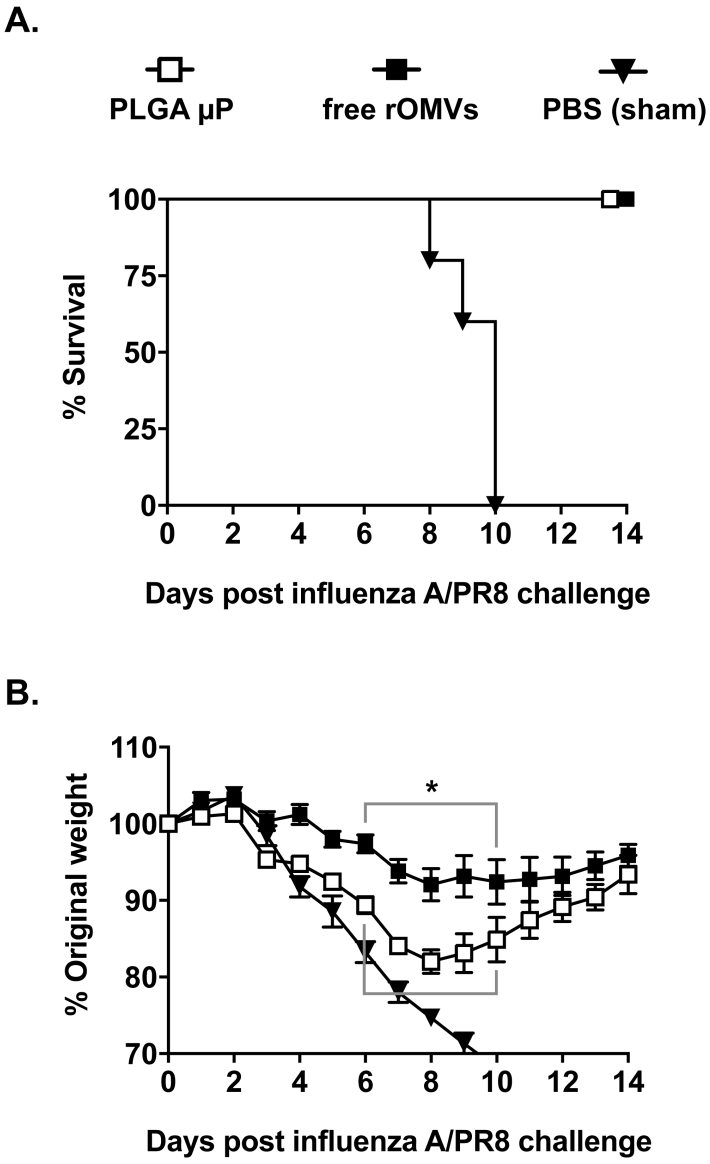

Figure 5: Mortality (A) and morbidity (B) of mice challenged with influenza A/PR8 at 26 weeks post prime vaccination (n=5 mice, except PLGA µP n=4). Error bars represent standard error of mean (* $p < 0.05$).

Discussion

PLGA μP loaded with M2e4xHet rOMVs resulted in effective and long-lasting protection from influenza A/PR8 challenge. While other vaccines have used PLGA μP to encapsulate inactivated influenza virus, influenza antigens, and influenza DNA, rOMVs have not previously been encapsulated by a PLGA system[17–19]. Though PLGA microparticles by themselves have been shown to enhance immunogenicity, most PLGA vaccine systems require the encapsulation of an adjuvant as well as peptides/proteins to generate an immunogenic response[20,21]. Because rOMVs directly couple adjuvant and antigen, no supplemental adjuvants needed to be added. Interestingly, when Singh et al. used PLGA μP to encapsulate inactivated influenza A virus (IAV), they found that the encapsulated system was less effective than a non-encapsulated IAV vaccine[22]. Instead, they determined that the best protection from influenza challenge was afforded when just an adjuvant (CpG) loaded PLGA particles were delivered along with IAV, first in a prime intramuscular dose, and then boosted in an intranasal dose. Hiremath et al. also developed a PLGA-based influenza vaccine system that encapsulated a cocktail of 4 conserved influenza A peptides, M2e virus like particles (VLPs), and adjuvant in PLGA nanoparticles (average diameter 260 nm)[23]. These nanoparticles were delivered to pigs twice intranasally in a prime/boost regimen and resulted in a reduction of symptoms and of viral titers during influenza challenge. Thus, there is some precedent for a M2e-VLP system being encapsulated in PLGA, though our system used larger PLGA microparticles and did not require a boost dose for efficacy.

Previous research has also investigated the ability to generate a single-dose influenza vaccine based on M2e, though not necessarily through use of PLGA μP[24]. Conjugation of a short M2e consensus sequence to the papaya mosaic virus was recently used to create a single

dose pandemic influenza vaccine. Following a single dose of this vaccine, 70% of BALB/c mice survived lethal influenza challenge and there was as strong positive correlation between IgG2a titers and survival[25]. While our vaccine did not elicit elevated IgG2a: IgG1 anti-M2e antibody titers, there still were significant quantities of IgG2a antibody present, which likely contributed to the protective response.

The rapid development of anti-M2e IgG titers by our PLGA μP vaccine was likely enhanced by the presence of free rOMVs in the PLGA μP formulation. Substantial research efforts have gone into characterizing the degradation of PLGA microparticles in tissues and characterizing the release profiles that results from PLGA microparticles of varying compositions and sizes[26]. Additionally, other systems have explored the delivery of antigen in a controlled release manner that mimics natural infection or a prime/boost dosing regimen[27]. However, our work found that the simple approach of suspending PLGA particles in an rOMV solution led to titers that were equivalent to those elicited in prime/boost dosing. Future work comparing our PLGA μP formulation to one where the entire prime plus boost dose (80 μg) is contained within the PLGA μP will help to better ascertain the benefit that free rOMVs offer in the initial priming.

One major challenge to controlled release vaccines is stabilization of the formulation. The PLGA μP vaccine described in this paper, which is suspended in an rOMV solution prior to delivery, requires storage at -20° C. Now that we have established that a single dose controlled release vaccine system for rOMVS is feasible, future work will be directed at developing formulation strategies to allow storage of the vaccines at warmer temperatures prior to use. One well-known downside to PLGA particles is that they create an acidic environment upon degradation, which can denature encapsulated antigens; groups have tried different approaches to

mitigate this problem[28]. Hanson et al. displayed antigens on lipid-enveloped PLGA particles, which kept the antigen away from the acidic PLGA core[29]. Tzeng et al. incorporated Eudragit® E PO into a PLGA microparticle-based inactivated polio virus (IPV) vaccine, which both prevented IPV from denaturing and generated a delayed burst release of IPV[30]. Because M2e is a linear epitope, rOMV denaturation due to the acidic environment that forms as PLGA microparticles degrade is less of a concern than it would be for a conformational epitope

While it is promising that both the PLGA μP and free rOMVs vaccines remained protective after 6 months, it is unknown how much longer that protection would be maintained; already, the mice in the PLGA μP group showed increased morbidity in the 26 week challenge vs. the challenge that took place at 10 weeks. Previously, a M2e-based influenza vaccine entered a Phase I clinical trial, but was hampered by high antibody attrition[31]. However, the lifespan of a laboratory mouse is only about two years, so the protection at 6 months past prime vaccination that our vaccines provided represents a significant portion of a mouse lifespan[32]. Some subunit vaccines, such as Gardasil™ for cervical cancer, produce titers that drop some, but then remain stable for yeas, maintaining protection (in humans)[33]. Further work exploring vaccination of aged mice, instead of 7-week-old mice, and use of other animal systems will allow a more nuanced view of the longevity of rOMV-based vaccines.

The splenocytes of PLGA μP and free rOMV vaacccinated mice produced IFNγ and IL-4 in response to M2e peptide stimulation, indicating a cellular response. Interestingly, PLGA μP vaccinated mice produced significantly more IFNγ in response to M2e peptide stimulation than splenocytes from free rOMVs vaccinated mice during the challenge that took place 10 weeks post prime vaccination. Because spleens were only collected after the first challenge, it is unknown whether this response was retained following the 26-week challenge. The PLGA μP

vaccinated mice lost more weight following the second challenge than the first, indicating that protection had waned somewhat during the time period. Average anti-M2e IgG titers were also lower at the 26-week time point, which could have contributed to the difference in morbidity, though the 26-week titers were not statistically different from the 10-week titers. Previously, it has been shown that encapsulating antigens and adjuvants in PLGA can lead to increased cellular response, due in part to enhancing antigen presentation through uptake by macrophages and dendritic cells[34]. Rubsamen showed that dendritic cells engulfed an average of three particles when they were 8 μm in size and 1 particle when they were 11 μm in size[35]. Additionally, other researchers have added dendritic cell targeting moieties to their microparticle formulations to try and enhance cellular uptake[36,37]. Further work with our PLGA μP is needed to determine the ideal PLGA μP size for optimizing potent—and long lasting—cellular responses.

In conclusion, vaccination of BALB/c mice vaccinated with a single dose influenza A vaccine, comprised of M2e4xHet rOMVs loaded into PLGA μP and suspended in an M2e4xHet rOMV solution (group PLGA μP), resulted in 100% survival following lethal influenza A/PR8 challenges at 10 weeks and 26 weeks post prime vaccination. The protective response is likely to due to both cellular and humoral contributions; following the 10-week challenge, splenocytes from both the PLGA μP vaccinated mice and free rOMVs vaccinated mice responded strongly to the M2e peptide, producing IFNγ and IL-4 in response. Additionally, while the average anti-M2e IgG titers decreased from 10 weeks to 26 weeks post prime vaccination, the difference was not significant. Overall, the PLGA μP represent a simple way to generate single dose rOMV vaccines.

References

1. McHugh, KJ, Guarecuco, R, Langer, R and Jaklenec, A (2015). Single-injection vaccines: Progress, challenges, and opportunities. *J. Control. Release* **219**: 596–609.

2. Danhier, F, Ansorena, E, Silva, JM, Coco, R, Le Breton, A and Préat, V (2012). PLGA-based nanoparticles: an overview of biomedical applications. *J. Control. release* **161**: 505–522.

3. Mundargi, RC, Babu, VR, Rangaswamy, V, Patel, P and Aminabhavi, TM (2008). Nano/micro technologies for delivering macromolecular therapeutics using poly (D, L-lactide-co-glycolide) and its derivatives. *J. Control. Release* **125**: 193–209.

4. Han, FY, Thurecht, KJ, Whittaker, AK and Smith, MT (2016). Bioerodable PLGA-Based Microparticles for Producing Sustained-Release Drug Formulations and Strategies for Improving Drug Loading. *Front. Pharmacol.* **7**.

5. Lü, J-M, Wang, X, Marin-Muller, C, Wang, H, Lin, PH, Yao, Q, *et al.* (2009). Current advances in research and clinical applications of PLGA-based nanotechnology. *Expert Rev. Mol. Diagn.* **9**: 325–341.

6. Anselmo, AC and Mitragotri, S (2014). An overview of clinical and commercial impact of drug delivery systems. *J. Control. Release* **190**: 15–28.

7. Silva, AL, Soema, PC, Slütter, B, Ossendorp, F and Jiskoot, W (2016). PLGA particulate delivery systems for subunit vaccines: Linking particle properties to immunogenicity. *Hum. Vaccin. Immunother.* **12**: 1056–1069.

8. Silva, AL, Rosalia, RA, Varypataki, E, Sibuea, S, Ossendorp, F and Jiskoot, W (2015). Poly-(lactic-co-glycolic-acid)-based particulate vaccines: particle uptake by dendritic cells is a key parameter for immune activation. *Vaccine* **33**: 847–854.

9. Mao, S, Xu, J, Cai, C, Germershaus, O, Schaper, A and Kissel, T (2007). Effect of WOW process parameters on morphology and burst release of FITC-dextran loaded PLGA microspheres. *Int. J. Pharm.* **334**: 137–148.

10. Tinsley-Bown, A., Fretwell, R, Dowsett, A., Davis, S. and G.H. Farrar (2000). Formulation of poly(d,l-lactic-co-glycolic acid) microparticles for rapid plasmid DNA delivery. *J. Control. Release* **66**: 229–241.

11. Rappazzo, CG, Watkins, HC, Guarino, CM, Chau, A, Lopez, JL, DeLisa, MP, *et al.* (2016). Recombinant M2e outer membrane vesicle vaccines protect against lethal influenza A challenge in BALB/c mice. *Vaccine* **34**: 1252–1258.

12. Baker, JL, Chen, L, Rosenthal, JA, Putnam, D and DeLisa, MP (2014). Microbial biosynthesis of designer outer membrane vesicles. *Curr. Opin. Biotechnol.* **29**: 76–84.

13. Kim, JY, Doody, AM, Chen, DJ, Cremona, GH, Shuler, ML, Putnam, D, *et al.* (2008). Engineered bacterial outer membrane vesicles with enhanced functionality. *J. Mol. Biol.* **380**: 51–66.

14. Chen, DJ, Osterrieder, N, Metzger, SM, Buckles, E, Doody, AM, DeLisa, MP, *et al.* (2010). Delivery of foreign antigens by engineered outer membrane vesicle vaccines. *Proc. Natl. Acad. Sci. U. S. A.* **107**: 3099–104.

15. Rosenthal, JA, Huang, C, Doody, AM, Leung, T, Mineta, K, Feng, DD, *et al.* (2014). Mechanistic insight into the Th1-biased immune response to recombinant subunit vaccines delivered by probiotic bacteria-derived outer membrane vesicles. *PLoS One* **9**: e112802.

16. Mosmann, TR and Coffman, RL (1989). TH1 and TH2 cells: different patterns of lymphokine secretion lead to different functional properties. *Annu. Rev. Immunol.* **7**: 145–73.

17. Hilbert, AK, Fritzsche, U and Kissel, T (1999). Biodegradable microspheres containing influenza A vaccine: immune response in mice. *Vaccine* **17**: 1065–1073.

18. Zhao, K, Li, G-X, Jin, Y-Y, Wei, H-X, Sun, Q-S, Huang, T-T, *et al.* (2010). Preparation and immunological effectiveness of a Swine influenza DNA vaccine encapsulated in PLGA microspheres. *J. Microencapsul.* **27**: 178–186.

19. Rajapaksa, TE, Stover-Hamer, M, Fernandez, X, Eckelhoefer, HA and Lo, DD (2010). Claudin 4-targeted protein incorporated into PLGA nanoparticles can mediate M cell targeted delivery. *J. Control. Release* **142**: 196–205.

20. Sharp, FA, Ruane, D, Claass, B, Creagh, E, Harris, J, Malyala, P, *et al.* (2009). Uptake of particulate vaccine adjuvants by dendritic cells activates the NALP3 inflammasome. *Proc. Natl. Acad. Sci.* **106**: 870–875.

21. Oyewumi, MO, Kumar, A and Cui, Z (2010). Nano-microparticles as immune adjuvants: correlating particle sizes and the resultant immune responses. *Expert Rev. Vaccines* **9**: 1095–1107.

22. Singh, SM, Alkie, TN, Nagy, É, Kulkarni, RR, Hodgins, DC and Sharif, S (2016). Delivery of an inactivated avian influenza virus vaccine adjuvanted with poly (D, L-lactic-co-glycolic acid) encapsulated CpG ODN induces protective immune responses in chickens. *Vaccine* **34**: 4807–4813.

23. Hiremath, J, Kang, K, Xia, M, Elaish, M, Binjawadagi, B, Ouyang, K, *et al.* (2016). Entrapment of H1N1 Influenza Virus Derived Conserved Peptides in PLGA Nanoparticles Enhances T Cell Response and Vaccine Efficacy in Pigs. *PLoS One* **11**: e0151922.

24. Price, GE, Soboleski, MR, Lo, C-Y, Misplon, JA, Quirion, MR, Houser, K V, *et al.* (2010). Single-Dose Mucosal Immunization with a Candidate Universal Influenza Vaccine Provides Rapid Protection from Virulent H5N1, H3N2 and H1N1 Viruses. *PLoS One* **5**: e13162.

25. Carignan, D, Thérien, A, Rioux, G, Paquet, G, Gagné, M-ÈL, Bolduc, M, *et al.* (2015). Engineering of the PapMV vaccine platform with a shortened M2e peptide leads to an effective one dose influenza vaccine. *Vaccine* **33**: 7245–7253.

26. Anderson, JM and Shive, MS (2012). Biodegradation and biocompatibility of PLA and PLGA microspheres. *Adv. Drug Deliv. Rev.* **64**: 72–82.

27. DeMuth, PC, Min, Y, Irvine, DJ and Hammond, PT (2014). Implantable Silk Composite Microneedles for Programmable Vaccine Release Kinetics and Enhanced Immunogenicity in Transcutaneous Immunization. *Adv. Healthc. Mater.* **3**: 47–58.

28. Wu, F, Zhou, Z, Su, J, Wei, L, Yuan, W and Jin, T (2013). Development of dextran nanoparticles for stabilizing delicate proteins. *Nanoscale Res. Lett.* **8**: 197.

29. Hanson, MC, Bershteyn, A, Crespo, MP and Irvine, DJ (2014). Antigen Delivery by Lipid-Enveloped PLGA Microparticle Vaccines Mediated by in Situ Vesicle Shedding. *Biomacromolecules* **15**: 2475–2481.

30. Tzeng, SY, Guarecuco, R, McHugh, KJ, Rose, S, Rosenberg, EM, Zeng, Y, *et al.* (2016). Thermostabilization of inactivated polio vaccine in PLGA-based microspheres for pulsatile release. *J. Control. Release* **233**: 101–113.

31. Deng, L, Cho, JK, Fiers, W and Saelens, X (2015). M2e-Based Universal Influenza A Vaccines. *Vaccines* **3**.

32. Goodrick, CL (1975). Life-Span and the Inheritance of Longevity of Inbred Mice. *J. Gerontol.* **30**: 257–263.

33. Schiller, JT and Lowy, DR (2015). Raising expectations for subunit vaccine. *J. Infect. Dis.* **211**: 1373–1375.

34. Luzardo-Alvarez, A, Blarer, N, Peter, K, Romero, JF, Reymond, C, Corradin, G, *et al.* (2005). Biodegradable microspheres alone do not stimulate murine macrophages in vitro, but prolong antigen presentation by macrophages in vitro and stimulate a solid immune

response in mice. *J. Control. Release* **109**: 62–76.

35. Rubsamen, RM, Herst, CV, Lloyd, PM and Heckerman, DE (2014). Eliciting cytotoxic T-lymphocyte responses from synthetic vectors containing one or two epitopes in a C57BL/6 mouse model using peptide-containing biodegradable microspheres and adjuvants. *Vaccine* **32**: 4111–4116.

36. Cruz, LJ, Rosalia, RA, Kleinovink, JW, Rueda, F, Löwik, CWGM and Ossendorp, F (2014). Targeting nanoparticles to CD40, DEC-205 or CD11c molecules on dendritic cells for efficient CD8+ T cell response: A comparative study. *J. Control. Release* **192**: 209–218.

37. Herrmann, VL, Hartmayer, C, Planz, O and Groettrup, M (2015). Cytotoxic T cell vaccination with PLGA microspheres interferes with influenza A virus replication in the lung and suppresses the infectious disease. *J. Control. Release* **216**: 121–131.

CHAPTER 5

DEVELOPMENT OF *E. COLI* NISSLE DERIVED RECOMBINANT OUTER MEMBRANE VESICLES CONTAINING TETRA-ACYLATED AND PENT-ACYLATED LIPOPOLYSACCHARIDES FOR USE AS AN INFLUENZA ADJUVANT PLATFORM

Introduction

Subunit vaccines often require the addition of an adjuvant to generate sufficient immune responses. Increased understanding of the innate immune system has led to the development of adjuvants that target pathogen recognition receptors (PRRs) in the innate immune system, allowing for a more tailored immune response[1]. One approach to adjuvant design is 'bottom up', and focuses on the exploration of how different combinations of specific PRRs can generate specific immune responses. An alternative approach to adjuvant design is 'top down' and uses complex, pathogen-mimetic particles to generate an immune response. Recently, *E. coli* derived recombinant outer membrane vesicles (rOMVs) have demonstrated potential as a potent adjuvant platform for subunit antigen delivery[2]. Because rOMVs are derived from a bacterial membrane, they naturally contain many pathogen associated molecular patterns (PAMPs), making them a complex, but efficacious, adjuvant system[3–6].

While the pathogen-mimetic nature of rOMVs can help to generate a robust immune response, the high lipopolysaccharide (LPS, or endotoxin) content in bacterial outer membranes can lead to injection site inflammation and post vaccination scarring. A strain of bacteria, Clearcoli® (CC), whose LPS synthesis pathway was engineered to create a cell membrane containing an LPS precursor lipid, lipid IVa, was recently engineered to assist the production of endotoxin-free recombinant proteins[7]. Previously, we have reported the further engineering of

CC to produce rOMVs. These CC rOMVs generated antibody titers against an antigen displayed on their surface equivalent to rOMVs derived from a probiotic strain of *E. coli,* Nissle 1917, despite the CC rOMVs lacking full LPS. Additionally, mice immunized with CC rOMVs displaying an influenza A virus derived antigen, M2e4xHet, were 100% protected from a lethal influenza challenge. While CC rOMVs appear to be a highly effective and safe adjuvant platform, they elicit a balanced IgG2a:IgG1 antibody ratio against displayed antigens, whereas rOMVs derived from Nissle 1917 elicit elevated IgG2a:IgG1 antibody ratios. IgG2a antibodies are desirable for two reasons. First as a means to neutralize a pathogen, and second to facilitate antibody mediated cellular cytotoxicity or antibody mediated phagocytosis[8–10]. Unlike Clearcoli® and other lab strains of bacteria, Nissle 1917 contains flagellin (in its flagella and fimbriae), a known TLR5 agonist, which may contribute to the observed Th1 biased immune response[11]. Therefore, we sought to engineer the LPS of *E. coli* Nissle 1917 to create a less pyrogenic rOMV but maintain the desired Th1 biased immune response.

There is precedence for engineering *E. coli* strains to produce OMVs with reduced toxicity[12]. LPS, also known as endotoxin, stimulates primarily through toll like receptor 4 (TLR4)[13]. While full LPS contains an O-antigen, inner and outer core, and lipid A region, only the lipid A portion contributes to TLR4 signaling[13,14]. The acyl chains of the lipid A region interact with MD-2 and TLR4, facilitating dimerization and signal transduction. Knock out of gene *lpxM* results in production of pent-acylated LPS, rather than the normal hex-acylated LPS, and has been used to reduce toxicity associated with rOMVs[15]. However, no work has yet used tetra-acylated LPS to produce rOMVs. While CC rOMVs do contain tetra-acylated lipid A, they do not contain complete LPS; they have only lipid IVa, no core region or O-antigen. Here, modified Nissle 1917 *E. coli* that contains pent-acylated or tetra-acylated LPS was generated

through a series of gene knock outs, similar to the approached used to generate CC from parent strain BL21(DE3). Unlike CC, no mutation was introduced into Nissle 1917 to remove the 3-deoxy-α-D-manno-octulosonic acid (KDO) portion of LPS. The modified Nissle 1917 strains were subsequently transformed with a plasmid containing an influenza antigen, M2e4xHet, and used to generate M2e4xHet rOMVs. These modified-LPS rOMVs were then compared to CC rOMVs and wild type Nissle rOMVs to better elucidate the impact of *E. coli* strain and LPS acylation on rOMV adjuvant potential.

Materials and Methods

P1 phage carrying gene knockouts created using Keio collection

P1 phage carrying DNA from Keio collection, which contain genes knocked out and replaced with kanamycin resistance (kan^R) genes, were generated as previously described[16]. Briefly, *E. coli* strains from the Keio collection containing the desired knockout (*lpxT, eptA, crcA, lpxM, lpxL,* or *lpxP*) were grown in LB overnight, then subcultured 1:100 into 2 mL LB with 5 mM $CaCl_2$, 10 mL $MgSO_4$, and 0.2% glucose for 1.5 h (Sigma-Aldrich, St. Louis, U.S). Subsequently, 50 µL of P1 phage was added and culture was grown until no longer turbid, indicating successful bacterial lysis (~4 h). Chloroform (10 µL) was added to the culture, the culture vortexed, then centrifuged (5 min, 12k rcf). The supernatant (phage lysate) was collected and stored at 4° C until needed.

Gene knockout in Nissle 1917 performed using P1 phage transduction

E. coli Nissle 1917 knock outs were generated as previously described[4]. Briefly, the strain to be modified was grown overnight, then 600 µL centrifuged and resuspended in 100 µL of Luria-Bertani (LB) broth (Thermo Fisher Scientific, Waltham, U.S.) (supplemented with 5 mM $CaCl_2$, 10 mM SO_4, and 0.2% glucose (Sigma-Aldrich, St. Louis, U.S.)) and 100 µL of phage lysate (containing the desired gene knock out). The culture was incubated (37° C, 2 h, 200 rpm), then 1 mL of LB and 100 µL of 1 M sodium citrate added to the tube and incubation continued for another hour. The culture was then centrifuged (12k rcf, 1 min), resuspended in 100 µL LB (with 100 mM sodium citrate), and plated on kan^+ (50 µg/mL) sodium $citrate^+$ (100 mM) Petri dishes (Corning, Corning, U.S.). Colonies were selected and streaked on kan^+, sodium $citrate^+$ plates. Colonies were then grown in LB overnight and sequenced to confirm replacement of

desired gene with kan^R gene.

Kanamycin resistance genes removed using plasmid pCP20

Removal of the kan^R resistance gene was facilitated through the use of plasmid pCP20. pCP20 contains a temperature sensitive origin of replication and contains genes for ampicillin resistance and FLP recombinase. Expression of FLP recombinase excises genes between FRT sites (which frame the kan^R gene)[17]. Briefly, *E. coli* Nissle strains containing the desired knock out were transformed with pCP20, then grown at 30° C overnight on amp^+ plates (50 μg/mL). Subsequently, colonies were selected, streaked on amp^+ plates (50 μg/mL), and grown overnight at 30° C. Colonies were then selected, streaked on antibiotic-free plates, and grown at 42° C overnight. Colonies were selected and each colony streak on a amp^+ plate, kan^+ plate, and antibiotic-free plate, then grown overnight at 37° C. Colonies that grew on the antibiotic free plate, but not the other two plates, were sequenced to confirm removal of kan^R gene and that the bacterial strain was correct.

Polymerase Chain Reaction (PCR) of Nissle strains confirms gene knock out

Polymerase chain reaction (PCR) was performed using Phusion polymerase (New England BioLabs, Ipswich, U.S.) according to manufacture's instructions for a 50 μL reaction. Primers used to verify gene knock out are same as used previously to create Clearcoli[7]. Gene *focA* was sequenced to verify that the strain being modified was Nissle 1917[18]. Genomic DNA was collected for sequencing using a simple boiling method. Briefly, strains were grown overnight in LB. 100 μL of sample was centrifuged (13.1k rcf, 1 min), supernatant removed, and pellet resuspend in nuclease free water. The sample was boiled for 10 min, centrifuged (13.1k rcf,

1min), then 2 µL of supernatant added per 50 µL PCR reaction.

Engineering and production of penta-acylated and tetra-acylated Nissle 1917 rOMVs

Starting with *E. coli* Nissle 1917 Δ*npI* (Nsl-wt), sequential gene knock out was used to produce penta-acylated (Nsl-5) and tetra-acylated (Nsl-4) strains. First, genes *lpxT* (encodes lipid A 1-diphosphate synthase), *eptA* (encodes phosphoethanolaminetransferase A), and *crcA* (encodes palmitoyl transferase for lipid A) were knocked out to create Nissle with a more uniform LPS composition. Pent-acylated Nissle (Nsl-5) was then created through knock out of *lpxM* (encodes lipid A biosynthesis myristoyltransferase). Tetra-acylated LPS was created by further knock out of *lpxL* (encodes lipid A biosynthesis lauroyltransferase) and *lpxP* (encodes lipid A biosynthesis palmitoleoyltransferase). Engineered strains were then transformed with a pBAD plasmid encoding a transmembrane protein, ClyA, followed by an influenza antigen, M2e4xHet, and grown up to produce rOMVs, as previously described[2]. Total surface protein in rOMVs was measured using a Pierce bicinchoninic acid (BCA) assay, performed according to manufacturer's instructions (Thermo Fisher Scientific, Waltham, U.S.). Presence of M2e4xHet antigen was confirmed via Western Blot with anti-His antibody (Sigma-Aldrich, St. Louis, U.S.).

Mouse immunization and challenge

Four cohorts of 7-week-old BALB/c mice (n=5) were subcutaneously vaccinated with either 40 µg of M2e4xHet CC rOMVs in PBS, 40 µg of M2e4xHet Nsl-4 rOMVs in PBS, 40 µg of M2e4xHet Nsl-5 rOMVs in PBS, or PBS. Following vaccination, mice were weighed daily for a week to assess the health impact of vaccination. All mice received a boost dose of the same composition of the prime dose 4 weeks post prime vaccination. At 10 weeks post prime

vaccination, mice were challenged with a lethal dose (50 FFU) of influenza A virus A/Puerto Rico/8/1934 (H1N1) (PR8) (BEI Resources, Manassas, U.S.) as previously described[2]. Briefly, mice were lightly anesthetized with isoflurane, then a 50 μL dose of PR8 (1 FFU/mL in PBS) delivered intranasally. Mice were monitored twice daily and weighed once daily to assess their response to the influenza challenge. Mice that lost more than 30% of their original weight, or exhibited signs up severe distress, were euthanized.

Toll like receptor (TLR) stimulation studies

TLR studies were carried out as previously described[2]. Briefly, HEK-Blue TLR5-KD cells (InvivoGen, San Diego, CA) were plated at $0.15x10^6$ cells/mL in 96 well plates (100 μL/well) and grown overnight. Subsequently, cells were transfected with 5xNF-kβ-luciferase reporter plasmid and TLR4/MD-2/CD14, mTLR4/MD-2/CD14, TLR2, or mTLR2 and grown for 28h. Cells were then incubated with rOMVs (100 ng/mL), LPS (100 ng/mL), or Pam3Cys (100 ng/mL) for 16, followed by removal of media and cell lysis to free luciferase. Luciferase activity was measured via addition of 100 μL D-luciferin substrate to 20 μL of lysate and resulting luminescence read using a Veritas luminometer (Promega, Madison, WI).

Macrophage stimulation studies

Macrophages (TLR2 KO, TLR4 KO, and TLR2/4 KO) were plated at $2x10^5$ cells/well (500 μL per well) in 24 well plates (Corning, Corning, U.S.) in complete DMEM media (DMEM with 10% low endotoxin fetal bovine serum (FBS), 10 mM HEPES, 1 mM sodium pyruvate, 2 mM L-glutamine, 50 U/mL penicillin, and 50 U/mL streptomycin). Cells were then stimulated with rOMVs (1 μg/mL), LPS (100 ng/mL), or Pam3Cys (1 μg/mL) and incubated for 6h (37° C, 5%

CO_2, 6h). Subsequently, media was collected and analyzed for TNF-α via ELISA assay run according to manufacturer's instructions (Biolegend, San Diego, U.S.).

Whole blood pyrogenicity testing

Whole blood pyrogen test was performed as previously described[19]. Blood from healthy human donors was collected into heparinized tubes and rotated at room temperature (<2h) until use. 96 well plates were filled with 200 µL endotoxin free saline and either 20 µL of rOMVs (concentrations ranged from 10 µg/mL to 0.001 pg/mL) or 20 µL of endotoxin standards (concentration ranged from 10 EU/mL to 0.125 EU/mL), or 20 µL phosphate buffered saline (PBS). 20 µL of blood was added per well, then plates incubated (37° C, 5% CO_2, 18h). Following incubation, plates were centrifuged (500 rcf, 5 min, RT) and supernatants collected and used to perform an IL-1β ELISA according to manufacturer's instructions (Biolegend, San Diego, U.S.).

Enzyme-linked immunosorbent assay (ELISA)

M2e ELISA was performed as previously described[2]. Briefly, plates were coated with 2 µg/mL M2e1xCys peptide (SLLTEVETPIRNEWGSRSNDSSD) (LifeTein, Somerset, U.S.), 12h, 37° C) in PBS overnight. Plates were blocked, incubated with 2-fold serial dilutions of sera samples (2h, 37° C), incubated with biotinylated anit-IgG1, anti-IgG2a, or anti-IgG antibodies (1h, 37° C) (eBiosciences, San Diego, U.S.), incubated with avidin-HRP (30 min, 37° C) (Sigma-Aldrich, St. Louis, U.S.), then developed with 3,3,5,5-tetramethylbenzidine (TMB) (Thermo Fisher Scientific, Waltham) (20 min, 20° C). Plates were washed 3+ times with PBS-T (0.3% bovine serum albumin (BSA), 0.05% Tween20 (Sigma-Aldrich, St. Louis, U.S.)) between each step.

Statistics

Pyrogenicity data was analyzed using a Kruskal-Wallis test followed by comparisons to CC rOVMs using Dunn's test to account for multiple comparisons. TLR and macrophage data was compared using an ANOVA followed by comparisons to PBS using Dunnett's test to account for multiple comparisons. Weight loss data post vaccination was compared using a 2-way ANOVA followed by Dunnett's test to account for multiple comparisons to PBS. Mortality data post influenza challenge was compared using a log-rank test, followed by using the Bonferroni method to account for multiple comparisons to PBS. Weight loss data post influenza challenge was compared using a 2-way ANOVA followed by Dunnett's test to account for multiple comparisons to CC rOMVs.

Results

Tetra-cylated and Penta-acylated rOMVs have low pyrogenicity

Pyrogenicity of CC, Nsl-4, Nsl-5, and Nsl-wt rOMVs was assessed using a whole blood monocyte activation pyrogenicity test. In this test, IL-1β production by monocytes in response to rOMVs was correlated to IL-1β production by monocytes in response to known amounts of endotoxin. CC, Nsl-4, and Nsl-5 rOMVs all had statistically equivalent pyrogenicity that was approximately 5 log fold lower than that of Nsl-wt rOMVs (**Figure 1A**). The significantly lower pyrogenicity that Nsl-4 and Nsl-5 rOMVs have relative to Nsl-wt rOMVs suggests that they would make a safer vaccine option than Nsl-wt, with less inflammation following injection.

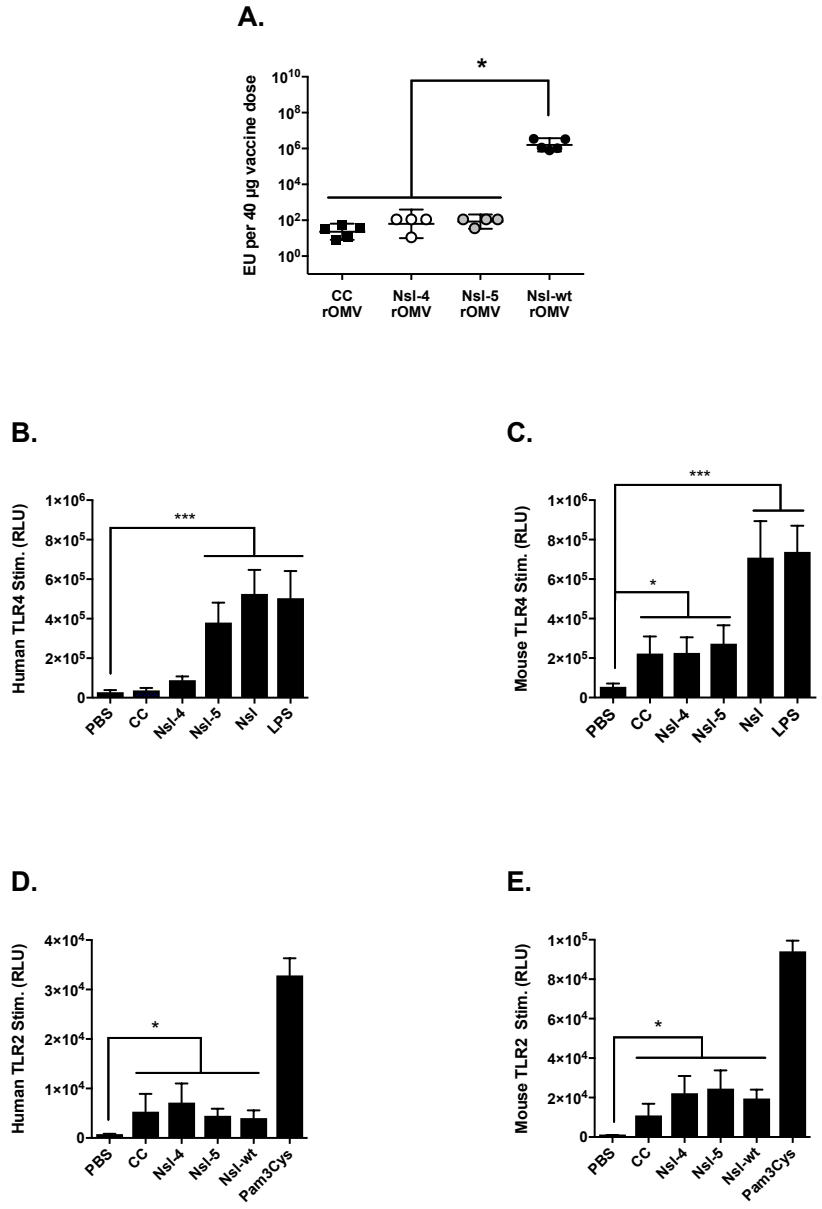

Figure 1: (A) Pyrogenicity of a 40 µg dose of rOMVs (* $p<0.05$). Error bars represent geomean average with 95% confidence intervals. Groups compared using Kruskal-Wallis test followed by comparisons to CC rOMVs using Dunn's test to account for multiple comparisons. (B-E) Cells transfected with a NFκβ luciferase reporter and TLR4/MD-2/CD14 (B), mTLR4/mMD-2/mCD14 (C), TLR2 (D), or mTLR2 (E) were incubated with rOMVs for 16h then measured for luciferase production. Error bars represent standard deviation of average. Groups compared using ANOVA followed by comparisons to PBS using Dunnett's test to account for multiple comparisons (* $p<0.05$, *** $p<0.001$).

Nissle LPS modifications impact TLR signaling

CC, Nsl-4, Nsl-5, and Nsl-wt rOMVs were incubated with cells transfected with individual TLRs to provide an enhanced understanding of rOMV signaling. Neither CC rOMVs nor Nsl-4 rOMVs stimulated cells transfected with TLR4, though both Nsl-5 and Nsl-wt rOMVs produced a response (**Figure 1B**). When cells transfected with mouse TLR4 (mTLR4) were incubated with rOMVs, CC, Nsl-4, and Nsl-5 rOMVs resulted in a moderate, but statistically significant ($p<0.05$), upregulation of signaling; mTLR4 transfected cells incubated with Nsl-wt rOMVs had high and statistically significant ($p<0.001$) upregulation of signaling (**Figure 1C**). CC, Nsl-4, Nsl-5, and Nsl-wt rOMVs all stimulated cells transfected with TLR2 and mTLR2 (**Figures D,E**). The ability of all rOMV types to stimulate TLR2 suggests that TLR2 may play a role in shaping the immune response following rOMV vaccination. While neither CC nor Nsl-4 rOMVs triggered human TLR4, CC, Nsl-4, and Nsl-5 rOMVs all stimulated murine TLR4. Thus, further investigation is needed to ascertain whether mTLR4 signaling is critical to achieving a protective response from rOMVs.

rOMVs stimulate macrophages in the absence of TLR4

To further investigate the importance mTRL4 stimulation by rOMVs, TLR4 knockout (KO), TLR2 KO, and wild type (WT) murine macrophages were incubated with CC, Nsl-4, Nsl-5, and Nsl-wt rOMVs (**Figures 2A-C**). Six hours post incubation, the amount of TNF-α in supernatants was quantified via ELISA. All 4 rOMV types resulted in statistically significant ($p<0.05$) TNF-α production following incubation with TLR4 KO macrophages (**Figure 2A**). Pure LPS did not significantly stimulate the TLR4 KO macrophages, confirming that LPS was not contributing to the response. All rOMV types also stimulated TLR2 KO macrophages, possibly due to TLR4

activity (**Figure 2B**). Pam3Cys did not stimulate TLR2 KO macrophages, confirming that the TNF-α produced was not due to TLR2 stimulation. Especially high levels of TNF-α were produced following incubation of WT macrophages with rOMVs, suggesting that synergistic signaling due to concurrent TLR2 and TLR4 stimulation could be occurring. While the macrophage data indicated that TLR4 stimulation was not necessary for rOMVs to elicit TNF-α production in macrophages, it also confirmed that signaling was taking place through more than TLR2.

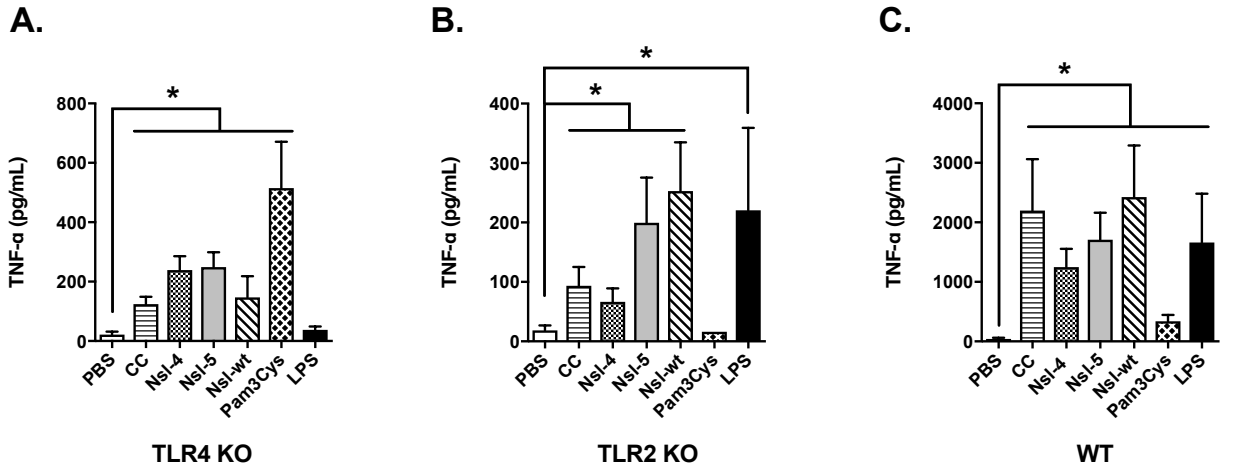

Figure 2: TLR4 knock out (KO) (A), TLR2 KO (B), and TLR2/4 KO (C) macrophages were incubated with rOMVs for 6h, then supernatant collected and TNF-α measured. Error bars represent standard deviation of average. Groups compared using ANOVA followed by comparisons to PBS using Dunnett's test to account for multiple comparisons (* $p<0.05$).

Nsl-4 and Nsl-5 rOMVs both lead to weight loss post vaccination

BALB/c mice were vaccinated with M2e4xHet CC rOMVs, M2e4xHet Nsl-4 rOMVs, M2e4xHet Nsl-5 rOMVs, or PBS to determine whether the modified Nsl rOMVs were able to elicit high anti-M2e titers with low vaccination side effects. Following vaccination, mice were

weighed daily to assess health following vaccination; mice that do not tolerate the vaccination well present with anorexia and weight loss. Mice that were vaccinated with CC rOMVs displayed no weight loss and were not statistically different from mice that received a PBS injection (**Figure 3A**). Mice that received Nsl-4 rOMVs had ~5% weight loss and took 2 days to recover back to the weight of mice that received only a PBS injection, though had minimal piloerection and displayed normal movement patterns (**Figure 3A**). Mice that received Nsl-5 rOMVs had ~10% weight loss and took 3 days to recover back to the weight of mice that received only a PBS injection (**Figure 3A**). Additionally, mice that received Nsl-5 rOMVs exhibited piloerection post injection and developed swelling followed by scarring at the injection site. The difference in weight loss between the Nsl-4 and Nsl-5 rOMVs demonstrates the reduction in inflammation that results between the pent-acylated and tetra-acylated lipid A structure, and suggests that Nsl-4 rOMVs are a safer platform than Nsl-5 rOMVs.

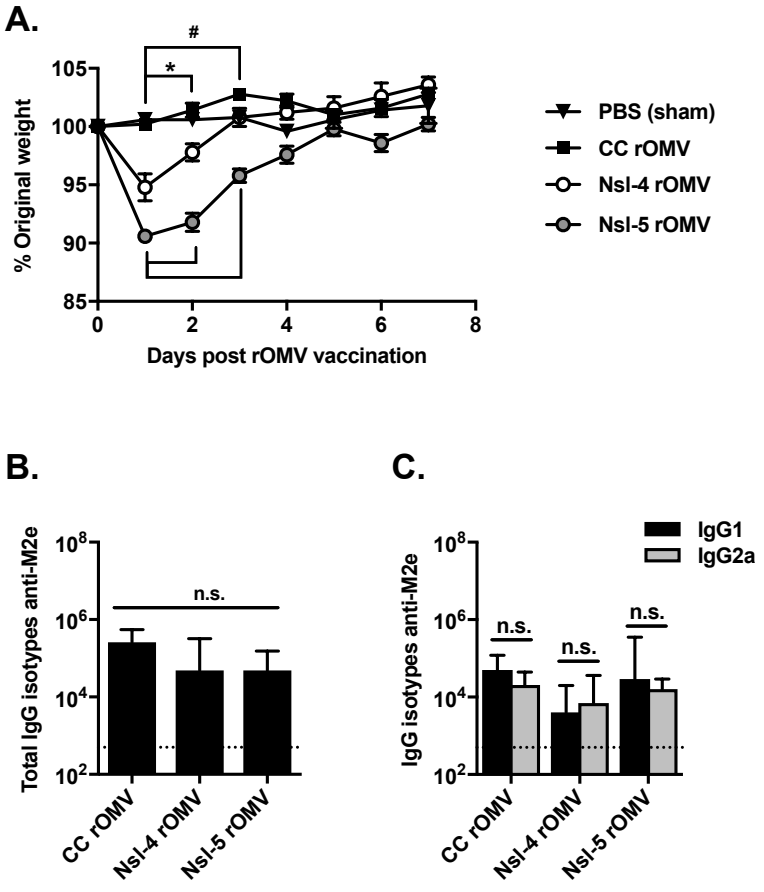

Figure 3: (A) Mice were weighed daily post vaccine prime. Dotted line equals titer of naïve sera. Error bars represent standard error of mean. Groups compared with 2-way ANOVA followed by using Dunnett's test to account for multiple comparisons to PBS (* $p<0.05$ PBS vs. Nsl-4; $^{\#}$ $p<0.05$ PBS vs. Nsl-5). (B,C) Total IgG (B) and IgG1 and IgG2a (C) anti-M2e titers were measured at 8 weeks post prime vaccination. Error bars represent 95% confidence interval of geometric mean. Groups compared using Kruskal-Wallis test followed by multiple comparisons that were corrected by Tukey's test.

CC, Nsl-4, and Nsl-5 rOMVs elicit high anti-M2e titers

Blood was collected from CC, Nsl-4, and Nsl-5 vaccinated mice 8 weeks post prime vaccination and sera analyzed for anti-M2e antibodies. CC, Nsl-4, and Nsl-5 rOMV vaccinated mice all produced high and statistically equivalent anti-M2e IgG titers (**Figure 3B**). Sera were further analyzed to compare IgG1 vs. IgG2a anti-M2e titers (**Figure 3C**). All three mice had statistically equivalent IgG1 and IgG2a anti-M2e titers. High levels of anti-M2e antibodies contribute to protection in influenza A challenge, suggesting that all three vaccines would offer good protection against influenza A challenge.

CC, Nsl-4, and Nsl-5 rOMVs protect mice in lethal influenza A challenge

BALB/c mice vaccinated with CC rOMVs, Nsl-4 rOMVs, Nsl-5 rOMVs, or PBS were challenged with a lethal dose of mouse adapted influenza strain A/Puerto Rice/8/1934 (H1N1) (PR8). Mice vaccinated with CC, Nsl-4, and Nsl-5 rOMVs demonstrated 100% survival (5/5 per cohort) against PR8 challenge. Additionally, all mice (5/5) vaccinated with PBS required euthanasia (**Figure 4A**). There was no significant difference in weight loss between any of the rOMV vaccinated mice (**Figure 4B**). Overall, the Nsl-4 and Nsl-5 rOMVs demonstrated that they were just as effective in protecting mice from influenza A challenge as CC rOMVs.

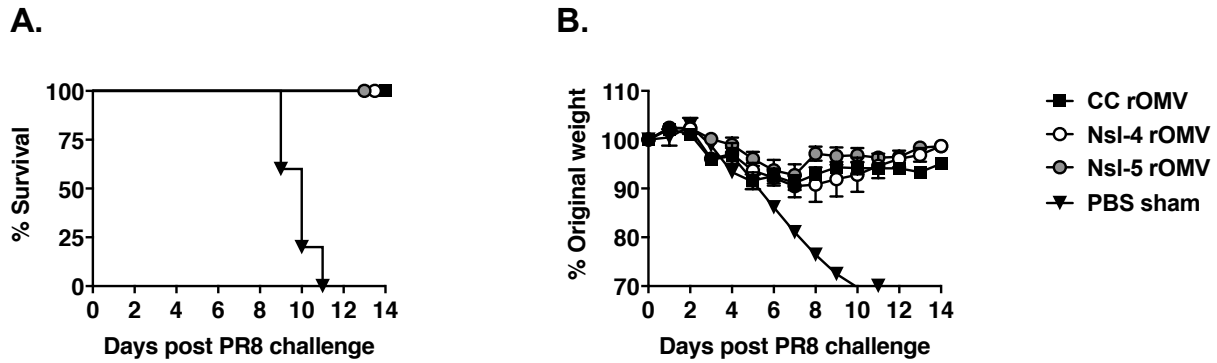

Figure 4: Mortality (A) and morbidity (B) of BALB/c mice following lethal dose (50 FFU) of influenza A/PR8. Error bars (B) represent standard error of the mean.

Discussion

Engineered *E. coli* Nissle strains containing only 4 or 5 acyl chains were able to successfully produce rOMVs containing the influenza antigen M2e4xHet. Previously, *E. coli* Nissle 1917 was engineered to have pent-acylated LPS through knock out of *lpxM,* though rOMVs from this modified Nissle strain were never tested in a challenge model[4]. However, other strains of *E. coli* have been engineered through *lpxM* knock out and used in both therapeutic and prophylactic vaccine models. OMVs derived from *E.coli* strain W3110, a K-12 derived strain with an *lpxM* mutation, were used to deliver siDNA as a cancer therapeutic[20]. Additionally, it was recently shown that *E. coli* strain JH8033, which lacks *lpxM,* could be further engineered to generate and display glycosylated rOMVs that protected against *Francisella tularensis* challenge[21]. While these groups generated pent-acyltaed *E. coli* strains via knock out of solely *lpxM,* the strains used in this paper (apart from Nsl-wt) also had genes *lpxT, eptA,* and *crcA* knocked out. Following the work produced by Needham et al, we decided to knock out these three genes, which all modify lipid A, to try and create Nissle strains with a more homogeneous lipid A profile[22]. Future work analyzing the LPS contained in Nsl-4 and Nsl-5 rOMVs using mass spectrometry will allow verification of the homogeneity of their LPS content.

The Nsl-4 and Nsl-5 rOMVs were able to successfully elicit high anti-M2e titers and protect mice from influenza challenge, though they still led to more weight loss post vaccination than CC rOMVs. Previously, rOMVs generated from *E. coli* Nissle 1917 were shown to have the advantage of eliciting a strong Th1 bias with elevated IgG2a:IgG1 antibody levels, even when used in BALB/c mice, a Th2 biased strain[4]. However, while CC, Nsl-4, and Nsl-5 rOMV vaccines all elicited anti-M2e IgG2a titers above those of naïve sera, none of the vaccines produced anti-M2e IgG2a titers that were statistically elevated relative to anti-M2e IgG1 titers.

Thus, wild type LPS appears to be critical to generating elevated IgG2a titers. Elevated IgG2a levels are only one component of a Th1 biased response, suggesting that further analysis of the cellular response to M2e4xHet rOMVs will provide a more nuanced view.

CC, Nsl-4, and Nsl-5 rOMVs all had statistically equivalent pyrogenicity, as measured by the whole blood monocyte activation test. However, Nsl-5 rOMVs stimulated both murine and human TLR4, whereas Nsl-4 and CC rOMV stimulated only mTRL4. The similar responses elicited by CC and Nsl-4 rOMVs in not stimulating TRL4, but stimulating mTLR4 was expected, as the lipid A region is the portion of LPS that interacts with the CD14/MD-2 complex, and both CC and Nsl-4 contain lipid A with 4 acyl chains. However, it was somewhat surprising that Nsl-5 rOMVs stimulated human TLR4, despite having the same level of pyrogenicity as Nsl-4 and CC rOMVs; possibly, the additional stimulation of TLR4 was insignificant due to other pathogen recognition receptors (PRR) being stimulated. It was also unexpected that CC and Nsl-4 rOMVs had the same level of pyrogenicity, despite Nsl-4 rOMVs containing the additional PAMPs flagellin and fimbrie. It is possible that the differences in pyrogenicity between the Nsl-4, Nsl-5, and CC groups were too subtle to detect using the pyrogenicity assay, but that other endotoxin measurement methods, such as the rabbit pyrogens test, would yield different results[23]. Overall, the low pyrogenicity of Nsl-4 and Nsl-5 rOMVs suggests that they are better vaccine candidates than Nsl-wt.

The *in vitro* macrophage work confirmed the TLR work, showing that rOMVs stimulated more than just mTLR4. Thus, while wild type mouse models are not ideal for testing rOMV efficacy, the macrophage data demonstrates that there is still potential for rOMVs to be sufficiently immunogenic for a human vaccine. Future work using TLR4 knock out mice and transgenic human TLR4/MD-2 mice will further demonstrate the translational potential of

rOMVs with LPS modifications[24]. Additionally, it will be interesting to see if TLR4 knock out mice lose weight post Nsl-4 and Nsl-5 vaccination, as wild type mice did. If it is specifically LPS stimulation of mTLR4 driving the inflammation and weight loss, then removal of mTLR4 should ameliorate these side effects. The macrophage data also indicated that just as mTLR4 stimulation was not necessary to elicit TNF-α production from macrophages, TLR2 stimulation was also not necessary. Future experiments using TLR2/4 knock out macrophages will demonstrate whether other PRRs are contributing to the immunogenicity of rOMVs. Previously, Nissle rOMVs were shown to stimulate through TLR2, TLR4, and TLR5, and to a lesser extent, TLR9[2,4]. Thus, it is likely that Nsl-4 and Nsl-5 rOMVs should continue to stimulate even TLR2/4 KO macrophages, though CC rOMVs may see a significant drop in their stimulation potential. In addition to work using murine macrophages, use of human-derived macrophages will allow species specific differences to be detected. As a whole, the macrophages responded similarly to all rOMVs tested; further work is needed to elucidate specific differences between the rOMV types.

In conclusion, we demonstrate the ability to use serial gene knock out in *E. coli* strain Nissle 1917 to engineer strains with pent-acylated and tetra-acylated LPS. These engineered Nissle strains were used to produce rOMVs displaying the influenza antigen M2e4xHet and successfully immunized mice against influenza, protecting them against a lethal PR8 challenge. While Nsl-4 and Nsl-5 rOMVs both led to weight loss in mice following vaccination, they had equivalent pyrogenicity to CC rOMVs in tests using human whole blood. Though further work is needed to determine whether Nissle 1917 derived rOMVs offer any superior benefits to ClearColi® derived rOMVs, overall, the Nsl-4 rOMVs represent a viable adjuvant platform with many of the same benefits as CC rOMVs.

References

1. Maisonneuve, C, Bertholet, S, Philpott, DJ and De Gregorio, E (2014). Unleashing the potential of NOD- and Toll-like agonists as vaccine adjuvants. *Proc. Natl. Acad. Sci. U. S. A.* **111**: 1–6.

2. Rappazzo, CG, Watkins, HC, Guarino, CM, Chau, A, Lopez, JL, DeLisa, MP, *et al.* (2016). Recombinant M2e outer membrane vesicle vaccines protect against lethal influenza A challenge in BALB/c mice. *Vaccine* **34**: 1252–1258.

3. Chen, DJ, Osterrieder, N, Metzger, SM, Buckles, E, Doody, AM, DeLisa, MP, *et al.* (2010). Delivery of foreign antigens by engineered outer membrane vesicle vaccines. *Proc. Natl. Acad. Sci. U. S. A.* **107**: 3099–104.

4. Rosenthal, JA, Huang, C, Doody, AM, Leung, T, Mineta, K, Feng, DD, *et al.* (2014). Mechanistic insight into the Th1-biased immune response to recombinant subunit vaccines delivered by probiotic bacteria-derived outer membrane vesicles. *PLoS One* **9**: e112802.

5. Kim, JY, Doody, AM, Chen, DJ, Cremona, GH, Shuler, ML, Putnam, D, *et al.* (2008). Engineered bacterial outer membrane vesicles with enhanced functionality. *J. Mol. Biol.* **380**: 51–66.

6. Baker, JL, Chen, L, Rosenthal, JA, Putnam, D and DeLisa, MP (2014). Microbial biosynthesis of designer outer membrane vesicles. *Curr. Opin. Biotechnol.* **29**: 76–84.

7. Mamat, U, Wilke, K, Bramhill, D, Schromm, AB, Lindner, B, Kohl, TA, *et al.* (2015). Detoxifying Escherichia coli for endotoxin-free production of recombinant proteins. *Microb. Cell Fact.* **14**: 1–15.

8. Schmitz, N, Beerli, RR, Bauer, M, Jegerlehner, A, Dietmeier, K, Maudrich, M, *et al.* (2012). Universal vaccine against influenza virus: Linking TLR signaling to anti-viral protection. *Eur. J. Immunol.* **42**: 863–869.

9. El Bakkouri, K, Descamps, F, De Filette, M, Smet, A, Festjens, E, Birkett, A, *et al.* (2011). Universal vaccine based on ectodomain of matrix protein 2 of influenza A: Fc receptors and alveolar macrophages mediate protection. *J. Immunol.* **186**: 1022–1031.

10. Carignan, D, Thérien, A, Rioux, G, Paquet, G, Gagné, M-ÈL, Bolduc, M, *et al.* (2015). Engineering of the PapMV vaccine platform with a shortened M2e peptide leads to an effective one dose influenza vaccine. *Vaccine* **33**: 7245–7253.

11. Vejborg, RM, Friis, C, Hancock, V, Schembri, MA and Klemm, P (2010). A virulent parent with probiotic progeny: Comparative genomics of Escherichia coli strains CFT073, Nissle 1917 and ABU 83972. *Mol. Genet. Genomics* **283**: 469–484.

12. Kim, SH, Kim, KS, Lee, SR, Kim, E, Kim, MS, Lee, EY, *et al.* (2009). Structural modifications of outer membrane vesicles to refine them as vaccine delivery vehicles. *Biochim. Biophys. Acta* **1788**: 2150–9.

13. Maeshima, N and Fernandez, RC (2013). Recognition of lipid A variants by the TLR4-MD-2 receptor complex. *Front. Cell. Infect. Microbiol.* **3**: 3.

14. Needham, BD and Trent, MS (2013). Fortifying the barrier: the impact of lipid A remodelling on bacterial pathogenesis. *Nat. Rev. Microbiol.* **11**: 467–81.

15. Kim, OY, Hong, BS, Park, KS, Yoon, YJ, Choi, SJ, Lee, WH, *et al.* (2013). Immunization with Escherichia coli outer membrane vesicles protects bacteria-induced lethality via Th1 and Th17 cell responses. *J. Immunol.* **190**: 4092–102.

16. Thomason, LC, Costantino, N and Court, DL (2001). *E. coli Genome Manipulation by P1 Transduction*. *Curr. Protoc. Mol. Biol.*, John Wiley & Sons, Inc.doi:10.1002/0471142727.mb0117s79.

17. Baba, T, Ara, T, Hasegawa, M, Takai, Y, Okumura, Y, Baba, M, *et al.* (2006). Construction of Escherichia coli K-12 in-frame, single-gene knockout mutants: the Keio collection. *Mol. Syst. Biol.* **2**.

18. Blum-Oehler, G, Oswald, S, Eiteljörge, K, Sonnenborn, U, Schulze, J, Kruis, W, *et al.* (2003). Development of strain-specific PCR reactions for the detection of the probiotic Escherichia coli strain Nissle 1917 in fecal samples. *Res. Microbiol.* **154**: 59–66.

19. Daneshian, M, von Aulock, S and Hartung, T (2009). Assessment of pyrogenic contaminations with validated human whole-blood assay. *Nat. Protoc.* **4**: 1709–1721.

20. Gujrati, V, Kim, S, Kim, S-H, Min, JJ, Choy, HE, Kim, SC, *et al.* (2014). Bioengineered Bacterial Outer Membrane Vesicles as Cell-Specific Drug-Delivery Vehicles for Cancer Therapy. *ACS Nano* **8**: 1525–1537.

21. Chen, L, Valentine, JL, Huang, C-J, Endicott, CE, Moeller, TD, Rasmussen, JA, *et al.* (2016). Outer membrane vesicles displaying engineered glycotopes elicit protective antibodies. *Proc. Natl. Acad. Sci.* **113**: E3609–E3618.

22. Needham, BD, Carroll, SM, Giles, DK, Georgiou, G, Whiteley, M and Trent, MS (2013). Modulating the innate immune response by combinatorial engineering of endotoxin. *Proc. Nat. Acad. Sci., USA* **110**: 1464–1469.

23. Graener, R and Werner, J (1986). Dynamics of endotoxin fever in the rabbit. *J. Appl. Physiol.* **60**: 1504–1510.

24. Hajjar, AM, Ernst, RK, Fortuno III, ES, Brasfield, AS, Yam, CS, Newlon, LA, *et al.* (2012). Humanized TLR4/MD-2 mice reveal LPS recognition differentially impacts susceptibility to Yersinia pestis and Salmonella enterica. *PLoS Pathog* **8**: e1002963.

CHAPTER 6

CONCLUSIONS AND FUTURE DIRECTIONS

Summary

Here, we demonstrate that rOMVs are a safe and viable adjuvant platform toward the development of a universal influenza vaccine. Previously, while rOMVs had indicated some potential as a vaccine adjuvant, high levels of LPS limited their translation in to the clinic. Through the engineering of probiotic *E. coli* strain Nissle 1917 (Nsl) to produce LPS that was pent-acylated (Nsl-5) and tetra-acylated (Nsl-4) rather than hex-acylated, we were able to generate rOMVs with reduced toxicity. Additionally, engineering a preexisting stain of *E. coli*, Clearcoli® (CC), to hypervesiculate, allowed production of rOMVs that contained only the LPS precursor lipid IVa. Each of these detoxified *E. coli* strains were used to produce rOMVs that displayed the influenza antigen M2e4xHet. Vaccination with M2e4xHet rOMVs from all three detoxified strains resulted in complete survival of BALB/c mice against lethal influenza challenge. Additionally, mice vaccinated with CC M2e4xHet rOMVs displayed complete survival against two different subtypes of influenza: H1N1 and H3N2. The protection elicited by CC rOMVs lasted for at least 6 months post prime vaccination. Single dose vaccination and using PLGA microparticles to encapsulate CC rOMVs was as effective as the prime/boost regimen. Furthermore, when CC rOMVs were used to vaccinate ferrets, ferrets had a two log reduction in lung viral titers during human pdmH1N1 challenge vs. ferrets that received a mock vaccine. While mice vaccinated with Nsl-4 and Nsl-5 rOMVs showed some side effects post vaccination, CC rOMVs were able to elicit these protective immune responses against influenza without causing excessive inflammation or weight loss following vaccination, further emphasizing their potential as a safe vaccine platform. While significant progress has been made

on making rOMVs a translatable adjuvant platform, much work is left to be accomplished, especially in further understanding the mechanisms of rOMV efficacy, and in improving characterization to allow for better batch-to-batch assessment.

Future direction 1: Determination of role of TLR4 in response to rOMVs

One of the most necessary future steps in this work is to test the immune response to rOMVs in a mTLR4 knock out mouse strain. Tetra-acylated LPS and lipid IVa both moderately stimulate mTLR4, but do not stimulate hTLR4. While the knock out macrophage experiments prove that mTLR4 stimulation is not necessary to elicit cytokine production from macrophages, wild type macrophages certainly had stronger responses to rOMVs than TLR4 knockout macrophages. At the time of the writing of this Disseration, mTLR4 knockout mice are being bred, which will allow the efficacy of rOMVs to be assessed in a model where mTLR4 does not contribute to any signaling. One downside is that the TLR4 knock out mouse is on a B6 background, which is a naturally Th1 biased mouse strain. Thus, the rOMVs may perform better in terms of immune bias in this strain than in an mTLR4 knock out BALB/c strain. In addition to the TLR4 knock out strain, several years ago, a humanized mouse model was developed that contains human TLR4 and MD2. Unfortunately, this strain is hard to access and also is on the B6 background. In addition to the mouse work, further characterization of how ferrets respond to lipid IVa and LPS with lipid A modifications is necessary so that the relevance of the ferret model can be better assessed. It is well established that ferrets are an excellent model for studying influenza and influenza vaccines; however, it is unknown how good of a model they are for studying inflammation due to LPS variants. Pyrogenicity of rOMVs in humans was assessed using the whole blood pyrogenicity test, which requires a pair of anti IL-1β antibodies for use in an ELISA

to monitor inflammation. Anti IL-1β antibody pairs do not exist for ferrets, but it is possible that ferret IL-1β might cross-react with anti IL-1β pairs intended for other species. It might also be possible to instead run qPCR on ferret monocytes incubated with rOMVs and look for upregulation in mRNA of inflammatory cytokines. Overall, determining the impact of mTLR4 on the response to rOMVs is critical for assessing their potential for translation to humans.

Future direction 2: Further exploration of E. coli Nissle 1917 derived rOMVs with tetra-acylated LPS

Nissle 1917 was engineered through a series of genetic knock outs to produce tetra-acylated LPS. However, mass spectrometry is needed to analyze the LPS contained in Nsl-4 rOMVs and determine (1.) whether it is in fact tetra-acylated and (2.) how homogenous the LPS structure is. The mice that received Nsl-4 rOMVs still lost weight relative to mice that received only PBS and mice that received CC rOMV injections. Though the mice that received Nsl-4 rOMVs did not show outward adverse effects, the weight loss indicates that there could be biocompatibility concerns. Histology of the injection site at different time points post injection will help to assess the level of inflammation occurring. Additionally, including an injection of alum as a control will help to determine how the inflammation from Nsl-4 rOMVs compares to that from a standard vaccine adjuvant. As mentioned above, it is important to determine the role that mTLR4 contributes to rOMV immunogenicity. It is possible that no weight loss would be seen in a TLR4 knockout mouse. The TLR data indicates that Nsl rOMVs contain TLR9, TLR5, and TLR2 agonists. Therefore, in addition to TLR4 knock out mice, it would be useful to ultimately test rOMVs in other knockout strains to better understand the mechanisms driving the response. Additionally, using MyD88 knock out mice would help to determine whether the bulk of the

response was in fact primarily TLR driven. It is quite possible that inflammasomes and other PRRs are contributing to the response. While theoretically Nsl-4 rOMVs should provide a more complex—and perhaps also more efficacious—stimulation of the innate immune system than CC rOMVs, which lack some of the PAMPS that Nsl-4 rOMVs contain, so far CC rOMVs appear to be the superior vaccine platform with respect to safety profile.

Future direction 3: Improved characterization of rOMVs

The scope of the current thesis centered on the detoxification of rOMVs and improving their safety profile while maintaining efficacy. However, for rOMVs to become a viable platform, improvements need to be made to their characterization: amount of antigen, distribution of antigen on rOMVs, concentration of rOMVs in a sample, and protein content within the lumen of rOMVs are all either difficult to determine, or are unknown. Currently, the amount of antigen present on rOMVs is estimated using a semi-quantitiative Western Blot. While Western Blots can give a rough estimate of antigen content, they are not nearly as accurate as an ELISA. By using anti-M2e antibodies and biotinylated anti-His antibodies, it may be possible to develop a sandwich ELISA that provides a more accurate measure of total M2e4xHet content in an rOMV preparation. The standard curve would be generated from His-purified M2e4xHet, using a BCA assay to determine its concentration. The second great unknown in rOMVs is how ClyA-antigen is distributed on the rOMV surface. Previous papers have published cryo-TEM images that clearly show ClyA dimerizing into pore like structures on OMV surfaces; however, no cyro-TEM images exist of rOMVs that display ClyA-M2e4xHet or ClyA-GFP. While we have many TEM pictures of ClyA-M2e4xHet rOMVs, the greater resolution of cryo-TEM, coupled with immunohistochemistry to label the antigens with gold dots, is needed to get a sense for the

distribution of ClyA-antigens on the rOMV surface. It is possible that different antigens result in different distributions on the rOMV surface. For example, Western Blot data indicates that there is a higher concentration of antigen in M2e4xHet rOMVs than in ClyA-GFP rOMVs. Do the ClyA-M2e4xHet rOMVs in fact contain more ClyA-M2e4xHet antigen per rOMV? Do all rOMVs contain about the same amount of ClyA-antigen, or does the amount per rOMV vary greatly? In addition to these questions, it is unknown whether the distribution pattern of ClyA-antigen on rOMV surfaces is strain specific. Engineering the LPS will likely impact the properties of the bacterial membrane, so it would not be surprising if it also impacted the distribution of ClyA. Finally, a simple way to measure the concentration of rOMVs in a preparation—not just the total protein concentration in the preparation—is necessary. Instruments, such as the Nanosight, may be useful for CC rOMVs; however, rOMVs derived from Nissle contain fragments of flagella, making rOMV concentration difficult to determine due to the highly polydispersed nature of the solution (flagella fragments are long and cylindrical whereas rOMVs are spherical). Currently, when injecting rOVMs, the total number of rOMVs is unknown. Finally, rOMVs remain a black box in terms of their content. Previous papers have found that rOMVs contain peptidoglycan fragments, DNA fragments, misfolded proteins, etc.; however, measuring all of these components on each rOMV preparation is currently impractical due to time and financial constraints. However, a better understanding of what is located within the interior space of rOMVs, and how variable that content is from batch to batch will be important to bring rOMVs to market. Thus, though we have seen consistent responses in mice to our CC M2e4xHet rOMVs, improvements to rOMVs characterization will allow for more confidence when dosing and for more nuanced conclusions to be drawn, paving the way for translation into the clinic.

Final thoughts

The detoxified rOMV platform holds much promise and there certainly are many more aspects to explore than the three future directions listed above. Studying the trafficking of rOMVs using confocal microscopy, optimizing the M2e antigenic sequence, exploring antigens from other pathogens, determining the adjuvanticity of ClyA-M2e4xHet, studying the cellular response to vaccination using cytotoxic T cell killing assays and adoptive transfer, exploring alternate delivery routes, and determining the impact on rOMV production of different growing conditions are all interesting questions that could be explored. It has been exciting to work on a project with such translational potential, and who knows, maybe in twenty years I'll walk into a health center for a flu vaccine and find that it's formulated with rOMVs. Overall, detoxified rOMVs have demonstrated great potential as a platform for influenza vaccines and could potentially be a great platform for other antigens as well.

APPENDIX I

Supplemental Information for Chapter 2

Sequences for expressed M2e peptides
Three codon optimized M2e-based sequences were expressed in *E. coli* and used to produce recombinant OMVs.

M2e1xS

Peptide:SLLTEVETPIRNEWGSRSNDSSD

Entire nucleotide sequence inserted into pBAD plasmid:
tctagaatgAGCCTGCTGACCGAAGTTGAAACCCCGATTCGTAATGAATGGGGTAGCCGT
AGCAATGATAGCAGCGATcatcaccatcaccatcactaaaagctt

M2e1xC

Peptide:SLLTEVETPIRNEWGCRCNDSSD

Entire nucleotide sequence inserted into pBAD plasmid:
tctagaAGCCTGCTGACCGAAGTTGAAACCCCGATTCGTAATGAATGGGGTTGTCGTTG
TAATGATAGCAGTGATcatcaccatcaccatcactaaaagcttgg

M2e4xHet

Peptide:SLLTEVETPIRNEWGSRSNDSSDgggsgggSLLTEVETPTRSEWESRSSDSSDgggsgg
gSLLTEVETPTRNEWESRSSDSSDgggsgggSLLTEVETLTRNGWGSRSSDSSD

Entire nucleotide sequence inserted into pBAD plasmid:
tctagaAGCCTGCTGACCGAAGTTGAAACCCCGATTCGTAATGAATGGGGTAGCCGTAG
CAATGATAGCAGTGATGGCGGTGGTAGCGGTGGTGGCTCACTGCTGACAGAGGTGG
AAACACCGACCCGTAGCGAATGGGAAAGCCGTAGTAGCGATAGCTCAGATGGCGGT
GGTAGCGGTGGTGGCAGTCTGCTGACGGAAGTAGAGACTCCGACCCGCAATGAGTG
GGAAAGTCGTTCAAGCGATTCATCAGATGGCGGTGGTAGCGGTGGTGGCAGCCTGC
TGACTGAGGTCGAGACACTGACACGCAATGGTTGGGGTTCACGTAGCTCTGATAGC
AGCGATcatcaccatcaccatcactaaaagctt

HEK293 stimulation via M2e4xHet-OMVs

TLR5 stimulation via M2e4xHet-OMVs was confirmed by using HEK293 cells in addition to HEK293 TLR5 KD cells

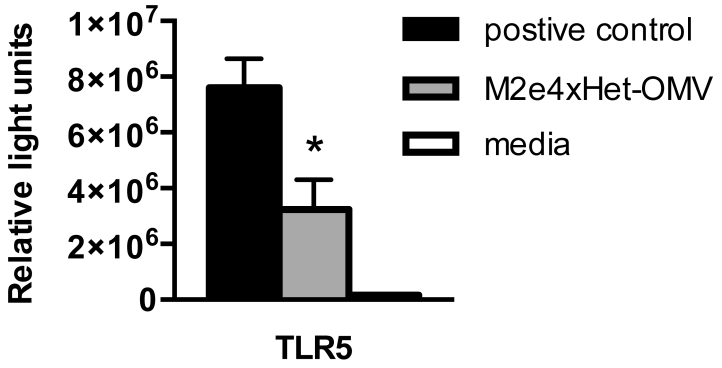

Figure S1: HEK293 cells transformed with CMV-β-galactosidase and 5xNF-κB-luciferase were stimulated with 4xHetM2e-OMVs (10 ng/mL), positive control (flagellin), or media. Addition of M2e4xHet-OMVs resulted in significant increase in luciferase production vs. media alone (* $p<0.0001$).

APPENDIX II

Supplemental Information for Chapter 3

Table S1: Primers used for PCR

Primer	Sequence (5'- 3')	Source
gutQ-F	GTCGATAAGCTGATTACCGACGC	Mamat 2015[1]
gutQ-R	GTGAAACTATTCGTCAGGCACTGG	Mamat 2015[1]
nlpI-F	ATTTACGCCGCGCATGTGTTTAG	This paper
nlpI-R	AGGGCCGTATCCGTCTGAGC	This paper

1. Mamat, U, Wilke, K, Bramhill, D, Schromm, AB, Lindner, B, Kohl, TA, *et al.* (2015). Detoxifying Escherichia coli for endotoxin-free production of recombinant proteins. *Microb. Cell Fact.* **14**: 1–15.

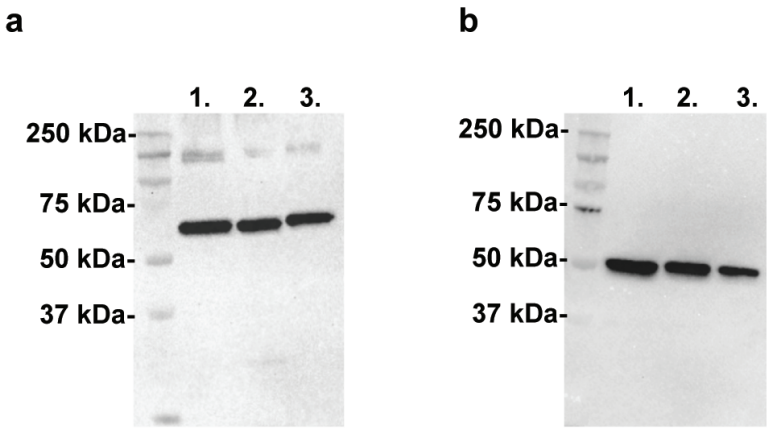

Figure S1: (**a**) Western blot of rOMVs expressing ClyA-GFP developed using anti-GFP antibody. Lane 1: ClyA-GFP CC rOMVs (2 µg), lane 2: ClyA-GFP BL21 rOMVs (2 µg), lane 3: ClyA-GFP purified protein (0.125 µg). (**b**) Western blot of rOMVs expressing influenza-based antigen ClyA-M2e4xHet developed using anti-His tag antibody. Lane 1: ClyA-M2e4xHet CC rOMVs (1 µg), lane 2: ClyA-M2e4xHet Nsl rOMVs (1 µg), lane 3: ClyA-M2e4xHet purified protein (0.2 µg). Both blots developed using chemiluminescence and imaged with Bio-Rad ChemiDoc Touch Imaging System (Bio-Rad, Hercules, CA).

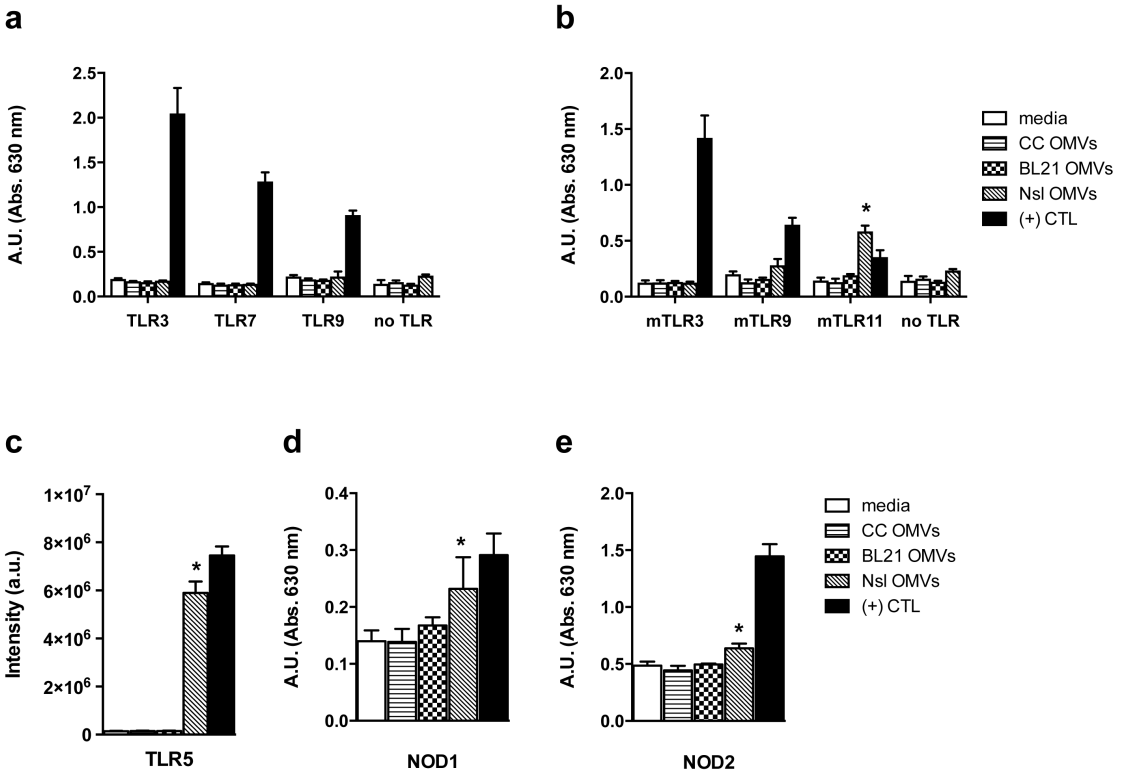

Figure S2: PRR signaling in response to rOMVs. (**a**) HEK-Blue^{TM} KD-TLR5 cells were transfected with human TLR2, 3, 7, and 9, then stimulated with CC, Nsl, and BL21 rOMVs (100 ng/mL). (**b**) HEK-Blue^{TM} KD-TLR5 cells were transfected with murine TLR2, 3, 9, and 11, then stimulated with CC, Nsl, and BL21 rOMVs (100 ng/mL). (**c**) HEK-293 cells were transfected with a 5xNF-kβ-luciferase reporter plasmid and TLR5, then stimulated with CC, Nsl, and BL21 rOMVs (100 ng/mL). (**d, e**) HEK-293 Blue^{TM} murine NOD1 (**d**) and NOD2 (**e**) reporter cells were stimulated with CC, Nsl, and BL21 rOMVs (100 ng/mL). Graphs analyzed using ANOVA followed by multiple comparisons to stimulation caused by media using Dunnett method of correction, * $p<0.01$. Error bars represent mean + SD (n=4).

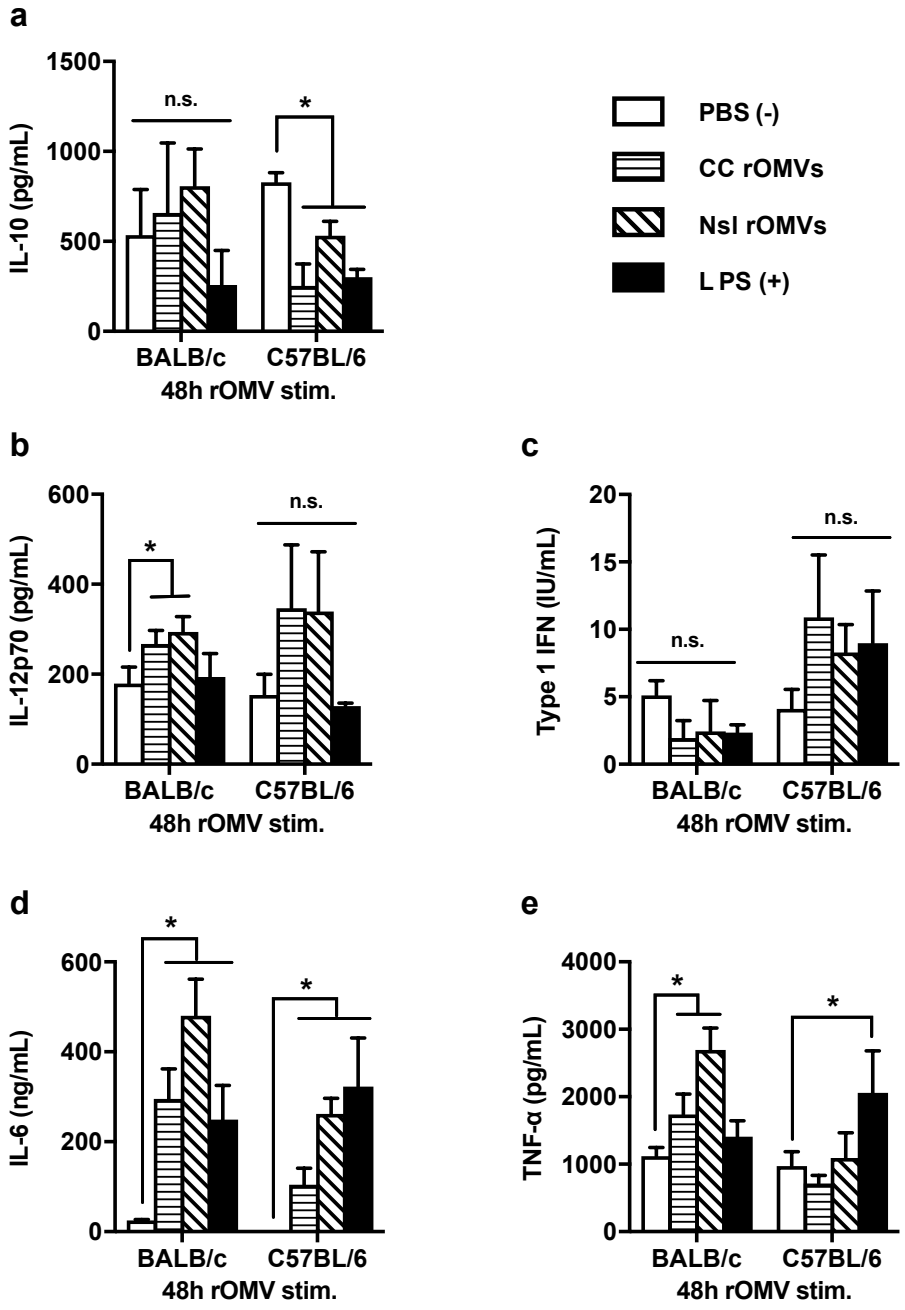

S3: BMDCs were isolated from BALB/c and C57BL/6 mice, then stimulated with CC rOMVs (100 ng/mL), Nsl rOMVs (100 ng/mL), LPS (100 ng/mL) or PBS. Media was collected 48h post stimulation and analyzed for IL-10 (**a**), IL-12p70 (**b**), type I IFN (**c**), IL-6 (**d**), and TNF-α (**e**). Error bars represent standard deviation. Samples analyzed via ANOVA followed by Holm multiple comparison test * $p<0.05$ (n=3).

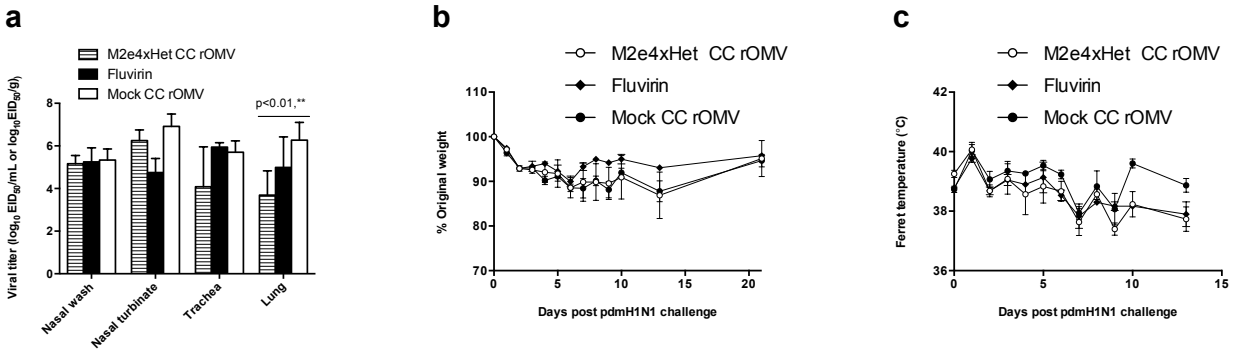

Figure S4: (**a**) Day 3 post influenza exposure, ferrets were assessed for viral titers. Groups analyzed with 2-way ANOVA, followed by multiple comparisons to mock CC rOMV using Bonferroni method of correction (n=3) ** $p<0.01$. (**b,c**) Weight loss (**b**) and temperature (**c**) were monitored in ferrets post influenza (pdmH1N1) exposure.